PHYTOPLANKTON PRODUCTIVITY AND MILANKOVITCH CYCLES IN THE CENOMANIAN-TURONIAN BRIDGE CREEK MEMBER OF THE GREENHORN FORMATION IN SOUTHEASTERN COLORADO

by

Scott David Rutherford

Thesis submitted to the Faculty of the Virginia Polytechnic Institute and State University in partial fulfillment of the requirements for the degree of

MASTER OF SCIENCE

in

Geological Sciences

APPROVED:

Dewey M. McLean, Chairman

Richard K. Bambach

J. Fred Read

December, 1994

Blacksburg, Virginia

PHYTOPLANKTON PRODUCTIVITY AND MILANKOVITCH CYCLES IN THE CENOMANIAN-TURONIAN BRIDGE CREEK MEMBER OF THE GREENHORN FORMATION IN SOUTHEASTERN COLORADO

by

Scott David Rutherford

Committee Chairman: Dewey M. McLean
Geological Sciences

(ABSTRACT)

Statistical analyses of palynomorph assemblages from the Upper Cretaceous Bridge Creek Member (Greenhorn Formation) near Pueblo, Colorado suggest that the micritic limestone/organic rich-shale cycles of the Bridge Creek may have been caused by a combination of fluctuating primary productivity and humid/arid climate cycles.

Species richness and evenness indices for palynomorph assemblages from 24 Bridge Creek beds were statistically analyzed using Analysis of Variance. The results indicate that assemblages for the limestone beds exhibit greater evenness and richness indices than do assemblage from the shale beds. Because phytoplankton communities typically exhibit lower evenness and richness values in eutrophic conditions, these results are consistent with possible surface water eutrophication during times of shale deposition. During times of high primary productivity, the aerobic oxidation of large amounts of organic matter settling to the sea floor may have consumed the oxygen available at depth creating an anaerobic environment and facilitating the preservation of organic carbon.

Riverine input to the seaway also contributed to cycle production. It appears that shale was deposited during humid periods when riverine runoff provided terrigenous

material necessary for shale deposition. The flow of isotopically-light fresh water to the seaway during times of shale deposition is supported by lighter $\delta^{18}O$ values in the shale beds.

The fluctuating primary productivity and humid/arid cycles may have been caused by Milankovitch Cycle-driven climate change. Climate models indicate that insolation fluctuations driven by the precessional or obliquity cycle may have periodically increased upwelling along the eastern margin of the Cretaceous Interior Seaway and influenced rainfall patterns. At appears that organic rich shale was deposited when upwelling, nutrient-rich bottom water stimulated planktonic productivity and rainfall transported terrigenous material to the seaway.

ACKNOWLEDGMENTS

I thank Dr. Dewey M. McLean of Virginia Polytechnic Institute and State University for his guidance and friendship over the course of this study, and Dr. Richard K. Bambach and Dr. J. Fred Read for reviewing the manuscript and making helpful suggestions. Thanks also to fellow graduate students J. Bret Bennington, Cole Davisson, Jane Parks, Eric Gardner, and Mike Pope for helpful discussions and, in some cases, a place to sleep. Special thanks are extended to my wife, LeAnn, who spent her honeymoon driving to Blacksburg so I could become a graduate student, and to my parents for their support over the years.

LIST OF FIGURES

LIST OF TABLES

INTRODUCTION

The earth's orbital parameters are not fixed but change cyclically. As the earth orbits the sun, it's rotational axis precesses, the angle between the axis and the ecliptic changes, and the orbit's ellipticity varies. These cycles, called Milankovitch cycles, after the Serbian mathematician, Milutin Milankovitch, are thought to cause cyclical variations in earth's climate and in the state of the biosphere.

The primary objective of this project is to examine how Milankovitch cycles influence the community structure and productivity of selected marine phytoplankton groups (dinoflagellates and coccolithophorids). A secondary objective of this study is to test the high resolution stratigraphic correlation potential of the phytoplankton assemblages.

To achieve these objectives, rock samples were collected from outcrops of the Upper Cretaceous Bridge Creek Member (Greenhorn Formation) near Pueblo, Colorado, and chemically macerated to extract the microfossils. The Bridge Creek Member was deposited during peak transgression of the Cretaceous Interior Seaway (Figure 1), and comprises decimeter-scale, alternating layers of limestone and shale that are believed to have been deposited as a function of Milankovitch-driven climate cycles (Barron et al., 1985; Gilbert, 1895).

Statistical analyses of phytoplankton communities observed during this study support coupling between Milankovitch cycles and marine phytoplankton communities. Analyses of dinoflagellate and coccolith assemblages suggest that fluctuating surface water fertility combined with riverine runoff produced the Bridge Creek cycles. Paleoclimate models suggests a possible link between Milankovitch cycles and phytoplankton productivity may occur via atmospheric circulation and upwelling.

Preliminary testing of high resolution stratigraphic correlation via phytoplankton assemblages was inconclusive. While there are indications that correlation is possible additional testing is needed.

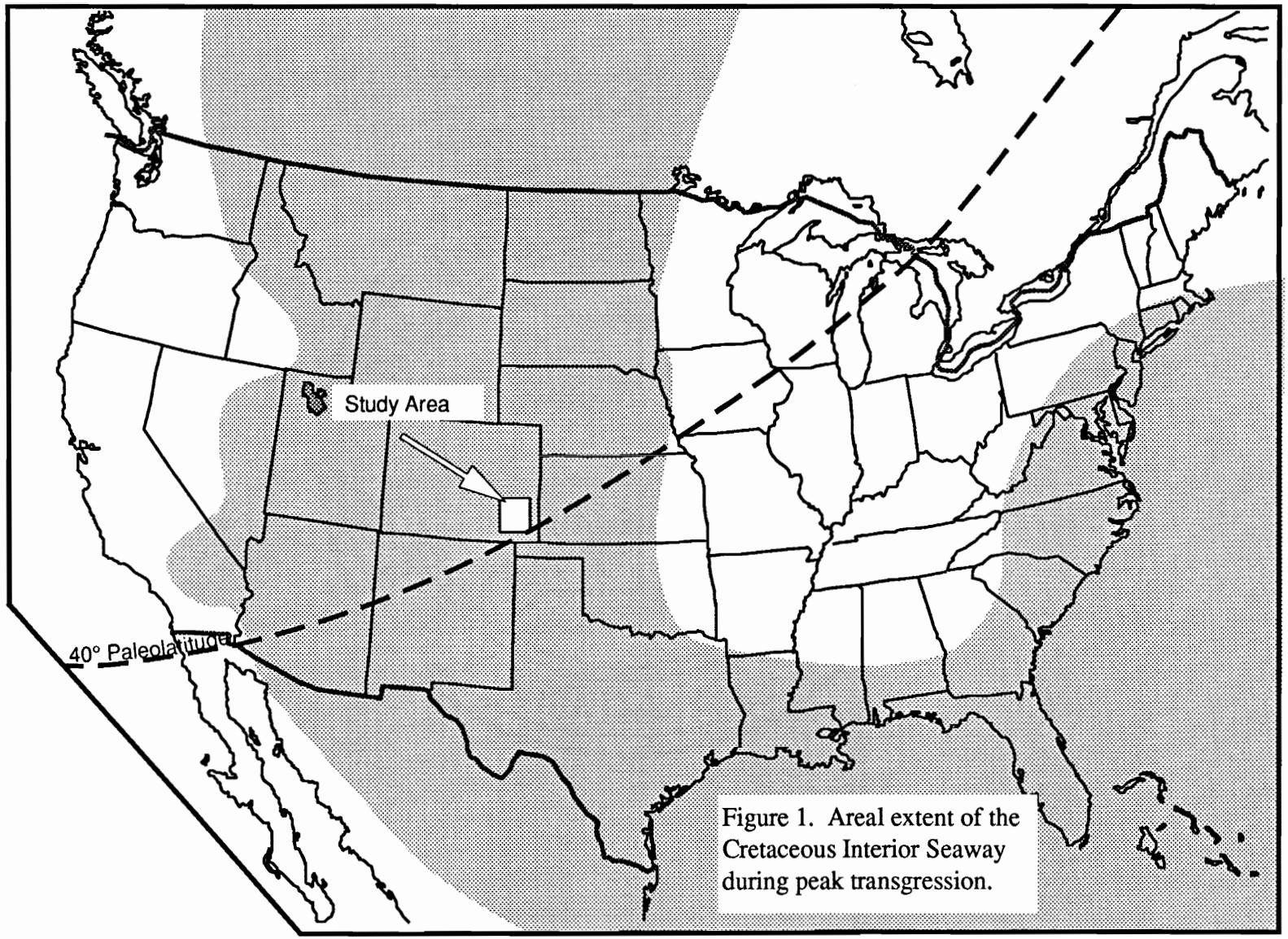

Figure 1. Areal extent of the Cretaceous Interior Seaway during peak transgression.

GEOLOGICAL SETTING

Samples for this study were collected by Dr. Dewey M. McLean from outcrops of the Greenhorn Formation in the Pueblo County Reservoir State Recreation Area (Figure 2). The Bridge Creek Member of the Greenhorn Formation is exposed where the Rock Canyon Anticline was breached by the Arkansas River. These outcrops are the Colorado Standard Reference Section of the Bridge Creek (Cobban and Scott, 1972).

During the Cretaceous Period, the study area was inundated by the Cretaceous Interior Seaway (Figure 1). The seaway initially flooded the continent during the Early Aptian, and by the Late Albian extended from the Gulf of Mexico to the Arctic Ocean. At peak transgression (Late Cenomanian to Early Turonian), the seaway was about 1,000 kilometers wide and 200 to 500 meters deep (Eicher, 1969).

A cross section of the seaway shows a typical foreland basin geometry (Figure 3). Uplift and erosion of the Sevier Highlands on the tectonically active western side of the seaway produced clastic sediments that were deposited in the seaway as the Frontier Formation. The low clastic input from the tectonically quiet, gently sloping, eastern margin of the seaway was conducive to the deposition of carbonate rich rocks that constitute the Benton and Niobrara Groups (Figure 3). The Bridge Creek, part of the Benton Group, was deposited in this area during maximum transgression of the seaway.

Rock Types

The Bridge Creek Member is composed of limestone and marlstone beds that alternate with shale beds (Plates 1 and 2). Additionally, bentonite layers are interspersed throughout the section. A brief description of each rock type follows.

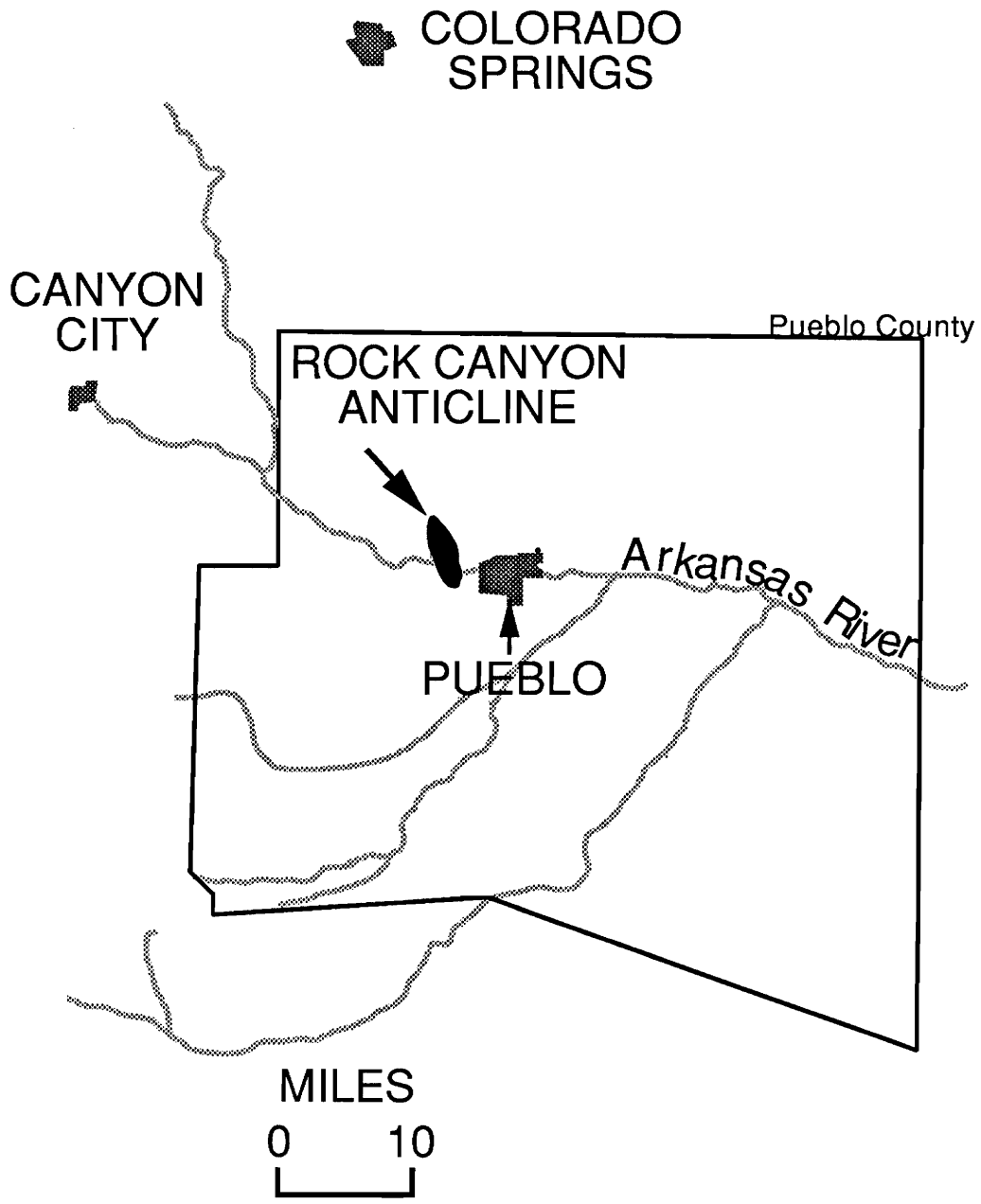

Figure 2. Locality map of Pueblo County and surrounding area. Samples for this study were collected from outcrops at the Rock Canyon Anticline.

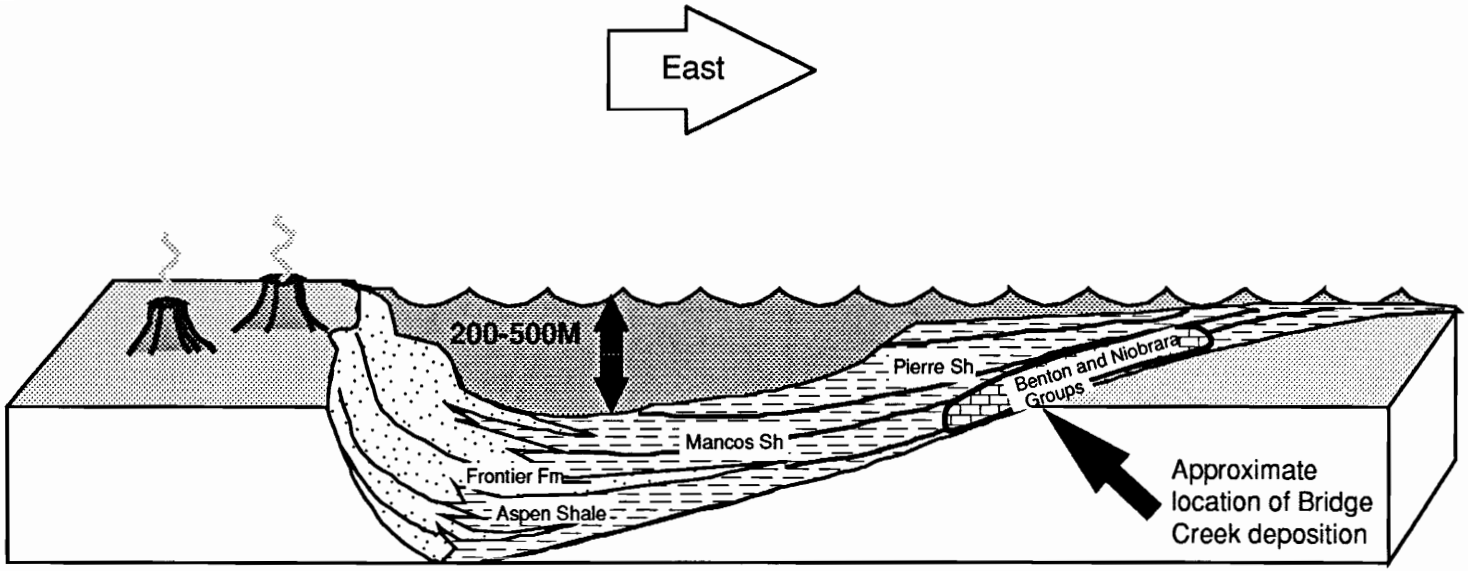

Figure 3. Generalized cross section of the Cretaceous Interior Seaway showing estimated water depth during the late Cenomanian. Carbonate rocks that compose the Benton and Niobrara Groups were deposited on the gently sloping, eastern side of the seaway.

Plate 1. Section of the lower Bridge Creek exposed along a railroad cut at the Rock Canyon Anticline near Pueblo Colorado.

Plate 2. The middle and upper Bridge Creek exposed at the Rock Canyon Anticline.

Limestone Units

The limestone beds of the Bridge Creek are bioturbated, range from 7.5 to 45.7 cm thick, contain 65.6 weight percent carbonate and 0.01 to 0.5 weight percent organic carbon (Pratt, 1984). These beds contain foraminifera tests and coccoliths in a micrite matrix. The limestone beds are increasingly argillaceous up-section and are replaced by marlstone in the upper third of the Bridge Creek. Vertical and horizontal burrows up to one centimeter in diameter are minimally distorted indicating early cementation of the limestone units.

Some limestone beds extend laterally over great distances. Hattin (1975) traced individual limestone beds for nearly 1,000 kilometers. Because the stratigraphic position of the limestone beds remains constant relative to bentonite beds, Hattin suggested that these traceable limestone beds are isochronous.

Marlstone Units

The Bridge Creek marlstone beds are calcareous, organic-rich strata, intermediate between limestone and calcareous, organic-rich shale. These units are 5.1 to 25.4 cm thick, have an average weight percent carbonate of 79.2, and organic carbon contents ranging from 0.5 to 1.5 weight percent (Pratt, 1984). The marlstone beds are poorly laminated and contain vertical and horizontal burrows 0.1 to 0.5 cm in diameter.

In the lower Bridge Creek, marlstones and limestones are interbedded with calcareous shale. In the upper Bridge Creek, marlstone is the dominant carbonate unit. Additionally, calcarenite layers are commonly associated with the upper Bridge Creek marlstone beds.

Shale Units

The Bridge Creek shale beds range from 3.8 to 42 cm thick, have an average weight percent carbonate of 65, and organic carbon contents ranging from 2 to 4 weight

percent. These units are laminated to moderately bioturbated and contain *Planolites* burrows.

Bentonite Units

Bentonite is chemically altered volcanic ash that forms a soft, light colored rock composed of clay minerals and silica. These volcanic ash beds are common in the Bridge Creek Member and are used to correlate limestone beds (Hattin, 1971). Bentonite layers range from 2 to 25 cm thick. The bentonites are a product of volcanic activity that occurred west of the seaway (Figure 3).

Stratigraphy

The Greenhorn Formation conformably overlies the Graneros Shale, and is conformably overlain by the Fairport Chalky-Shale Member of the Carlile shale. In Colorado, the Greenhorn Formation comprises the Lincoln Limestone Member, the Hartland Shale Member and the Bridge Creek Member (Figure 4).

The Lincoln Limestone Member is about 11.7 meters thick in the Rock Canyon area and is divided into lower and upper units (Sageman and Johnson, 1985). The lower unit is mostly laminated shale, whereas the upper unit consists of alternating shale and calcarenite.

In the Pueblo area, the Hartland Shale Member comprises about 16.75 meters of organic-rich calcareous shale that thins toward the east. Calcarenite beds one to five centimeters thick are interbedded with the shale.

The Bridge Creek Member (Figure 5) is subdivided into lower, middle, and upper units based on dominant rock types (Elder and Kirkland, 1985). The lower Bridge Creek is correlative with the upper Hartland Shale Member in Kansas (Figure 4) and ranges from the basal limestone bed (PBC-1) through bentonite marker bed PBC-20 (a thickness of about six meters in the Pueblo area). This interval comprises 15 to 20 cm thick, highly

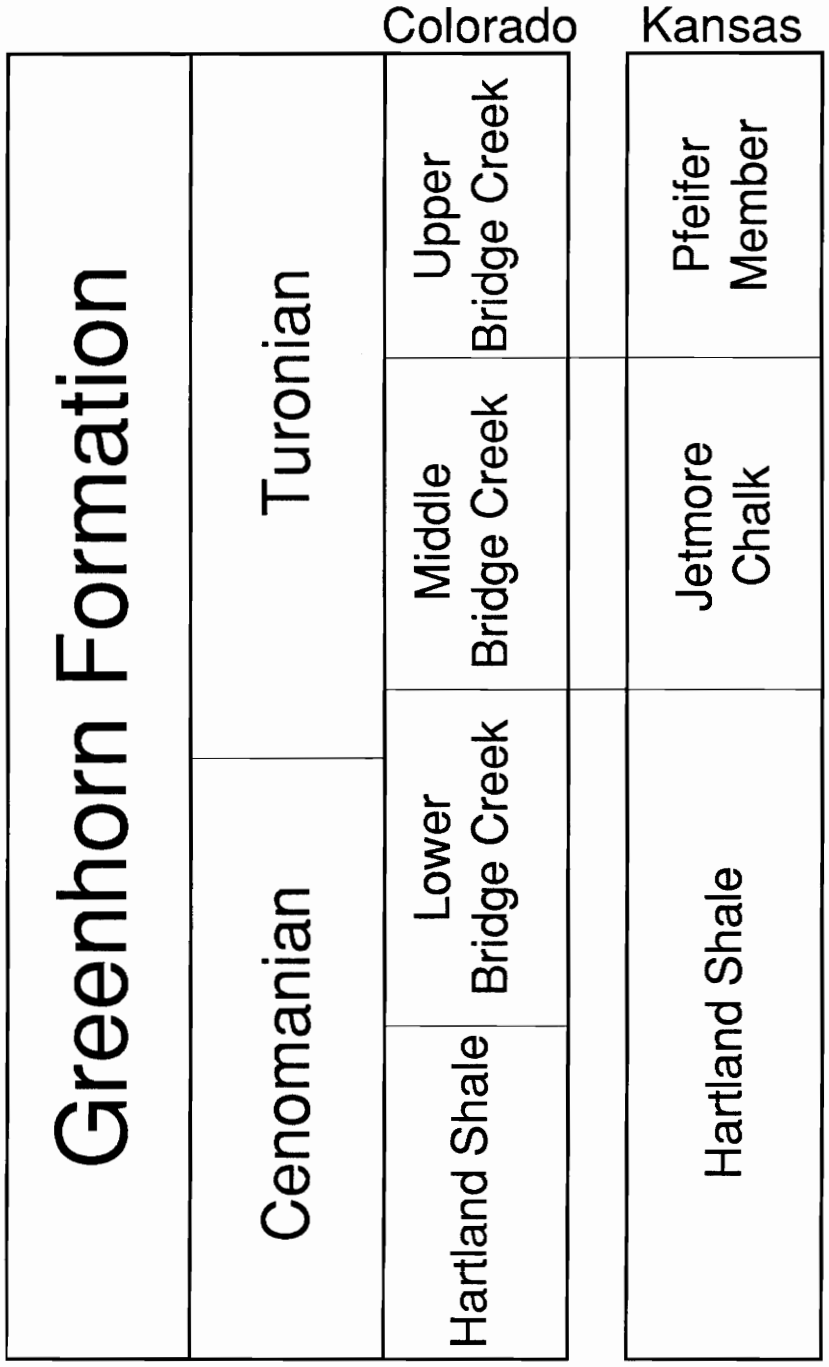

Figure 4. Stratigraphic correlation of the Bridge Creek between Colorado and Kansas.

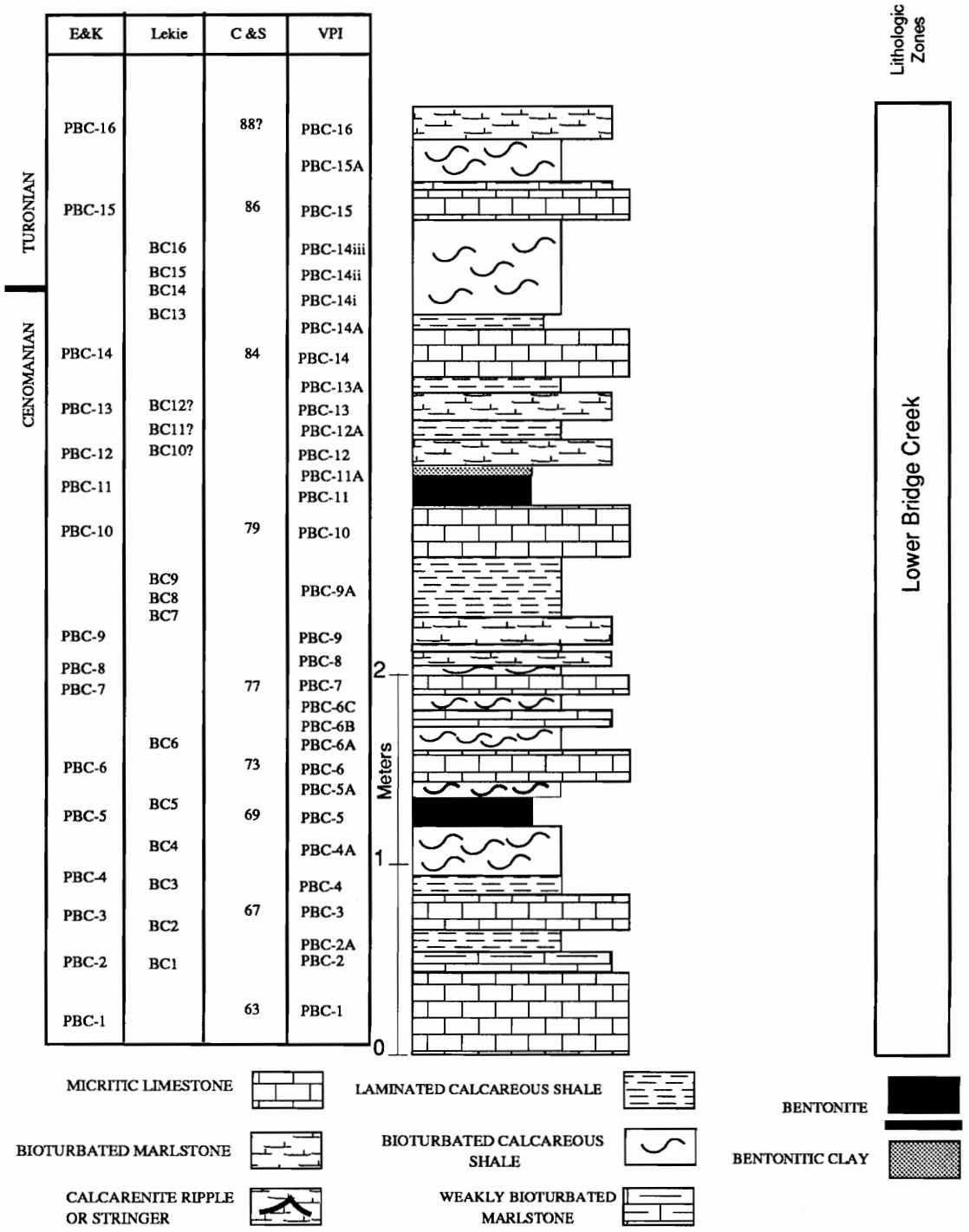

Figure 5. Stratigraphic column of the Bridge Creek at Rock Canyon (After Elder and Kirkland, 1985). Bed designations: E&K= Elder and Kirkland (1985), C&S= Cobban and Scott (1972), Leckie= Leckie (1985), VPI= this study

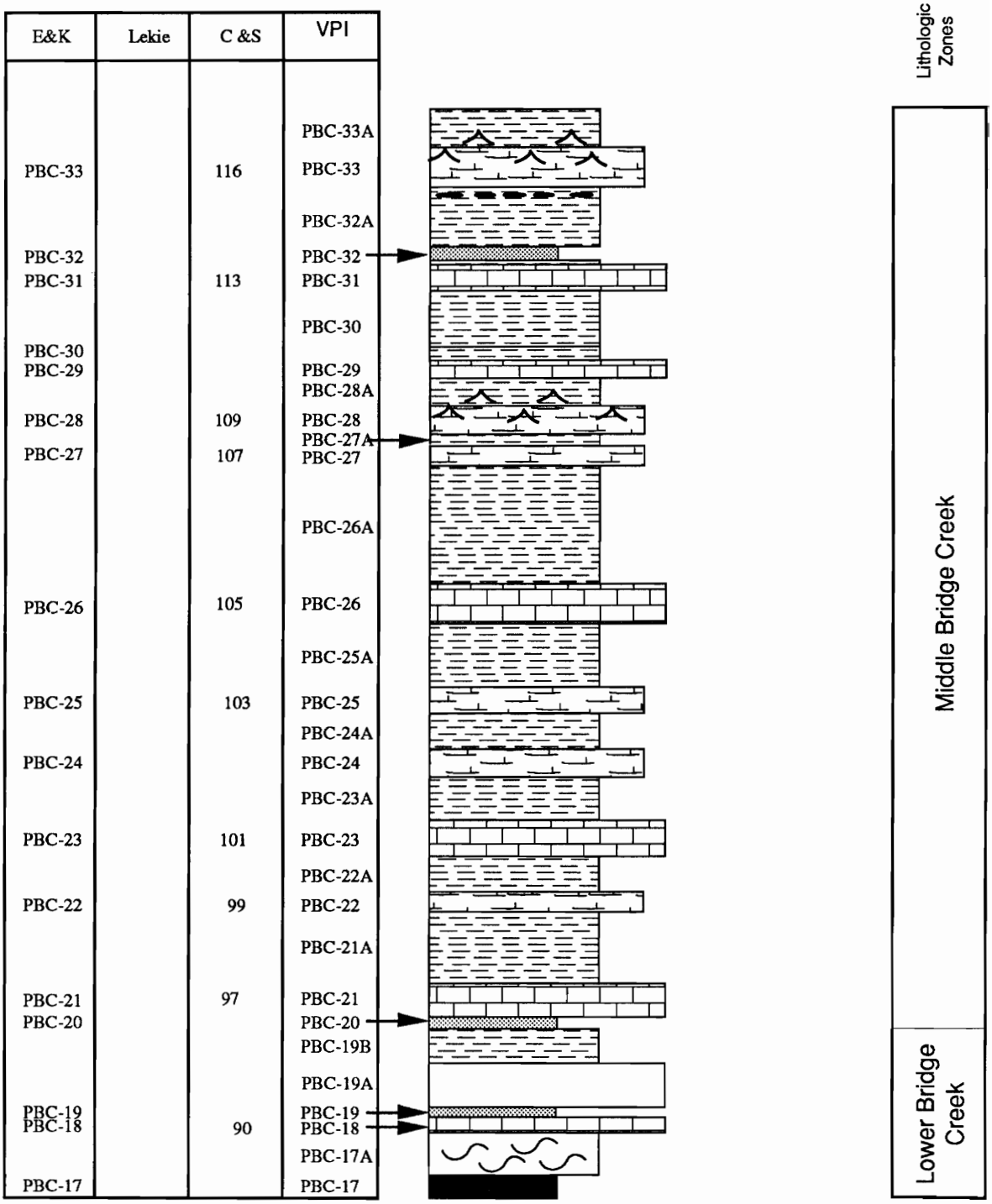

Figure 5, Continued. The middle Bridge Creek.

E&K	Lekie	C &S	VPI
PBC-40		124	PBC-40
			PBC-39A
PBC-39		122	PBC-39
PBC-38			PBC-38
PBC-37			PBC-37
			PBC-36A
PBC-36			PBC-36
			PBC-35A
PBC-35		120	PBC-35
			PBC-34A
PBC-34		118	PBC-34

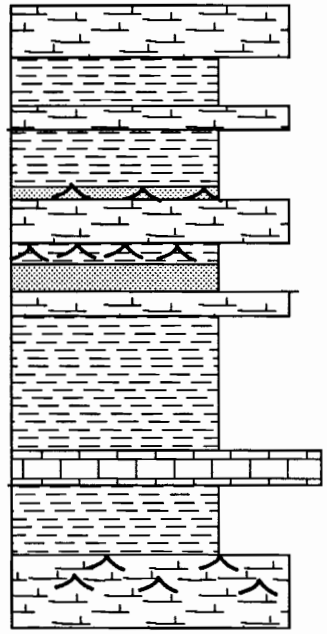

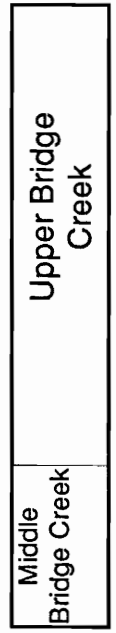

Figure 5, Continued. The upper Bridge Creek.

bioturbated, micritic limestone beds that alternate with 30 to 100 cm thick calcareous, organic-rich shale beds. The lower Bridge Creek was deposited during a time of sea-level rise and reduced terrigenous input, relative to the underlying Graneros Shale (Elder and Kirkland, 1985).

The middle Bridge Creek correlates with the Jetmore Member in central Kansas (Figure 4). This interval begins at the base of limestone bed PBC-21 and ends at limestone bed PBC-35 (approximately 4.4 meters of section at the Pueblo locality). The middle Bridge Creek is composed of 10 to 20 cm thick micritic limestone beds interbedded with 30-50 cm thick calcareous, organic-rich shale beds. It was deposited during maximum transgression of the seaway at a time when oxygen and salinity concentrations were equal to the open ocean (Elder and Kirkland, 1985).

The upper Bridge Creek is correlative with the Pfeifer Member in central Kansas (Figure 4). This interval begins at the base of shale bed PBC-35A and ends at the Bridge Creek/Carlile Shale contact, PBC-53 (about 3.5 meters of section in the Pueblo area). The upper Bridge Creek is characterized by 20-30 cm thick organic-rich shale beds interbedded with 7-15 cm thick marlstone beds and 1-6 cm thick calcarenite beds. Elder and Kirkland (1985) interpreted the absence of limestone beds and the presence of calcarenite beds to represent increased bottom currents and increased terrigenous input compared to the lower and middle Bridge Creek.

Anoxia and Organic-Rich Shale Deposition

Oxygen concentration at the sediment/water interface influences the deposition of organic rich shale. When sufficient oxygen is available, organic matter is degraded before it can be stored in sediments. Under anoxic conditions, however, organic matter is stored in sediments because degradation proceeds more slowly.

Oxygenated environments can be depleted of oxygen via aerobic degradation of organic detritus because aerobic degradation consumes 138 moles of 0_2 for each mole of organic matter oxidized. If the rate of aerobic degradation exceeds the delivery of dissolved oxygen an oxygen minimum zone develops. Organic-rich shale is deposited where the oxygen minimum zone intersects the sediment/water interface (Figure 6).

Water column stratification is often cited as the main cause of anoxia and organic-rich shale deposition. However, recent studies suggest that anoxia can be caused by high planktonic productivity and the associated settling of organic detritus to the sea floor (Southam et al., 1982). For example, Calvert and Price (1971) argue that sapropel formation in the Mediterranean Sea resulted from high surface water productivity. Sapropel is an unconsolidated ooze of algal remains decaying in an anaerobic environment. During the time of the last sapropel formation (8,000 to 12,000 years ago), flow from the Nile River into the Mediterranean was much greater than today because of increased rainfall over equatorial Africa. Nutrients transported by the Nile River to the Mediterranean resulted in a Mediterranean Sea that was more productive than today.

Sheu's (1983) study of sediments of the Orca Basin, a hypersaline, anoxic basin in the northern Gulf of Mexico, suggested that high surface water productivity produced the high percentage of organic carbon in the sediments.

In addition, Calvert and Price (1971) cite high surface water productivity near coastal upwelling zones as the cause of anoxic sediments in Peru and Namibia.

Anoxia may not be required to preserve organic-rich sediments. In the Gulf of California, the weight percent of organic carbon in sediments deposited under anaerobic conditions is indistinguishable from the weight percent of organic carbon in sediments deposited under aerobic conditions (Figure 7). In this example, benthic oxygen concentration does not affect the weight percent of organic carbon in sediments.

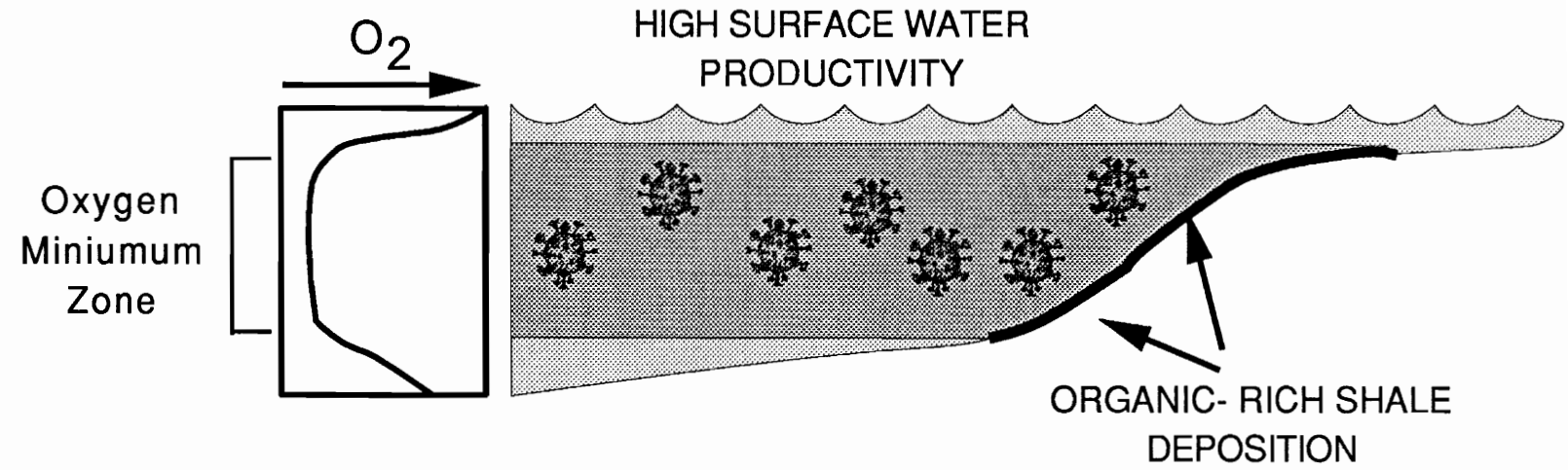

Figure 6. Oxygen minimum layer resulting from the consumption of oxygen by oxidation of organic matter. Where the oxygen minimum layer intersects the sediment/water interface, organic rich sediments are preserved.

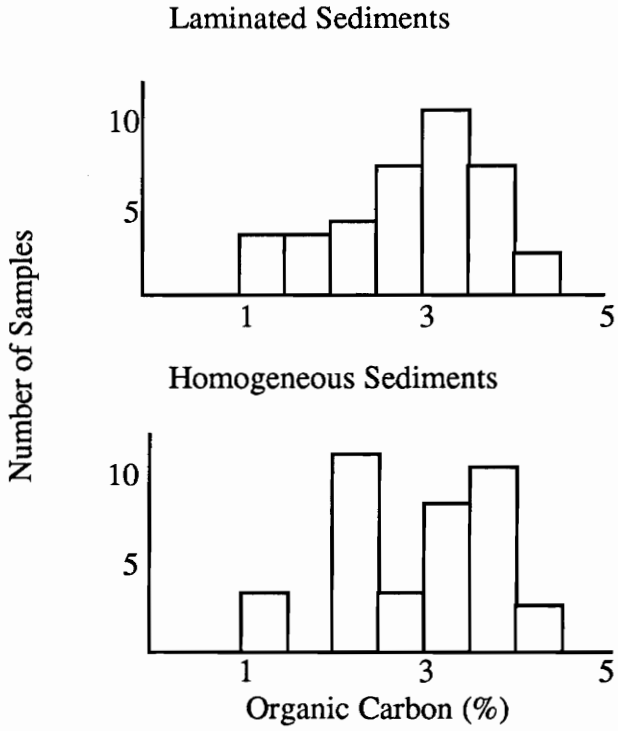

Figure 7. Organic carbon (% dry weight) content of homogeneous and laminated sediments from the Gulf of California (From Calvert 1987). The histograms show that the percent of organic carbon is the same in anaerobic sediments and aerobic sediments.

Anaerobic degradation is another important aspect of organic carbon preservation. Under anaerobic conditions, denitrification ($2.5C_{organic} + 2NO_3^- + 2H^+ = N_2 + 2.5CO_2 + H_2O$), and sulfate reduction ($SO_4^{2-} + 2C_{organic} + 2H_2O = H_2S + 2HCO_3^-$) break down organic matter.

The role of sulfate reducing bacteria in anaerobic decay may be underestimated. Calvert (1987) and Jørgensen (1982) showed that anaerobic sulfate reduction and aerobic oxidation can be equally effective at breaking down organic matter.

That significant decay of organic matter takes place in anaerobic conditions below the sediment surface was shown by Murray et al. (1978) and Martens and Klump (1984). Their studies found that the concentration of organic carbon in sediments decreases exponentially with depth.

Sedimentation rate is another important factor in organic carbon preservation. In the modern Pacific Ocean, surface sediments consisting of greater than 0.5 weight-percent organic carbon are limited to areas of high planktonic productivity and high sedimentation rates, such as continental shelves and the Arafura Sea (Figure 8). Müller and Suess (1979) showed that there is a strong correlation between the accumulation of organic carbon and sedimentation rate when normalized to surface water productivity.

To summarize, organic-rich sediments are deposited at times when the amount of organic matter settling through the water column exceeds the rate of aerobic and anaerobic degradation. This occurs when planktonic productivity is high, or when the oxygen delivery to the sea floor is low. Rapid burial of organic matter facilitates the preservation of organic-rich sediments.

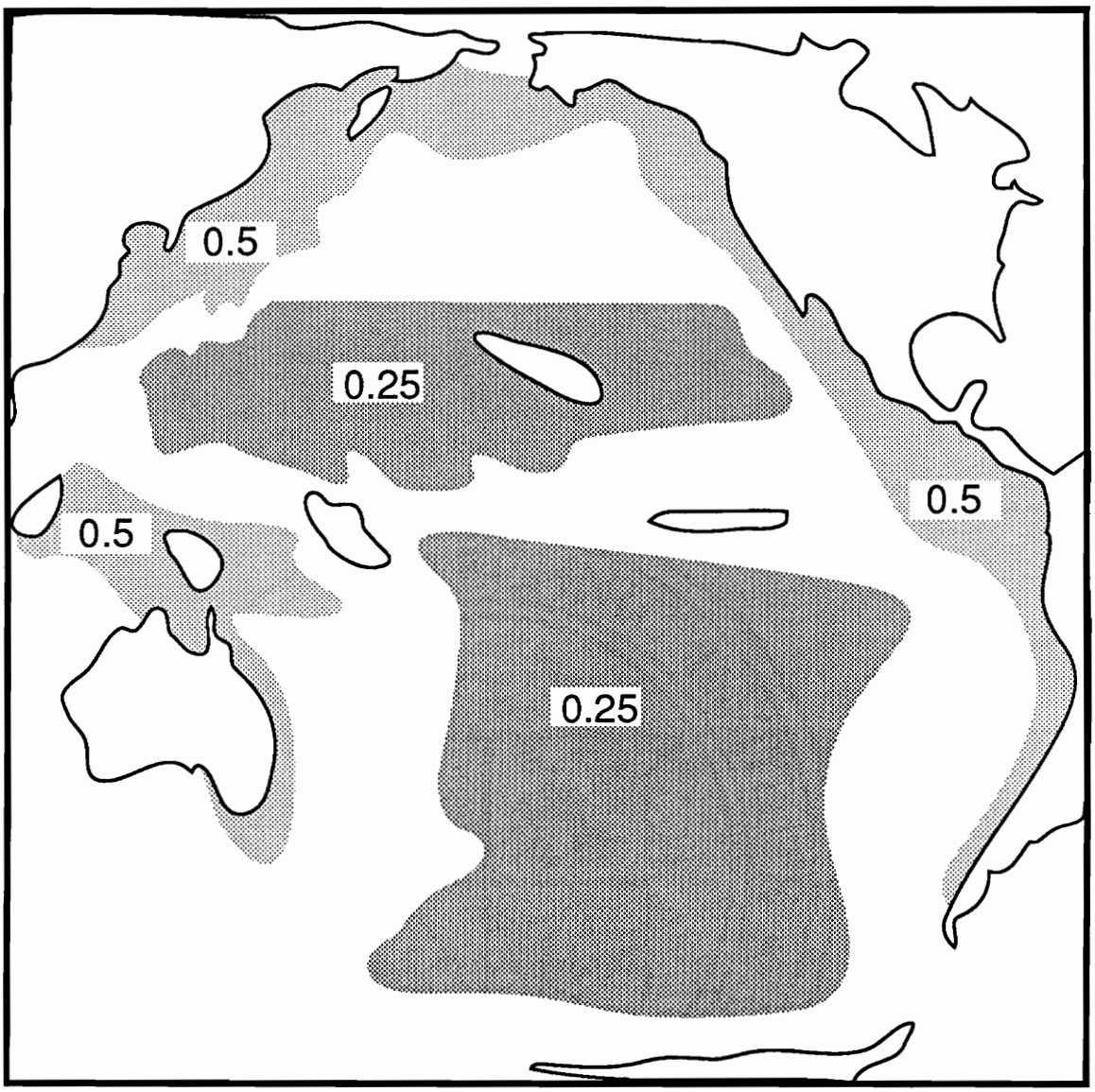

Figure 8. Distribution of organic carbon (% dry weight) in Pacific Ocean surface sediments (From Calvert, 1987). Sediments with greater organic carbon content occur in areas of high productivity.

Milankovitch Cycles and Climate

Four of the earth's orbital characteristics, eccentricity, obliquity, axial precession, and the precession of the equinoxes, are not fixed but change cyclically. These astronomical cycles are termed Milankovitch cycles after the Serbian mathematician, Milutin Milankovitch. The existence of Milankovitch cycles has been known for centuries–the ancient Greeks knew about axial precession (Ferris, 1989). How these cycles affect earth's climate was not known until Croll's work in the late 1800's (Croll, 1875). He stated that, although changes in the earth's orbital parameters are not sufficient to directly alter climate, they might trigger a series of events which do affect earth's climate.

In the early 1900's, Milankovitch, seeking to explain the occurrence and regular recurrence of ice-ages, mathematically demonstrated that changes in the earth's orbital parameters influence the amount of solar radiation striking the earth at different times of the year. These changes, he stated, drive the ice ages. While Milankovitch forcing can trigger climatic change, its effect on climate occurs through atmospheric and oceanic feedback systems (Croll, 1875).

The remainder of this section is a discussion of each orbital cycle. Although these cycles constructively and destructively interfere with one another, each cycle is discussed independently of the others for clarity.

The Eccentricity Cycle

The eccentricity cycle is a change in the ellipticity of the earth's orbit that affects the annual heat budget of the entire planet (Figure 9). The length of the semi-major axis of the earth's orbit fluctuates with an average quasi-period of 95ky. The eccentricity value is calculated as follows.

$$e = \frac{\sqrt{a^2 - b^2}}{a}$$

Where: a = the length of the semi-major axis of the ellipse, and
b = the length of the semi-minor axis of the ellipse.

The eccentricity value ranges from 0.005 to 0.0607, and is currently 0.0167 (Berger, 1980).

At maximum ellipticity, the earth receives maximum solar radiation when the earth is closest to the sun (perihelion) and minimum solar radiation when the earth is farthest from the sun (aphelion). At minimum ellipticity, the earth receives about the same intensity of solar radiation throughout the year because the difference between aphelion and perihelion is at a minimum.

The strength of the eccentricity cycle is insufficient to directly influence earth's climate. However, the cycle is expressed in the geological record through climatic feedback (Croll, 1875; Einsele and Ricken, 1991; Hays, et al., 1976. The Pennsylvanian Cyclothems of middle North America and the eustatic sea-level fluctuations of the Pleistocene (Mesolella, et al., 1969) apear to be the result of eccentricity-cycle forcing.

The Obliquity Cycle

Obliquity refers to the angle between the earth's axis and a line perpendicular to the ecliptic (Figure 10). The obliquity cycle effects seasonal intensity by varying insolation distribution across the northern and southern hemispheres. Maximum northern hemisphere insolation (boreal summer) occurs when the northern hemisphere is tilted toward the sun and minimum insolation occurs when the hemisphere is tilted away from the sun. As obliquity increases, seasonal intensity also increases. If the obliquity was zero, seasons

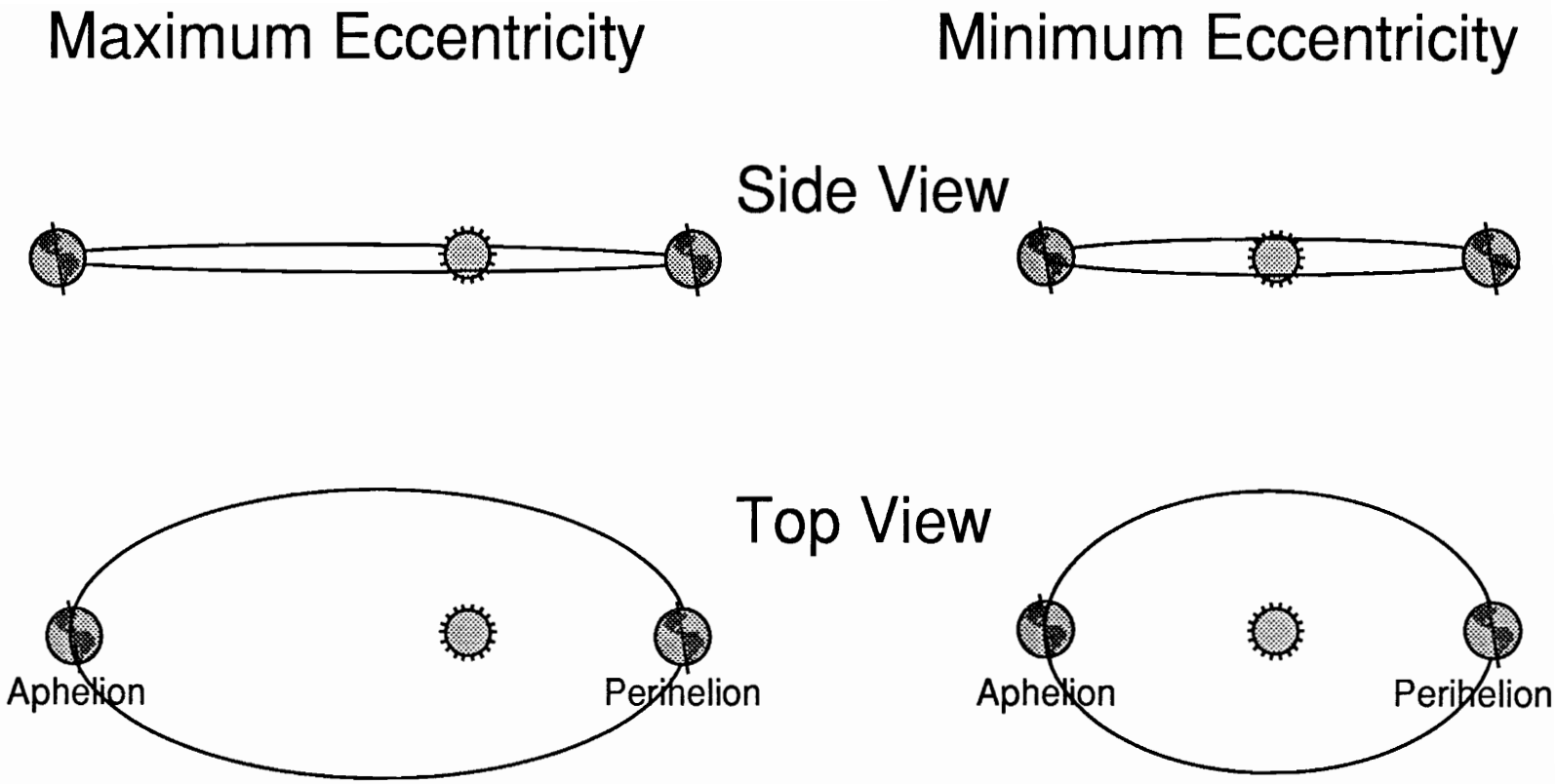

Figure 9. The 100 Ky Milanovitch Eccentricity Cycle. The shape of the earth's orbit changes from elliptical (maximum eccentricity) to more circular (minimum eccentricity).

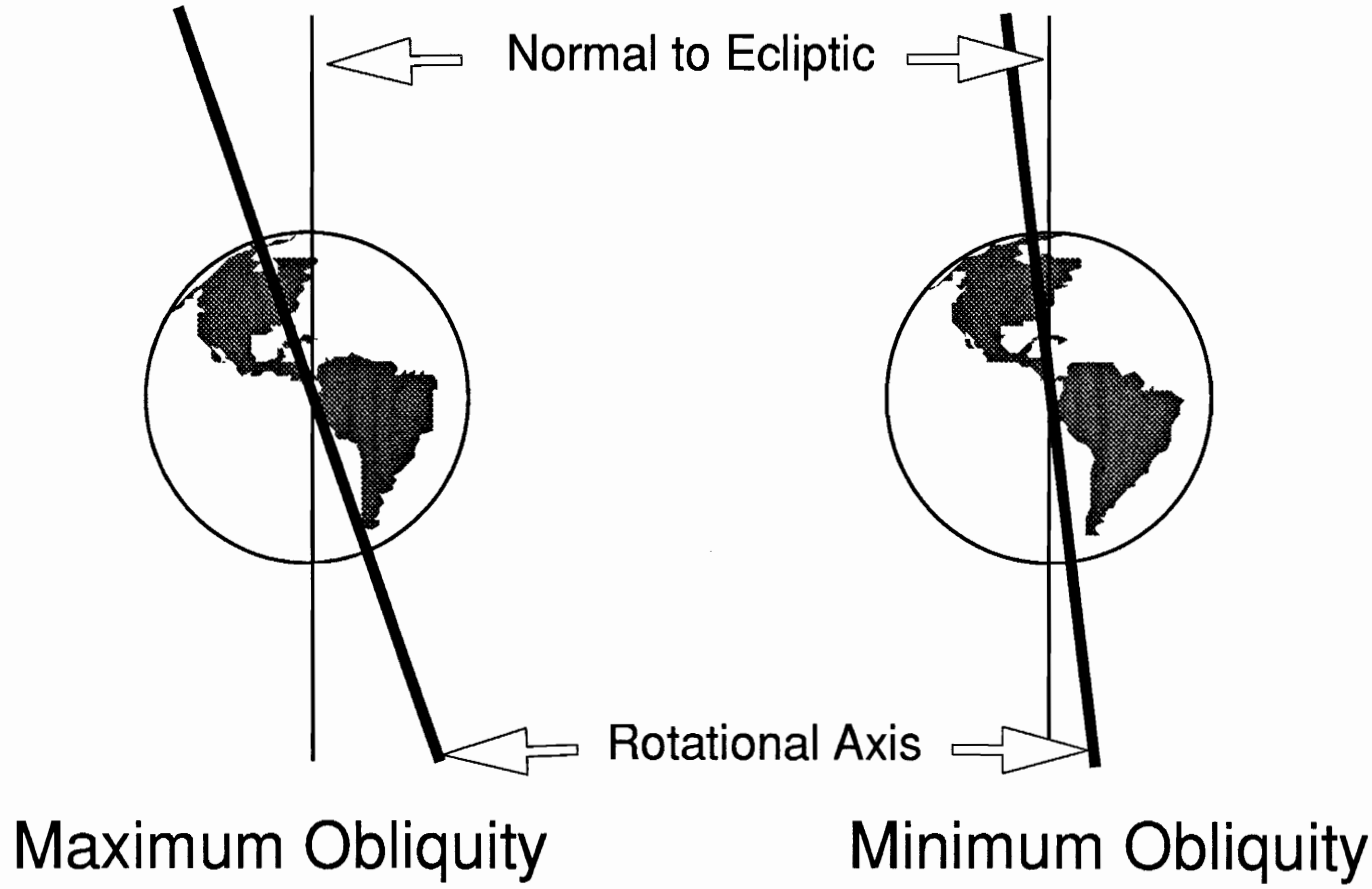

Figure 10. The 40 Ky Obliquity Cycle. The tilt of the earths axis with respect to the ecliptic changes.

would not exist. The obliquity varies from 22°2' to 24°27' (the current value is 23°27') with a quasi-period of 41ky (Berger, 1980).

Axial Precession and Precession of the Equinoxes

The torque created by the rotating earth is continually changing the orientation of the earth's axis. The cyclic gyration of the axis, called axial precessesion, has an average quasi-period of 25,700 years (Figure 11). Axial precession influences earth's climate through the fourth cycle, precession of the equinoxes (Figure 11). The 21 ky quasi-period of this cycle is a consequence of the 25,700 ky axial precession quasi-period and the clockwise movement of perihelion (Berger, 1980).

The precessional cycles influence season intensity by shifting the position of boreal summer with respect to perihelion (Figure 11). For example, if boreal summer coincides with perihelion, the seasons are intensified, and if boreal summer coincides with aphelion, the seasons are attenuated.

Milankovitch Cycles in the Geologic Record

Milankovitch Cycles are expressed in the geologic record as stable isotope cycles, sedimentary cycles, and eustatic sea-level oscillations.

Stable Isotope Cycles

The ratio of ^{16}O to ^{18}O in sea water varies as a function of global ice volume (Shackleton, 1967). Because light oxygen, ^{16}O, is preferentially evaporated from sea water and stored in glaciers and ice caps, sea water becomes relatively enriched in ^{18}O when global ice volume is high. The carbonate skeletons of marine organisms record the $^{16}O/^{18}O$ ratio of the sea water in which they were secreted.

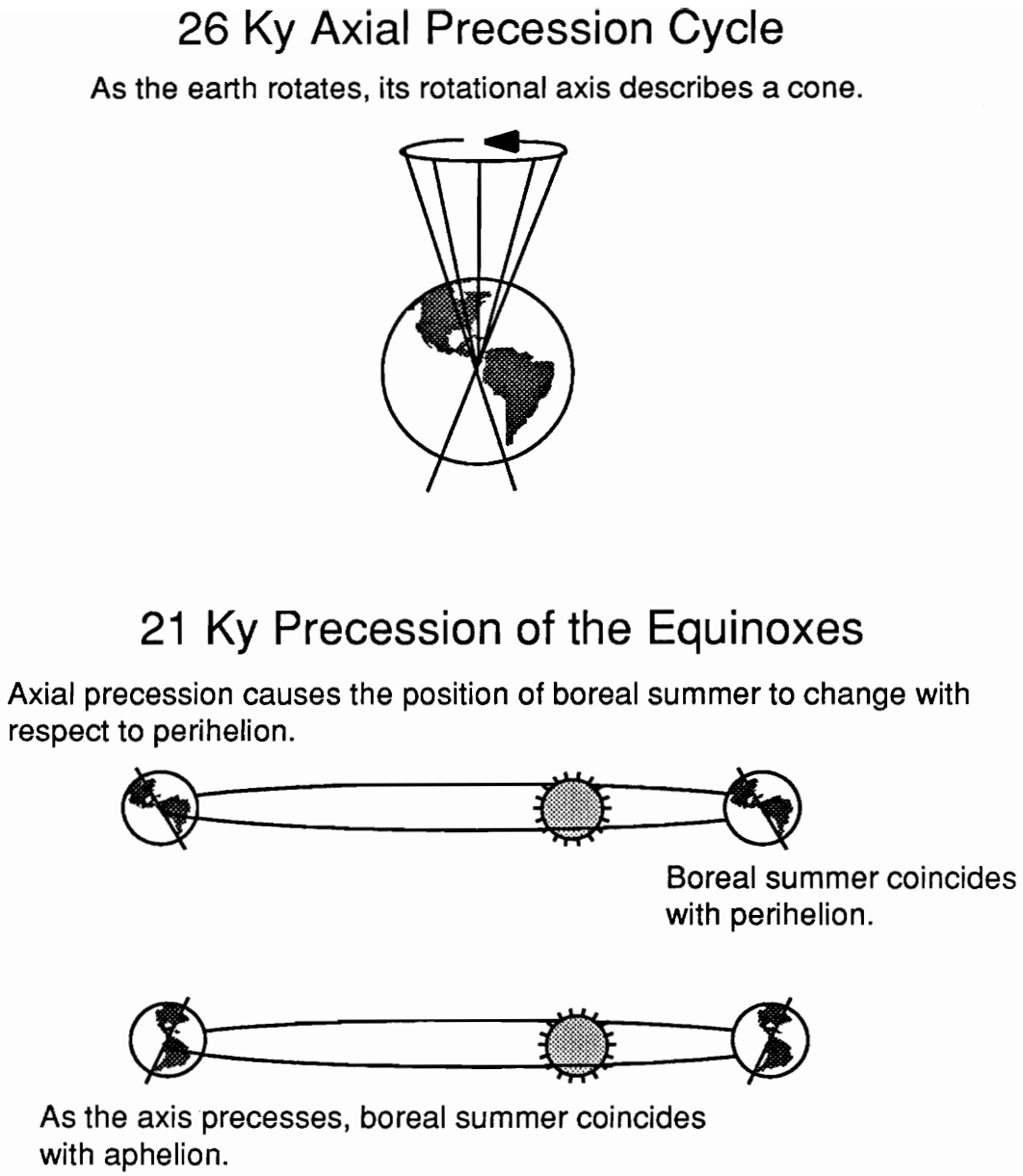

Figure 11. The 26 ky Axial Precession Cycle (top) causes the position of boreal summer to move with respect to perihelion (bottom). The different cycle periods are due to the clockwise movement of perihelion.

Oxygen isotopes were used in the first study linking Milankovitch cycles to sedimentary cycles. Hays et al. (1976) studied the $\delta^{18}0$ record in two deep sea cores from the southern Indian Ocean. The $\delta^{18}0$ values were obtained from tests of the planktonic foraminifera *Globegerina bulloides* and converted into a time series for spectral analysis. The $\delta^{18}0$ cycles in the cores correspond to the Milankovitch precession, obliquity, and eccentricity cycles.

Sedimentary Cycles

Lime-shale cycles resembling those of the Bridge Creek, may be produced by Milankovitch forcing. Einsele (1982) proposed three mechanisms for producing lime-shale cycles: productivity cycles, dilution cycles, and dissolution cycles. A discussion of each follows.

Productivity Cycles

In the productivity cycle, the input of terrestrial material remains constant relative to planktonic carbonate production. Limestone is deposited when CO_3 productivity is high, and shale is deposited when productivity is low. Einsele and Ricken, 1991 estimate that a five to ten-fold increase in carbonate production is necessary to produce the thick-limestone/thin-shale couplets produced by the productivity cycle.

Thunell et al. (1991) suggested that productivity cycles produced the lime-shale couplets preserved in Pleistocene strata of Southern Italy. They concluded that nutrient rich bottom water carried to the surface by periodic upwelling stimulated carbonate production.

Dilution Cycles

Dilution cycles form via fluctuating terrigineous input, and constant planktonic carbonate production. Assuming the time of deposition is the same for limestone and shale, the greater sedimentation rate during shale deposition (planktonic carbonate plus increased terrigineous input) produces thick shale units and thin limestone units.

Cycles in the Cretaceous Lower Chalk of southeastern England are attributed to the dilution model by Arthur et al. (1986) who based their conclusion on decreased calcisphere abundance and increased insoluble residue and organic carbon in the shale units.

Dissolution Cycles

Dissolution cycles occur when the carbonate dissolution rate fluctuates while clastic input remains constant. The dissolution model produces thick limestone units and thin shale units. Cycles formed by this model resemble those formed by the productivity model (Einsele, 1982).

This model may be linked to the productivity model via fluctuations in the lysocline depth and carbonate compensation depth (CCD). When carbonate productivity is high, the increased flux of biogenic carbonate to the sea floor depresses the CCD thereby reducing the carbonate dissolution rate.

An example of dissolution cycles occurs in the Cretaceous of the Swiss Alps in which water-temperature fluctuations, driven by climate change, are cited as the mechanism driving the depositional cycles (Brückner, 1953).

Eustatic Sea-Level Fluctuations

Eustatic sea-level fluctuations are governed by global ice volume. When Milankovitch forcing cools the earth, global ice volume increases and sea level drops.

Milankovitch forced sea-level oscillations are evident in sea-level fluctuations during the Pleistocene (Mesollela et al., 1969), in the Devonian (Goodwin and Anderson, 1985), and in the Cambrian (Koerschner and Read, 1989).

METHODS

Four categories of methods were used in this investigation: rock sample collection, sample preparation, compilation of palynological data, and calculation of weight percent carbonate data.

Rock Sample Collection

Rock samples were collected from outcrops eight kilometers west of Pueblo, Colorado, in the Pueblo County Reservoir State Recreation Area (Figure 2). The Bridge Creek Member is exposed where the Arkansas River has eroded into the Rock Canyon Anticline (Plates 1 and 2).

The outrcrop and collecting implements were cleaned to prevent contamination between samples. Samples were double bagged and labeled.

Sample Preparation

Palynomorphs were recovered using standard palynological maceration techniques as outlined below:

1. About 60 grams of rock were crushed into pellet sized pieces and digested in concentrated hydrochloric acid (HCL) for 24 hours and in concentrated hydrofluoric acid (HF) for 24 hours.
2. Samples were next treated with sodium hypochlorite (NaClO), acidified by a few drops of concentrated HCl, to remove partially oxidized organic material and by dilute Ammonium Hydroxide (NH_4OH) to further oxidize unwanted organic material, and to dissolve products of the NaClO treatment.
3. At this stage both palynomorphs and mineral grains remain. To separate out the palynomorphs from the mineral residue, both were placed in a zinc

bromide ($ZnBr_2$) solution of specific gravity 2.0 and centrifuged for 30 minutes. The palynomorphs floated and were decanted into test tubes and rinsed to remove the $ZnBr_2$.

4. Clay sized particles were removed via sieving with a 20μm sieve and/or differential centrifugation.
5. Palynomorphs were darkened for microscopic examination by acetolization in a 10:1 mixture of acetic anhydride and sulfuric acid (H_2SO_4). Test tubes containing the organic residue and the acetolization mixture were placed in a boiling water bath for 20-30 minutes and then rinsed to neutrality.
6. Strewn mounts of the surviving residue were made using a glycerin jelly mounting medium and 22 mm X 22 mm cover slips of #0 thickness. The slides were sealed with clear enamel.

Compilation of Palynological Data

Specimens counts were made by traversing the slide from west to east. A total of 4,225 dinoflagellate, acritarch, and chlorophyte cysts representing 64 taxa were identified from 24 samples.

Poor and inconsistent preservation made reliable identification of many taxa uncertain to impossible in which case palynomorphs were assigned arbitrary letter designations. Justification for this classification is three fold: (1) this is not a taxonomic study, (2) any classification scheme is a form classification to some extent since a single thecate form may produce many types of cysts, (3) finding several hundred adequately preserved specimens per sample was not possible.

Calculation of Weight Percent Carbonate

Weight percent carbonate was measured by the following process in which triplicate verification runs indicate an error of ± 2%.

1. Four to six grams of rock were crushed to a powder and placed in a pre-weighed cup.
2. After the sample weight was determined, the sample was placed in concentrated HCl either for 24 hours or until addition of HCl no longer produced a reaction.
3. Samples were then washed to neutrality, dried, and weighed to determine the percentage of material dissolved.

PROJECT RESULTS AND DISCUSSION

The results of this investigation are presented in four parts: Lithologic Cycles, Biostratigraphy, Milankovitch Cycle/Phytoplankton Productivity Link, and Correlation Using Phytoplankton Assemblages. The Lithologic Cycles section includes information on both the history of Bridge Creek study and the results of spectral analysis performed during this investigation.

Lithologic Cycles

Gilbert (1895) recognized that the lime-shale couplets in the Bridge Creek may have been produced by orbitally-driven climate changes. He stated that humid/arid climate cycles generated the Bridge Creek rock cycles by the following mechanism. During humid periods, flourishing land vegetation produced organic acids that increased limestone dissolution on land. The dissolved limestone was transported to the seaway where it was deposited as the limestone beds of the Bridge Creek. During arid periods, shale was deposited because the flow of dissolved limestone to the seaway lessened as land vegetation withered and organic acid production decreased.

Gilbert was aware of three orbital cycles: the annual cycle, the eccentricity cycle, and the precessional cycle. Of these, he favored the precessional cycle as driving the Bridge Creek rock cycles. A century later, however, Gilbert's proposal remains controversial.

Time Series Analysis

The first step in searching for a link between Milankovitch Cycles and phytoplankton assemblages was to determine if the Bridge Creek lime-shale alternations are periodic cycles or random alternations. The lime-shale alternations appear regular upon

initial inspection of the outcrop (Plates 1 and 2), but consider the following example. Flip a coin 50 times in succession. If the coin lands heads up, a 10 cm thick layer of limestone is deposited, and if the coin lands tails up, a 10 cm thick shale layer is deposited. After 50 flips, lime-shale cycles of various thickness result. To see if the Bridge Creek cycles are random alternations spectral analysis was used.

Spectral analysis is a statistical technique that analyzes time series data (data collected through time). Time series data are composed of three parts: trend, cycles, and a random component. Trend is defined as a long-term increase or decrease, cycles are the hidden periodicity that spectral analysis defines using sine and cosine terms, and the random component consists of irregular fluctuations resulting from experimental error or confounding variables.

The use of spectral analysis in stratigraphy assumes that each rock type accumulated at a constant rate, even though different rock types need not accumulate at the same rate. This assumption is generally considered valid for pelagic sediments and there is no evidence that the Bridge Creek violates the assumption.

The data used for this spectral analysis are code numbers that represent lithology. To create the data set, a 12 meter section of the Bridge Creek was sampled at 8 cm intervals (Figure 12). At each sampling point the rock type was recorded. The 8 cm sampling interval sampled each bed at least once (excepting bentonite beds less than 2 cm thick), and thicker units more than once. This method produced a data set that accounts for both lithology and bed thickness.

The spectral analysis results are shown on a spectrogram with cycle frequency on the X-axis and spectral density on the Y-axis (Figure 13). Peaks on the spectrogram show the strength of a frequency. Note the strong spectral peak on Figure 13 at a frequency of 0.183 cycles per observation. This indicates that the lime-shale alternations are not random, but exhibit cyclicity with a dominant frequency of one cycle every 42 cm.

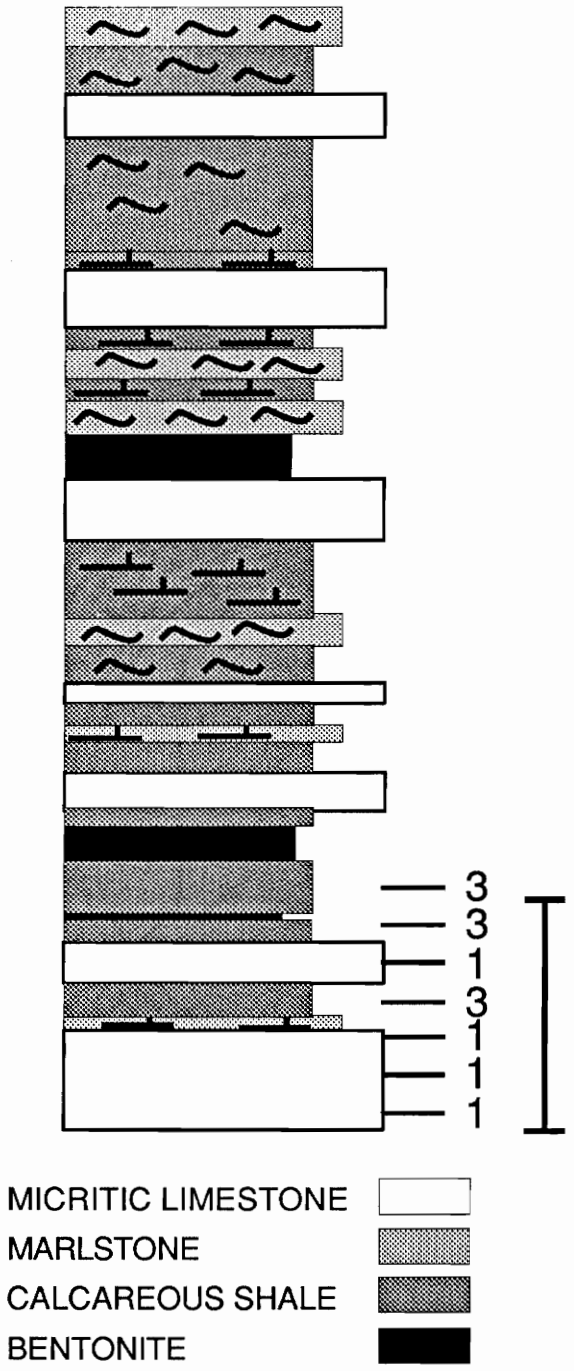

Figure 12. Sampling Scheme for Spectral Analysis. Each sample was assigned a code number to represent lithology. Scale bar equals one meter. Sample points are not to scale.

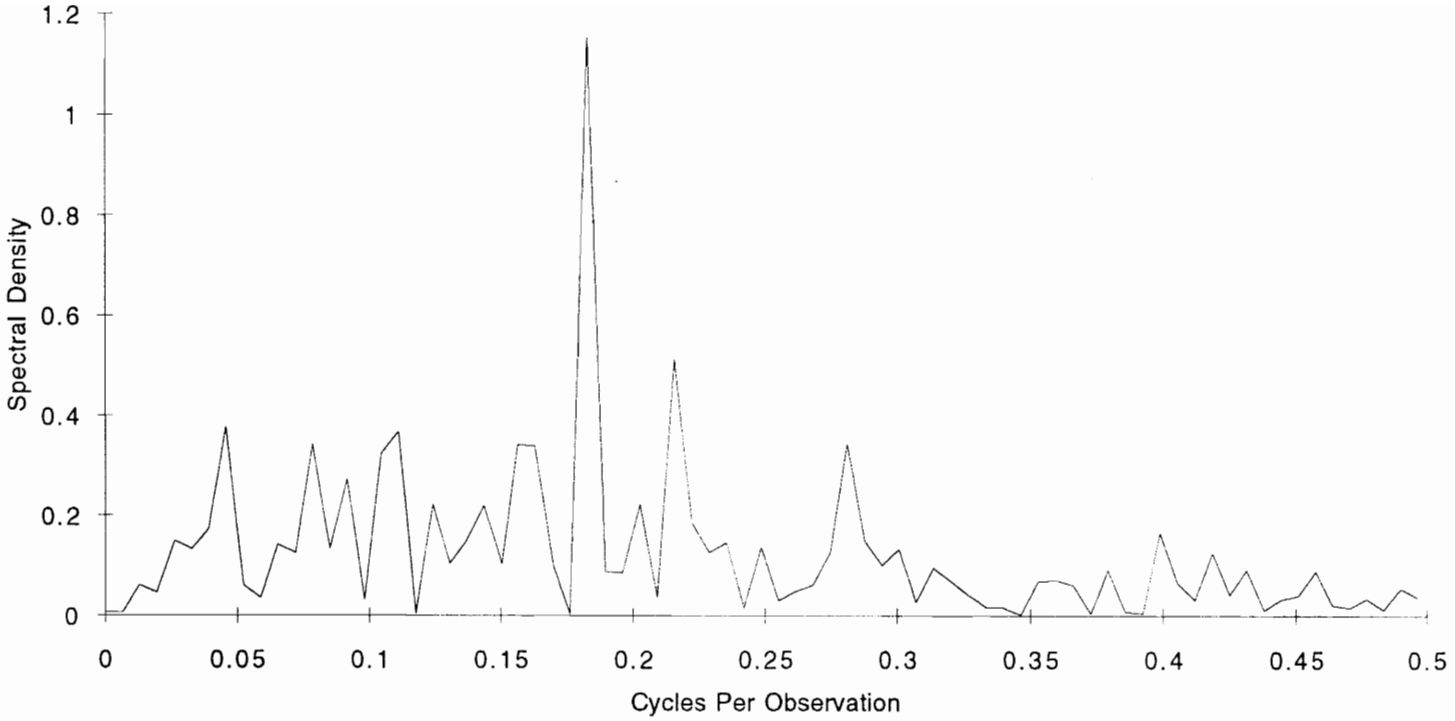

Figure 13. Spectrogram produced by spectral analysis when all lithologies are considered.

To ensure that the observed spectral peak was not an artifact of the arbitrary codes used to represent lithology, the analysis was performed two additional times, once coding limestone data points as 1 and others as 0, and once coding shale data points as 1 and others as 0. This would allow the contribution of each lithology to the overall spectral peak to be independently evaluated. An overlay of these two plots on the original spectrogram shows that a shale peak and a limestone peak correspond with the overall spectral peak (Figure 14). Based on this analysis, the dominant cycle frequency of one cycle per 42 cm seems to accurately represents the Bridge Creek cycles.

The stratigraphic cycles identified by spectral analysis can be converted to time by using sedimentation rate. The average rate of Bridge Creek accumulation is estimated to be between 0.5 and 1.0 cm/ky (Elder, 1985). Using the faster rate, the cycle period identified by the spectral analysis correlates with the 41 ky Milankovitch obliquity cycle. This interpretation agrees with Fischer et al. (1985) and Barron et al. (1985). If different decompaction curves and other plausible sedimentation rates are considered, however, the true period may range from less than 20 ky to more than 80 ky.

Biostratigraphy

This section integrates the palynological data collected during this study with other biostratigraphical data.

Macrofaunal Biostratigraphy

The Bridge Creek has been biostratigraphically zoned via different fossil groups. For this study, modified ammonite zones proposed by Cobban and Scott (1972) and bivalve biozones of Kauffman (1977) are used (Figure 15).

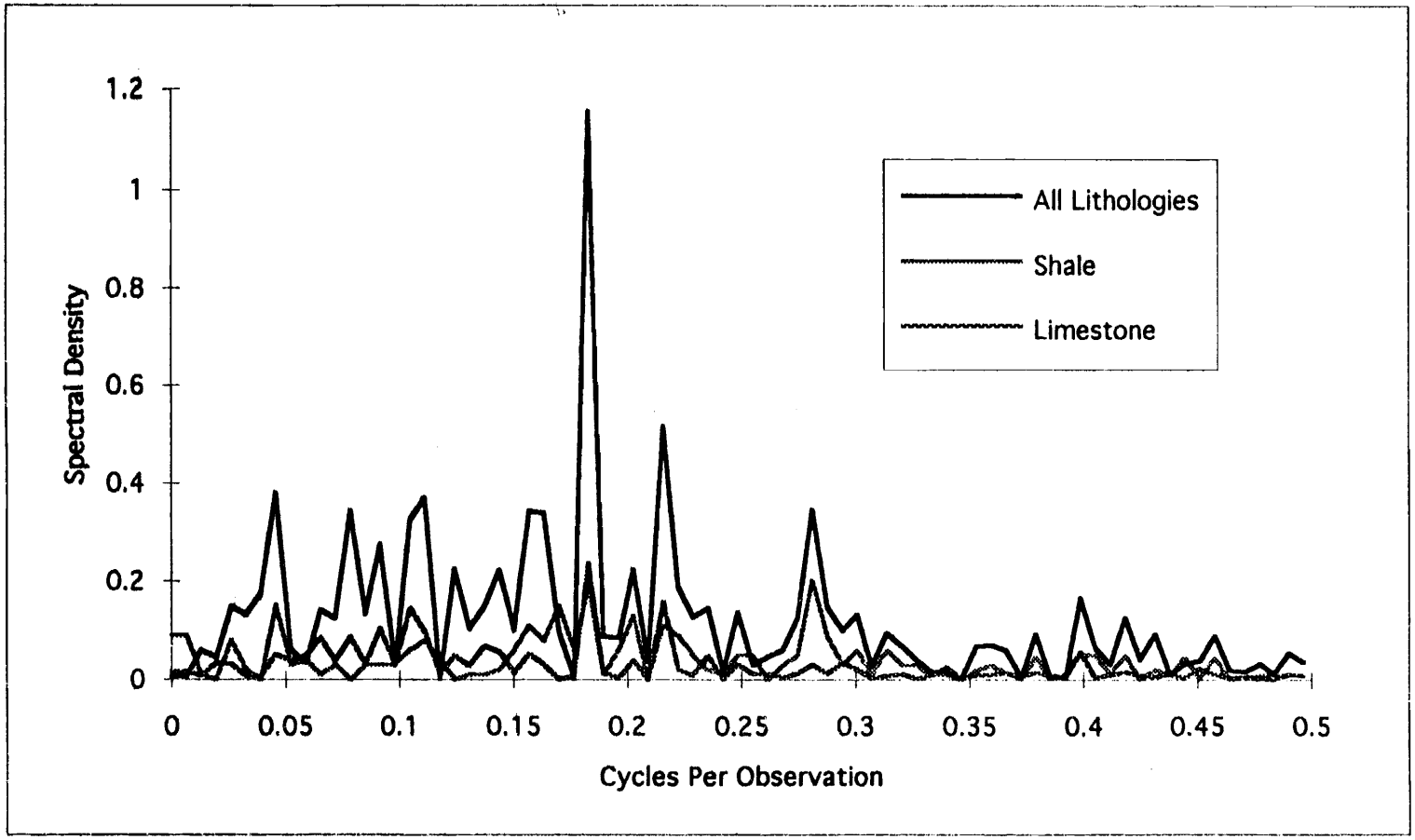

Figure 14. Spectrogram overlay comparing limestone, shale, and overall spectrograms. Note that a limestone peak and a shale peak coincide with the strong overall peak at 0.183 cycles per observation.

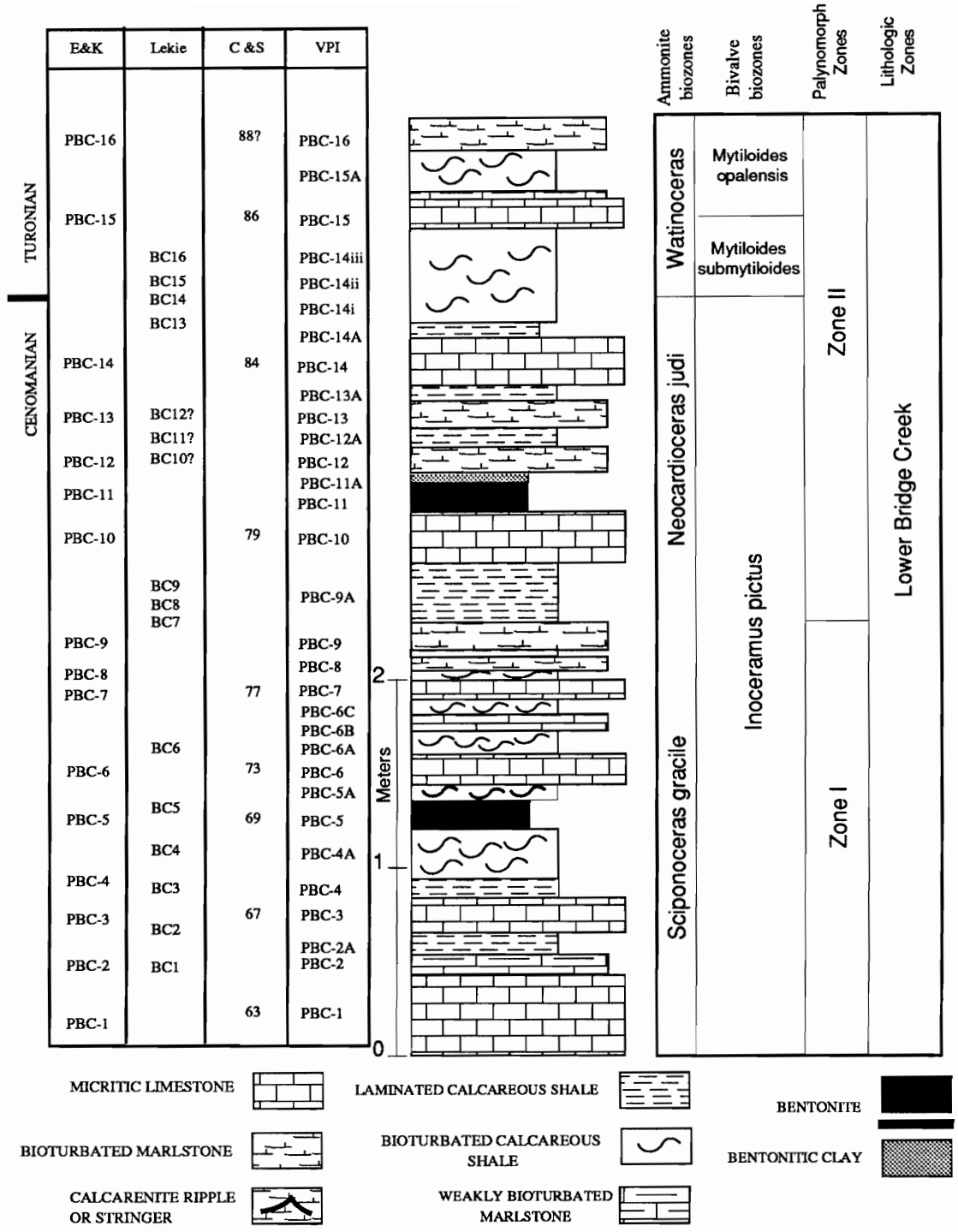

Figure 15. Stratigraphic column of the Bridge Creek at Rock Canyon (After Elder and Kirkland, 1985). Bed designations: E&K= Elder and Kirkland (1985), C&S= Cobban and Scott (1972), Leckie= Leckie (1985), VPI= this study

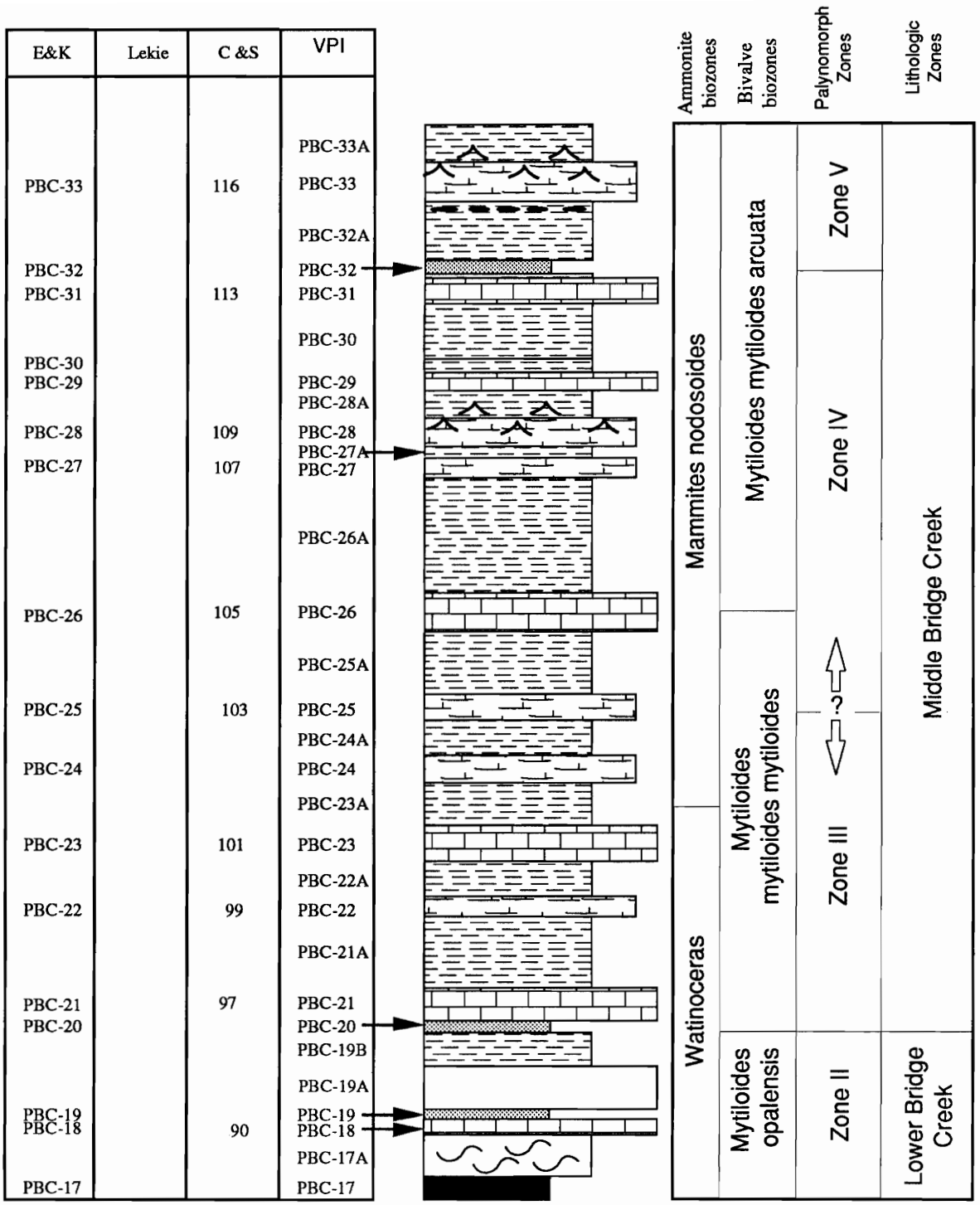

Figure 15 Continued. The middle Bridge Creek.

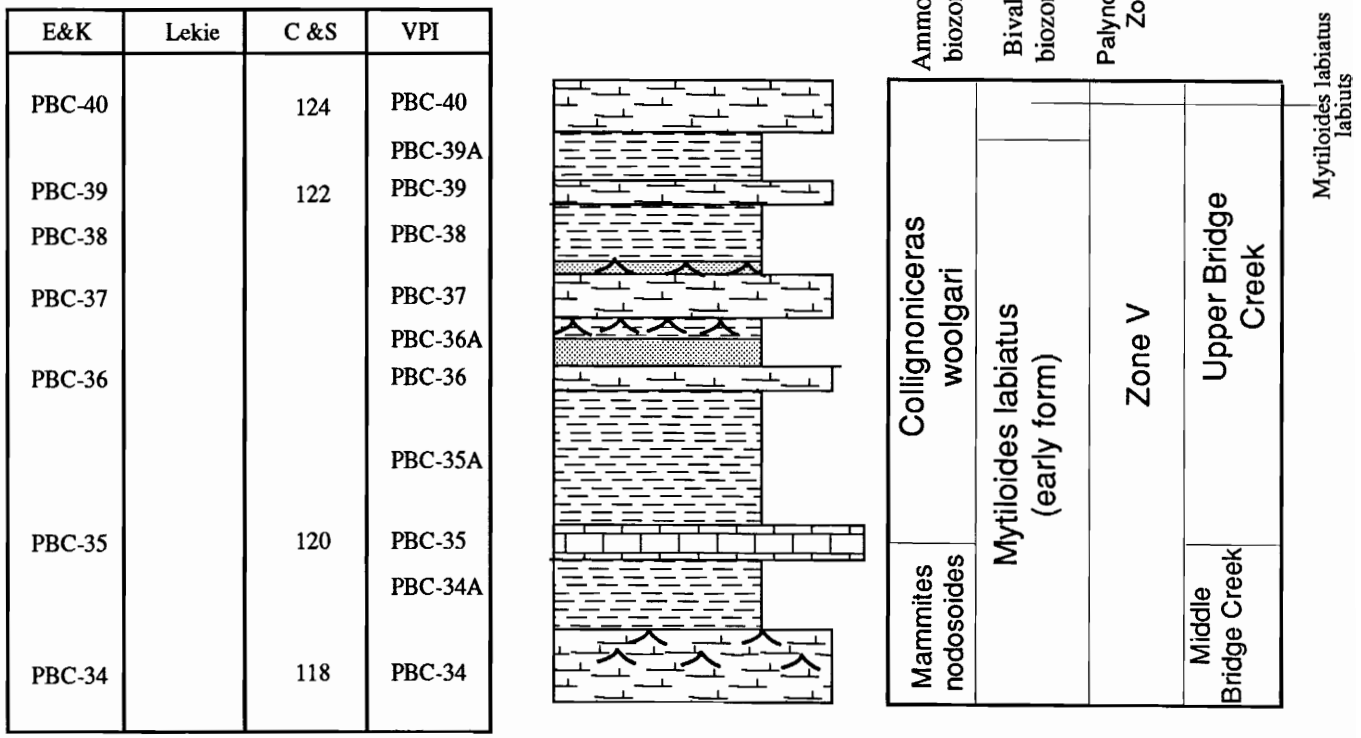

Figure 15, Continued. The upper Bridge Creek.

The Bridge Creek is divided into several ammonite biozones. The *Sciponoceras gracile* biozone extends from the base of the Bridge Creek to bed PBC-9. The *Neocardioceras juddi* biozone extents from bed PBC-9 to the Cenomanian-Turonian boundary, which occurs in bed PBC-14i. The *Watinoceras* biozone extends from the Cenomanian-Turonian boundary to bed PBC-23A. The *Mammites nodosoides* biozone begins at bed PBC-23A and ends in bed PBC-35, and the *Collignoniceras woollgari* biozone begins at bed PBC-35 and ends at the Bridge Creek/Carlile Shale contact.

Figure 15 also shows biostratigraphic zones based on bivalves. With the exception of biozone boundaries at the Cenomanian-Turonian stage boundary, the bivalve biozone boundaries do not coincide with the ammonite biozone boundaries.

Dinoflagellate Biostratigraphy

Q-mode cluster analysis was used to divide the Bridge Creek into informal dinoflagellate zones. Cluster analysis groups samples according to a similarity coefficient calculated from species abundances. Two samples containing identical species abundance distributions would group together with a similarity coefficient of one.

The first step in cluster analysis is to compare the species abundances in each sample with every other sample and then to compute a matrix of similarity coefficients. The two samples that are most similar (i.e. have the greatest similarity coefficient) form the beginning of the first cluster. An average of this cluster is then compared to the remaining samples. The ungrouped sample that is most similar to the cluster average is added to the cluster. This process continues until all the samples are placed in a group.

There are many methods to calculate similarity coefficients and to determine a cluster average for subsequent comparisons. In this analysis the Czekanowski coefficient was used. The Czekanowski coefficient is calculation as follows.

$$Coefficient = \frac{2 * W}{Sum(i) + Sum(k)}$$

Where:

sum(i) = the total number of individuals in sample "i",

sum(k) = the total number of individuals in sample "j", and

$W = \sum_{i=1}^{S}\left[\min\left(X_{ij}, X_{ik}\right)\right]$, the number of individuals of each species shared by both samples.

The correlation coefficients calculated from the dinoflagellate data were used to produce the dendrogram in Figure 16. The branch point of two samples is scaled to the correlation coefficient shown at the top of the dendrogram.

The cluster analysis was used to divide the Bridge Creek into five informal palynomorph zones as follows (see Figure 15). Zone I extends from the base of the Bridge Creek through bed PBC-9 and is dominated by *Paleohystrichosphaera infusoriodes*. The Palynomorph Zone I/II boundary coincides with a planktonic foraminifera zone boundary identified by applying cluster analysis to foraminifera data published by Leckie (1985; Leckie reported species as very rare, rare, common, and abundant; for quantitative analysis, percentages were assigned as 1, 5, 10, and 25, respectively). In Zone I, the relative percentages of the 10 overall most abundant taxa are shown on Figure 17.

Zone II ranges from bed PBC-9A through bed PBC-19A, and contains three dominant taxa: *Paleohystrichosphaera infusoriodes, Spiniferites spp.*, and *Cyclonophelum spp.*. The Palynomorph Zone II/III boundary coincides with both the Lower/Middle lithologic zone boundary and the *Mytiloides opalensis/Mytiloides mytiloides mytiloides* bivalve biozone boundary.

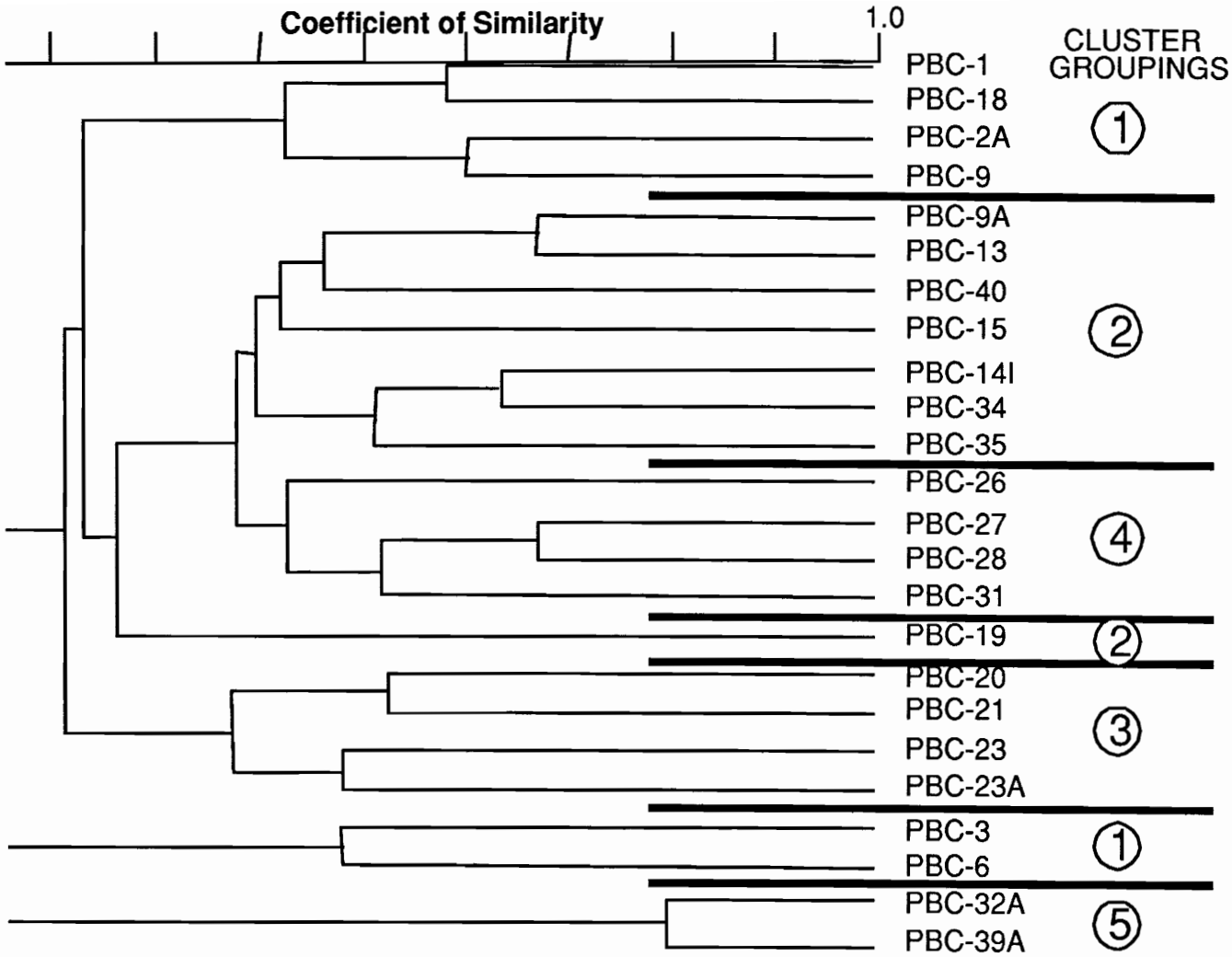

Figure 16. Q-mode cluster diagram for dinoflagellate data. The numbers on the right are the Bridge Creek Dinoflagllate Zones as determined by the cluster groupings.

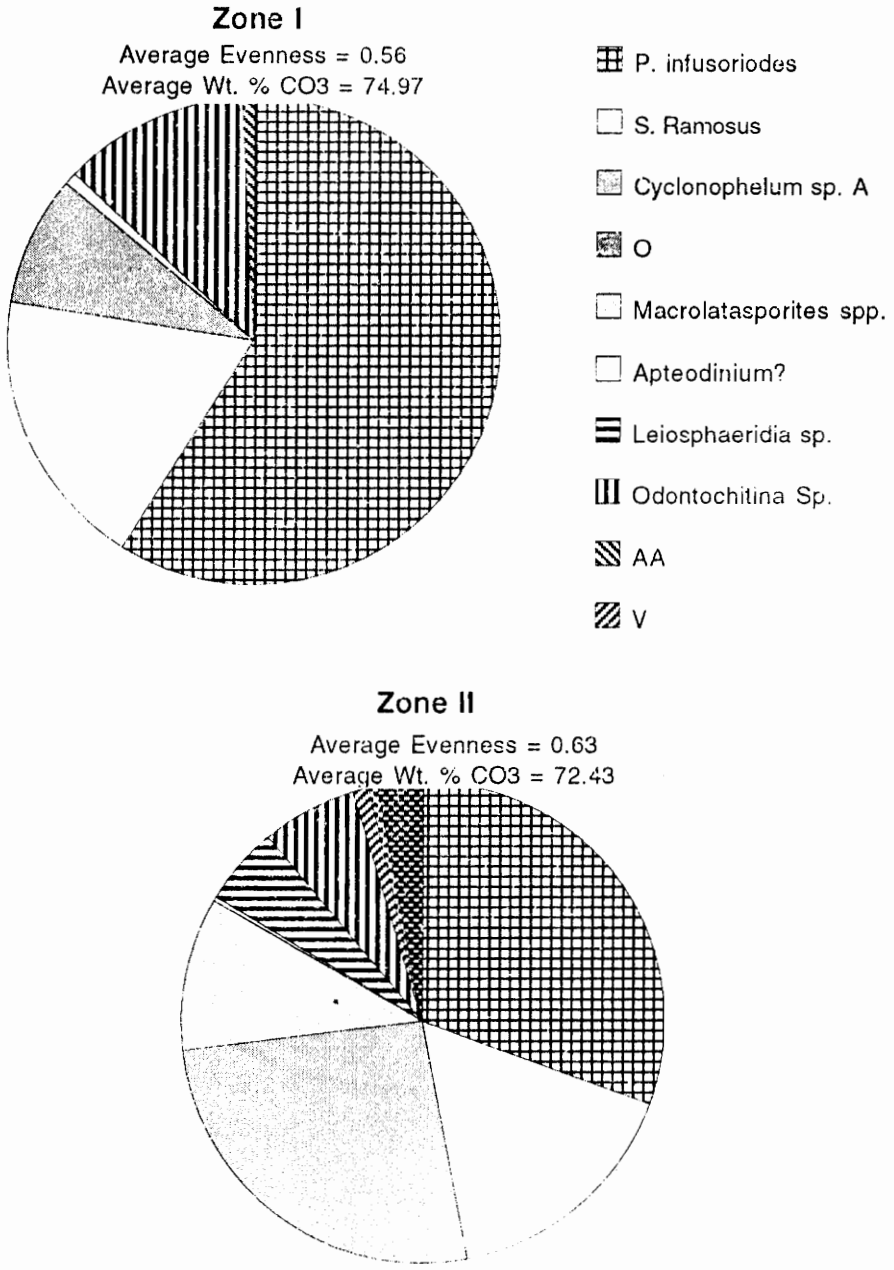

Figure 17. Pie charts show the relative percentage of the ten overall most abundant species. For each zone, average evenness and average weight percent carbonate increase as species represented on pie charts become more evenly distributed.

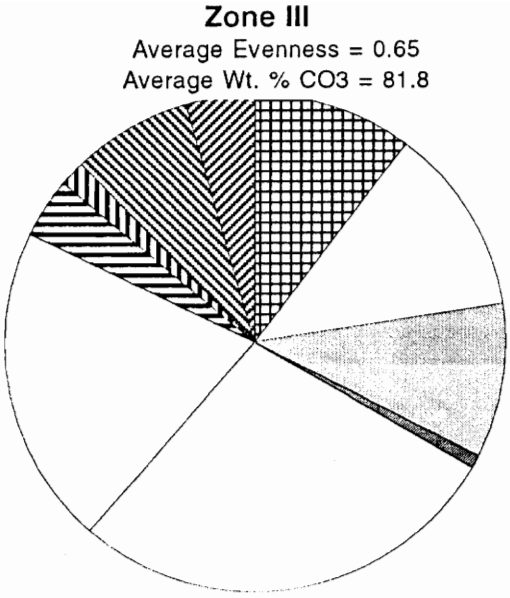

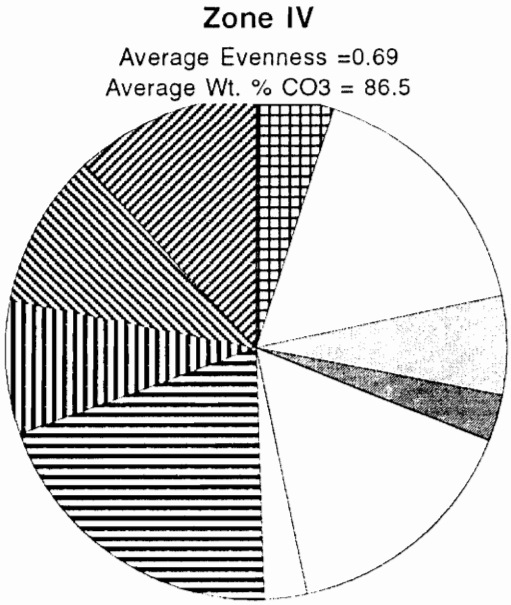

Figure 17, Continued. Relative percentage of the ten overall most abundant species.

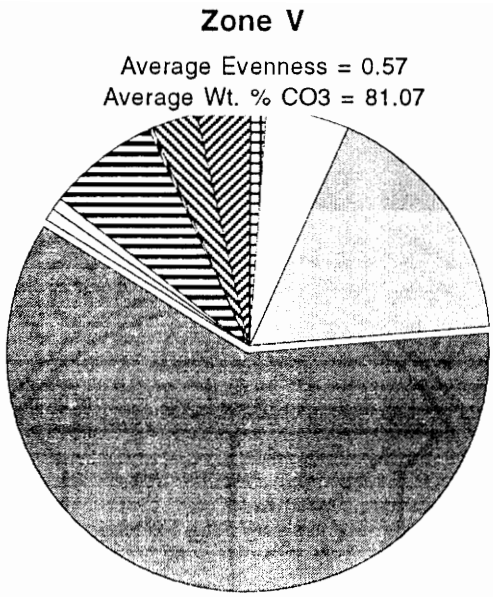

Figure 17, Continued. Relative percentage of the ten overall most abundant species.

The pie chart on Figure 17 indicates that the percentages of the ten overall most abundant taxa are more evenly distributed in Zone II than in Zone I. The visual evidence is supported by the average evenness value for this zone.

Zone III begins at the top of bed PBC-19A and ends between beds PBC-23A and PBC-26. This zone is dominated by *Macrolatasporites spp.* and *Apteodinium? spp.* Poor sample recovery from this interval precluded determining the exact location of the Zone III/IV boundary. Although the exact position of the Zone III/IV palynomorph boundary is unknown, it appears to correlate with either the *Watinoceras/Mammites nodosoides* ammonite biozone boundary or the *Mytiloides mytiloides mytiloides/Mytiloides mytiloides arcuata* bivalve biozone boundary.

The pie chart on Figure 17 and the average evenness value indicate that evenness in Zone III increased relative to Zone II.

Zone IV begins in the PBC-23A to PBC-26 interval and ends at the base of bed PBC-32A. The most abundant taxa in this zone are *Spiniferites, Leiosphaeridia,* and *Macrolatasporites.*

The Zone IV evenness index is greater than that of Zone III. The trend of increasing evenness from Zone I through Zone IV suggests that surface water fertility decreased through time.

Zone V ranges from the base of PBC-32A through bed PBC-40 and is dominated by palynomorph form "O". The low evenness index for this cluster suggests eutrophication of surface water, perhaps associated with a sea level fall suggested by Elder and Kirkland (1985). This interval also contains the greatest concentration of calcarenite beds, stringers, and starved calcarenite ripples in the Bridge Creek.

Potential Milankovitch Cycle/Phytoplankton Productivity Linkage

This section describes the methods used to search for a link between palynomorph assemblages and the lithologic cycles of the Bridge Creek, and discusses the findings of this research. Community characteristics and Multivariate Analysis of Variance (MANOVA) techniques were used to explore potential linkages.

Community Characteristics

Evenness and richness indices were calculated to provide measures of community structure and productivity. The indices used in this study were calculated by the FORTRAN programs "Richness" and "Evenness" listed in Appendix A.

Richness is a measure of the number of species in a sample when adjusted for sample size. The richness index used in this study is the Margalef Index as described in Ludwig and Reynolds (1988). Margalef's index was chosen over other evenness indices because it is well known in statistical ecology and relatively simple to calculate. Given "n" as the total number of individuals in a sample and "S" as the number of species in the sample, richness is calculated using the following equation.

$$R = \frac{S-1}{\ln(n)}$$

Evenness is a measure of the relative proportion of species in a sample. Samples with a few dominant taxa have low evenness values, whereas samples with an even distribution of species abundances have high evenness values. A modification of Hill's index was used in this study because it is not strongly affected by species richness. An example given in Ludwig and Reynolds (1988) illustrates this point. Table 1 shows that the addition of a single individual of a species can affect the evenness values of several

Table 1 – Comparison of Evenness Indices

Sample	# of species	Individual Abundance	Pielou Index	Sheldon's Index	Heip's Index	Hill's Index	Modified Hill's
1	3	500,300,200	0.94	0.93	0.90	0.94	0.91
2	4	500,299,200,1	0.75	0.71	0.61	0.94	0.90

common indices. Notice that the modified Hill's index is only slightly affected by the addition of a single individual of a new species. The modified Hill's index is calculated using the following equation:

$$Hill = \frac{\left(\frac{1}{\lambda} - 1\right)}{e^{H} - 1}$$

Where: $\lambda = \sum_{i=1}^{S}\left(\frac{n_i}{n}\right)^2$ and $H = \sum_{i=1}^{S}\left[\left(\frac{n_i}{n}\right)\ln\left(\frac{n_i}{n}\right)\right]$

Where: S = the number of species in the population,

n = the number of individual in the sample, and

n_i = the number of individuals of the "ith" species.

Evenness and richness are indicators of surface water fertility. Phytoplankton communities from oligotrophic environments exhibit greater evenness and richness values than do communities from eutrophic environments (Harris, 1986). At times when surface waters are rich in nutrients (eutrophic), a few species of phytoplankton reproduce rapidly and out-compete the other species, producing a community with low evenness and low richness. Red tides, which are algal blooms dominated by a single species of alga, are an example of this phenomenon. Increased nutrient input to the surface waters via increased upwelling or runoff after a heavy rain can produce red tides (Harris, 1986).

The evenness and richness indices were plotted on an X-Y graph with lithology represented by the plot symbol (Figure 18). Limestone samples plot above the dashed line, shale samples plot below the line, and marlstone samples are scattered on both sides of the line. This indicates that limestone samples have greater evenness values than do the shale samples.

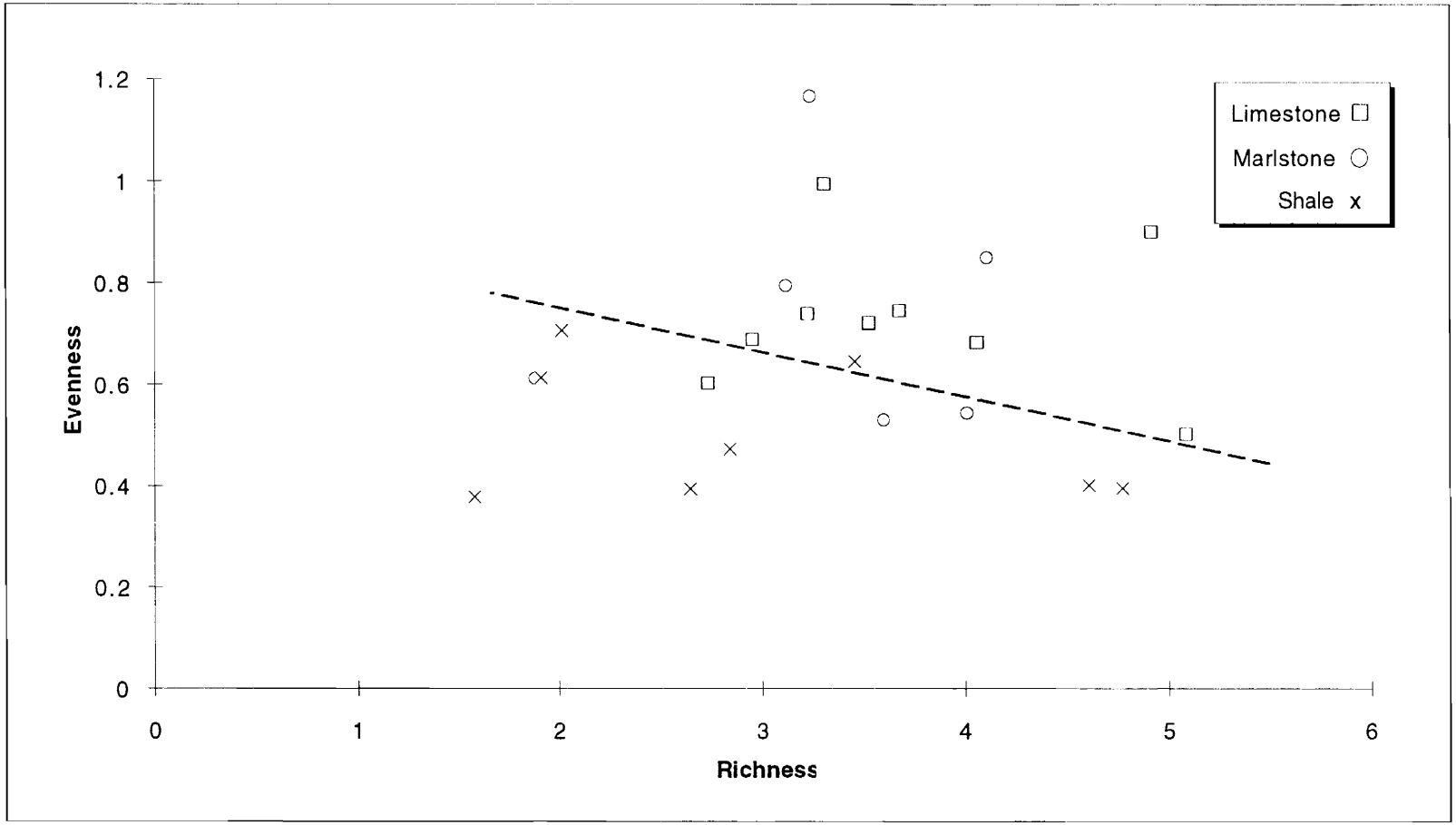

Figure 18. Plot of Evenness versus Richness with data points coded by lithology. Note the limestone samples plot above and to the right of the dashed line while the shale samples plot below and to the left of the line. This suggests that surface water ferility was greatest when shale was being deposited.

Analysis of Variance (ANOVA) was used to further investigate the relationship between rock type and the evenness and richness indices. The ANOVA compares the means of several groups based on the null hypothesis that the groups being tested are not different. The ANOVA breaks variance into two components: within-group variation and between-group variation (Figure 19). Groups differ if the ratio of between-group variation to within-group variation (expressed as an F-value) is greater than a critical ratio. If the calculated F-value exceeds the critical ratio, multiple comparison procedures are used to identify which group or groups are different.

The ANOVA is used in lieu of the t-test when more than two groups are being compared because it controls the experiment-wise Type I error rate. Type I errors are false-positive errors, meaning that the null hypothesis is rejected when it is true. For example, if a two-sample t-tests is performed at the 95% confidence level, there is a 5% chance that Type I error will occur. If several comparisons are performed, the probability of incorrectly rejected the null hypothesis by chance increases with each comparison. The ANOVA controls the Type I error rate by comparing all groups simultaneously.

The ANOVA results are expressed as the probability (P-value) of obtaining an F-value more extreme than the one calculated. Generally, a P-value less than 0.05 indicates that at least one group is different from the others. This would be equivalent to the statement "if one rejects the null hypothesis that all groups are the same, they will be correct 95% of the time."

The ANOVA was performed on three sample groups, limestone, marlstone, and shale. The results indicate that species richness is the same for each group (P-value > 0.05; Table 2). The ANOVA performed on evenness, however, indicates that at least one group is different (P-value < 0.05). To determine which group or groups are different, multiple comparison test were performed. The results of these tests (Fisher's LSD and Dunkan's

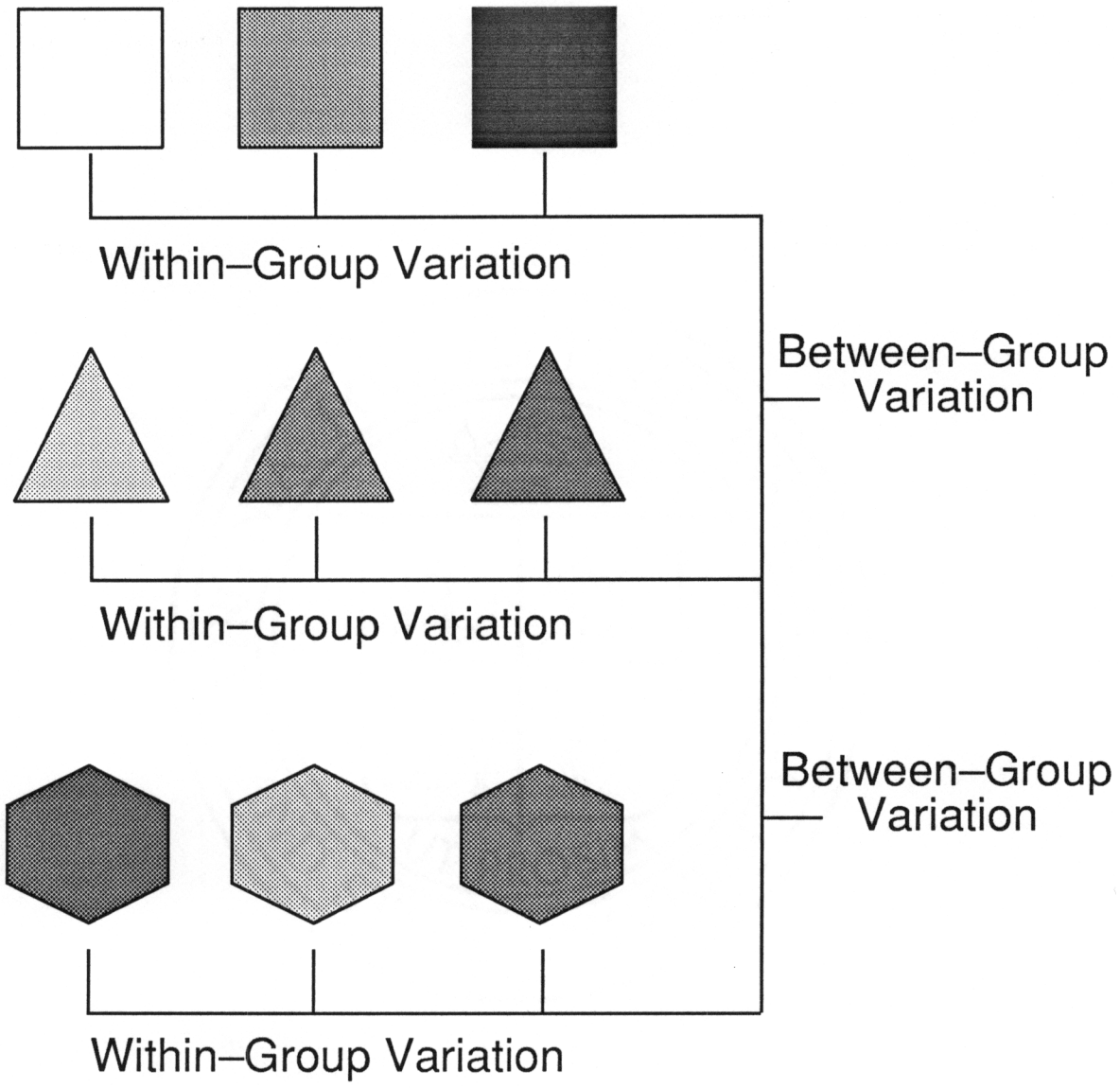

Figure 19. The ANOVA compares within-group variation to between-group variation. In this example, the shapes represent between group variation and the shading represents within group variation.

Table 2 – ANOVA Table for Species Richness

Source	Degrees of Freedom	Sum of Square	Mean Square	F-Value	Prob>F
Between Groups	2	2.3124	1.1562	1.28	0.2975
Within Groups	21	18.089	0.8998		
Total	23	21.13	2.0		

multiple range test) indicate that the evenness indices of the limestone group are significantly different than those of the shale group, but neither is significantly different from the marlstone group (Table 3).

The ANOVA results and the average evenness values suggest that the marlstone depositional environment is intermediate between the limestone and shale environments: The two extremes differ but neither extreme is significantly different from the intermediate.

Inspection of the richness data reveals two shale samples that may be outliers with respect to the other shale samples. These samples are exceptionally low in weight percent carbonate and high in species richness, relative to the other shale samples (Figure 20). The ANOVA results are different if these two data points are removed from the analysis. The ANOVA table for richness with the two outliers removed (Table 4) indicates that species richness in at least one lithologic group is different than the others (P-value < 0.05). Multiple comparison procedures indicate that species richness in the shale group is significantly lower than in the limestone and marlstone groups.

To summarize, qualitative and quantitative analyses of the evenness and richness indices of the dinoflagellate assemblages indicates that the limestone assemblages have more species and a more even distribution of species than do the shale assemblages. These analyses suggest possible surface water eutrophication during times of shale deposition.

Multivariate Analysis of Variance

Multivariate Analysis of Variance (MANOVA) was used to analyze the phytoplankton assemblage according to rock type. Support for a Milankovitch cycle/phytoplankton community link would be enhanced if the limestone beds and shale beds can be shown to contain distinct assemblages.

Table 3 - ANOVA Table for Evenness

Source	Degrees of Freedom	Sum of Squares	Mean Square	F-Value	Prob>F
Between Groups	2	0.243	0.121	4.32	0.0268
Within Groups	21	0.590	0.028		
Total	23	0.834			

Results of Multiple Comparison Procedures for Evenness

Lithology	Mean	Shale	Marlstone	Limestone
Shale	0.500			Significant
Marlstone	0.583			
Limestone	0.729	Significant		

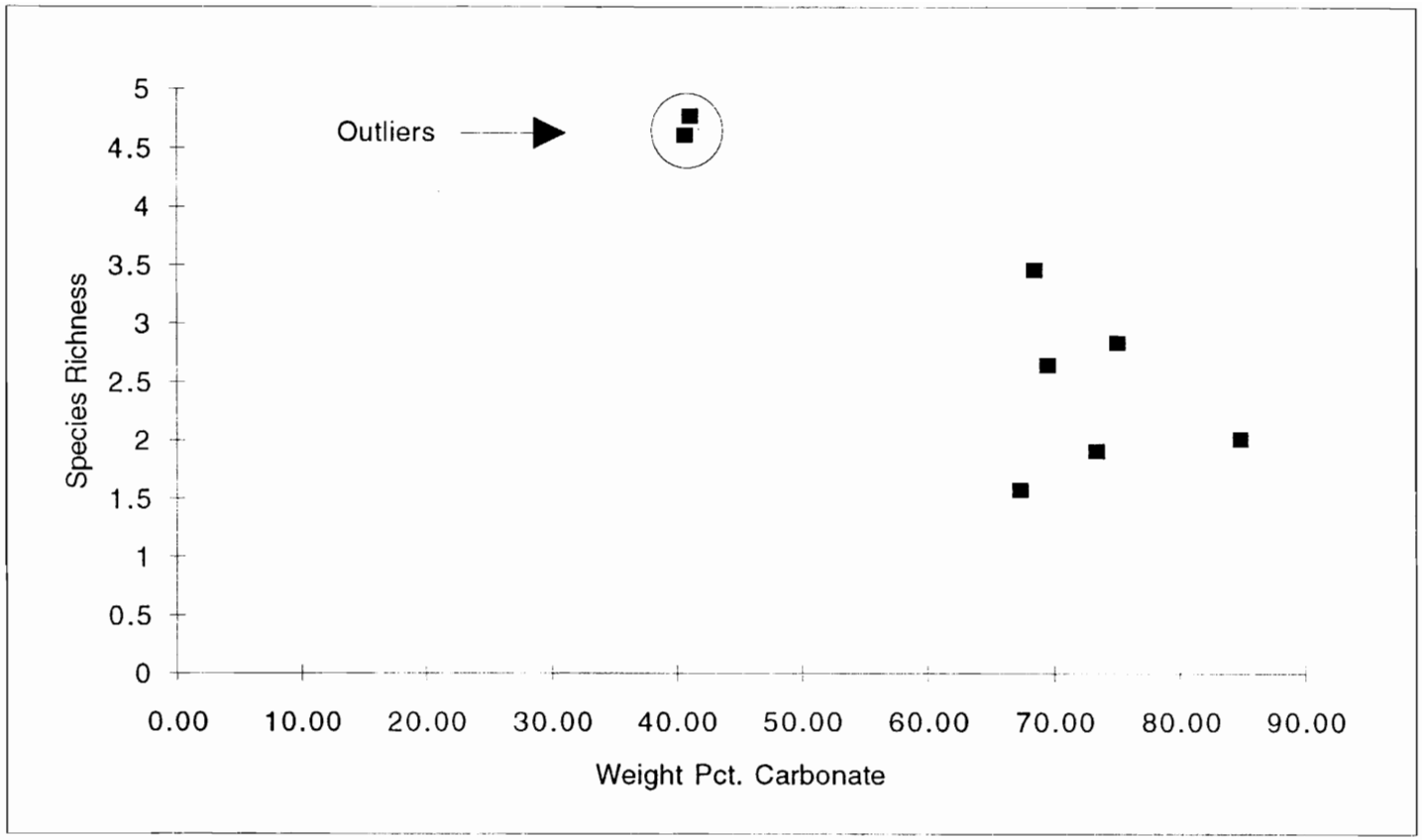

Figure 20. Plot of weight percent carbonate versus species richness for shale samples. Notice the two outliers with relatively low weight percent carbonate and high species richness.

Table 4 - ANOVA Table for Richness With Shale Outliers Removed

Source	Degrees of Freedom	Sum of Squares	Mean Square	F-Value	Prob>F
Between Groups	2	6.30042	3.150209	5.361644	0.014248
Within Groups	19	11.1634	0.587545		
Total	21	17.4638			

Results of Multiple Comparison Procedures for Richness

Lithology	Mean	Shale	Marlstone	Limestone
Shale	2.401		Significant	Significant
Marlstone	3.32	Significant		
Limestone	3.69	Significant		

MANOVA is more sensitive to differences between multivariate groups than the ANOVA because it considers several variables simultaneously. Figure 21 shows two groups that are not significantly different when two variables are evaluated individually. When the variables are considered simultaneously, however, the two groups are significantly different.

MANOVA has two limitations that were addressed prior to running the analysis. First, to normalize the data and ensure homogeneity of variance among groups, the Freeman-Tukey arcsine transformation was used as follows:

$$Trans(I,J) = 0.5 * \text{Arcsin}\sqrt{\frac{total(I,J)}{tot(I)+1}} + \text{Arcsin}\sqrt{\frac{total(I,J)+1}{tot(I)+1}}$$

Where:

total(I,J)= the number of individuals of the "jth" species in the "ith" sample,

and

tot(I)= the total number of individuals in the "ith" sample.

Second, to maintain the statistical power of the test, only the 12 overall most abundant species were used.

The samples were weighted according to the total number of individuals in the sample. Samples with more individuals and, thus, more information, were weighted more heavily in the analysis. MANOVA was performed on samples grouped by rock type.

The ANOVA table generated by SAS® is shown in Table 5. Unlike ANOVA, there are four accepted tests of significance for MANOVA. These are: Wilks' Lambda, Pillai's Trace, the Hotelling-Lawley Trace, and Roy's Greatest Root. This raises the question of which test to use, especially in cases where the tests disagree on whether the null hypothesis should be rejected or accepted. Of the four tests, Wilk's Lambda is the most

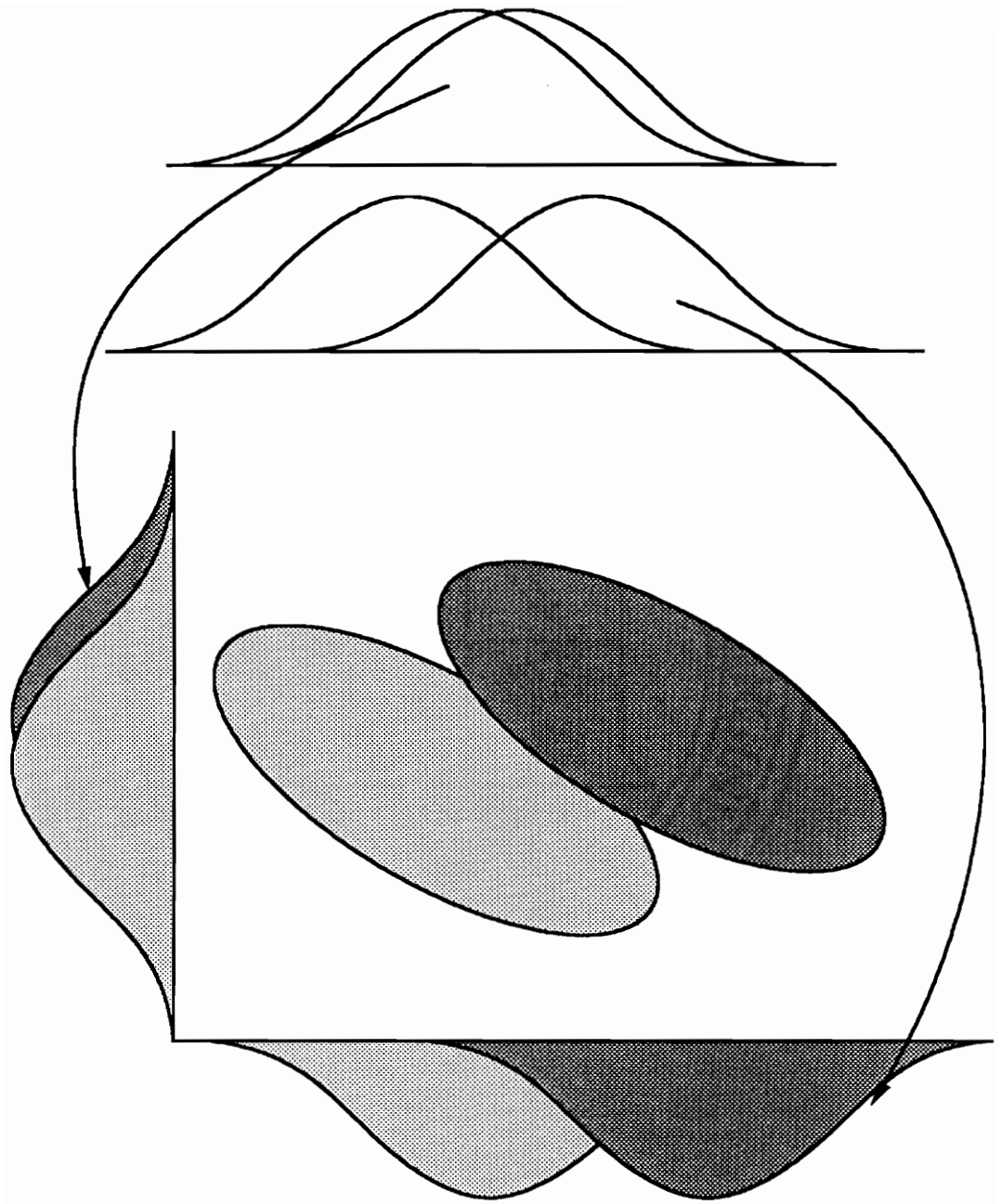

Figure 21. Two groups may not differ when variables are considered individually. When the variables are sonsidered simultaneously, however, the two groups may be significantly different.

Table 5 - MANOVA Results

Statistic	Value	F	Num DF	Den DF	Pr > F
Wilks' Lambda	0.087527	1.9834	24	20	0.0620
Pillai's Trace	1.376204	2.0223	24	22	0.0507
Hotelling-Lawley Trace	5.126937	1.9226	24	18	0.0793
Roy's Greatest Root	3.691828	3.3842	12	11	0.0262

commonly used, and Pillai's trace is the most robust (Bray and Maxwell, 1985). For a complete discussion of the MANOVA see Bray and Maxwell (1985).

All four tests indicate that at least one group is different from the others at the alpha = 0.10 level, and Pillai's Trace and Roy's Greatest Root are significant at the alpha = 0.05 level. Unfortunately, there are no good multivariate multiple comparison tests to determine which group or groups differ.

In conclusion, the MANOVA, which analyzed the palynomorph data directly, and the measurements of community structure (evenness and species richness) suggest a potential link between phytoplankton assemblages and the stratigraphic cycles of the Bridge Creek.

Stratigraphic Correlation Using Phytoplankton Assemblages

The Bridge Creek is an ideal testing ground for phytoplankton assemblage-based stratigraphic correlation because: (1) the alternating depositional environment allows for the establishment of new communities, (2) the isochronous limestone beds provide a method of checking regional correlations made by biostratigraphic methods, and (3) the environment of deposition was generally similar over broad areas of the Cretaceous Interior Seaway (Hattin, 1985).

To test correlation, two of the original 24 samples were randomly selected and designated as "unknown" samples meaning that the stratigraphic position of the sample was not known. The correlation test used the palynomorph assemblages to determine which of the original samples (referred to as "known" samples because the stratigraphic position of the sample was known) correlated with the "unknown" samples.

Two distance measurements, the Bray-Curtis group distance, and the Chord Distance, were used to correlate each unknown sample to one of the original samples.

Both measurements are popular in the ecological literature and have been used successfully over a wide range of ecological studies (Ludwig and Reynolds, 1988).

The Bray-Curtis group distance is calculated as the percent similarity between two samples as follows:

$$PS_{jk} = \left(\frac{2W}{A+B}\right)(100)$$

Where:

$W = \sum_{i=1}^{S}\left[\min\left(X_{ij}, X_{ik}\right)\right]$, the minimum of the "shared" species abundances between samples "j" and "k",

$A = \sum_{i=1}^{S} X_{ij}$, the total number of individuals in sample "j", and

$B = \sum_{i=1}^{S} X_{ik}$, the total number of individuals in sample "k".

The larger the Bray-Curtis group distance the more similar the species abundance distributions.

The Chord Distance projects the two samples as points on a circle. The distance between the two samples is the length of the chord connecting the two points on the circle. Therefore, samples which are similar have short chord distances. The chord distance is given by:

$$CRD_{jk} = \sqrt{2\left(1 - c\cos_{jk}\right)}$$

Where:

$$c\cos_{jk} = \frac{\sum_{i=1}^{S}\left(X_{ij}X_{ik}\right)}{\sqrt{\sum_{i}^{S}X_{ij}^{2}\sum_{i}^{S}X_{ik}^{2}}}$$

Where:

X_{ij} is the abundance of the "ith" species in the "jth" sample, and

X_{ik} is the abundance of the "ith" species in the "kth" sample.

The Bray-Curtis Group Distance and the Chord Distance between the first "unknown" sample, PBC-19, and each "known" sample were calculated (Table 6). The table lists each "known" sample in the left column and the correlation coefficients between each "known" sample and the "unknown" sample of interest. For the test to be successful, the distance measurements must indicate that the "unknown" sample (in this case PBC-19) is most similar to the original sample PBC-19. The Bray-Curtis Group Distance correctly identified the bed from which "unknown" number one was collected. The Chord Distance, however, incorrectly identified the sample as PBC-23.

For the second "unknown" sample, PBC-23, the Chord Distance correctly identified the sample, but the Bray-Curtis Group Distance incorrectly identified the sample as PBC-31 (Table 7).

The results of this test suggest that this approach to high resolution correlation may not be appropriate. Perhaps the problem lies in the actual species distributions across space and time. It is possible that when similar surface water conditions recur, phytoplankton communities of similar composition also recur. Hence, an individual bed does not have unique species abundance distributions.

Alternatively, perhaps the sampling and analysis methods are affecting the outcome of the tests. Exposure of strata to weathering and maceration techniques may bias the relative proportions of palynomorphs in successive preparations of the same sample. Although this seems unlikely considering the size of the fossils, perhaps it should be tested.

Table 6 - Distance Measurements for Unknown Sample PBC-19

Sample	Bray-Curtis	Chord Distance
PBC-1	4.361	1.405
PBC-2A	6.72	1.397
PBC-3	2.083	1.361
PBC-6	2.37	1.406
PBC-9	0.7326	1.406
PBC-9A	5.575	1.392
PBC-13	3.947	1.396
PBC-14i	1.522	1.408
PBC-15	10.26	1.349
PBC-18	6.07	1.407
PBC-19	**23.27**	1.413
PBC-20	3.604	1.406
PBC-21	20.92	1.406
PBC-23	6.452	**1.346**
PBC-23A	3.046	1.409
PBC-26	4.5	1.39
PBC-27	4.324	1.384
PBC-28	3.774	1.374
PBC-31	5.612	1.363
PBC-32A	0.625	1.413
PBC-34	4.898	1.408
PBC-35	4.036	1.375
PBC-39A	3.333	1.411
PBC-40	4.926	1.382

Table 7 - Distance Measurements for Unknown Sample PBC-23

Sample	Bray-Curtis	Chord Distance
PBC-1	5.357	1.399
PBC-2A	8.05	1.38
PBC-3	14.44	1.262
PBC-6	6.557	1.393
PBC-9	3.252	1.402
PBC-9A	3.745	1.409
PBC-13	5.195	1.404
PBC-14i	2.817	1.41
PBC-15	18.97	1.284
PBC-18	2.89	1.401
PBC-19	0	1.414
PBC-20	0	1.414
PBC-21	3.65	1.392
PBC-23	21.38	**0.9152**
PBC-23A	8.989	1.372
PBC-26	16.16	1.26
PBC-27	12.65	1.259
PBC-28	14.08	1.193
PBC-31	**29.21**	1.066
PBC-32A	2.36	1.407
PBC-34	7.447	1.39
PBC-35	18.06	1.17
PBC-39A	5.042	1.394
PBC-40	9.434	1.382

Finally, the fact that the Bray Curtis Group Distance and the Chord Distance disagreed on which "known" sample was most similar to the "unknown" sample suggests that additional testing is necessary to determine which of the multitude of distance measurement is most reliable.

In conclusion, high resolution correlation using phytoplankton assemblages as tested in this study may be possible, but additional testing is necessary. In two test cases, one of the two distance measurements used correctly identified the stratigraphic position of an unknown sample.

DEPOSITIONAL MODELS

Presently, three models, the Salinity Stratification Model, the Carbonate Productivity Model, and the Organic Productivity Model, attempt to link Milankovitch cycle-induced climate cycles and the Bridge Creek sedimentary cycles. Each model has strengths and weaknesses, as discussed below.

Salinity Stratification Model

The Salinity Stratification Model is based on studies of the organic geochemistry and petrogenesis of the Rock Canyon section of the Bridge Creek. Pratt (1984) noted the correlation between the abundance of current-induced sedimentary structures and the degree of bioturbation. Because the abundance of benthic organisms varies with oxygen concentration, Pratt suggested that anaerobic conditions prevailed during the deposition of non-bioturbated, organic rich, shale beds, and aerobic conditions existed during the deposition of bioturbated limestone. Because sedimentary structures, such as ripples, are more abundant in the limestone beds than the shale beds, benthic oxygen concentration at the sediment-water interface was construed to be dependent upon the delivery of dissolved oxygen by benthic currents. The frequency and intensity of benthic currents was a function of seaway stratification.

Pratt suggested that humid/arid climate cycles produced the Bridge Creek rock cycles through a series of steps beginning with salinity stratification. Salinity stratification occurred during humid periods when fresh water entering the seaway accumulated as a brackish surface layer. Stratification prevented the downward mixing of oxygen required to oxidize organic material, thereby preserving organic carbon. In this model the enhanced

preservation of organic carbon, combined with terrestrial detritus transported by intensified river runoff, produced the Bridge Creek shale beds.

During arid periods, the brackish surface layer weakened and salinity stratification failed, permitting the downward mixing of oxygen, and enhancing the destruction of organic matter. The destruction of organic material and reduced terrestrial detritus associated with river runoff produced the limestone beds.

The Salinity Stratification Model is not supported by planktonic foraminifera studies (Eicher and Diner, 1985). Most modern planktonic foraminifera are stenohaline. If a brackish layer capped the seaway during shale deposition, the planktonic foraminifera assemblages from the shale beds would exhibit low diversity and abundance as compared to the assemblages from the limestone beds. The planktonic foraminifera assemblages from the Bridge Creek shale beds, however, are as diverse as assemblages from coeval strata deposited in the open Tethyan Ocean (Eicher and Diner, 1985). This observation suggests that surface water salinity in the Cretaceous Interior Seaway approximated normal marine values.

Also, seaway circulation models do not support the Salinity Stratification Model. Circulation models suggest that a salinity gradient of 1‰ to 2‰ would produce salinity stratification if the seaway depth exceeded 300 meters (Jewell, 1993). Estimated precipitation, evaporation, and runoff based on modern environments and output from general circulation models suggest that fresh water flowing to the seaway could produce vertical salinity gradients of 7‰ within one year (Jewell, 1993). Thus, the circulation model satisfies half of the Salinity Stratification Model by indicating that salinity stratification could easily be established.

The other half of the salinity stratification hypothesis requires that the seaway be unstratified when limestone was deposited. This presents a problem—either in the circulation model or in the Salinity Stratification Model—because it is difficult to unstratify

the seaway to deposit limestone. In a seaway with water depths ranging from 300 to 400 meters and a vertical salinity gradient of less than 2‰, a simulated winter storm of three days duration with 60 m/s winds was needed to mix oxygen to the sea floor (Jewell, 1993).

Thermohaline circulation is another method that could unstratify the seaway. Thermohaline circulation during the Cretaceous was weak, relative to today, however, and may not have been strong enough to unstratify the seaway (Brass et al., 1982). Thus the salinity stratification theory is weakened because the seaway could not be unstratified to produce bioturbated limestone beds.

Another problem with the Salinity Stratification Model relates to the lateral distribution of carbon-rich strata in the Cretaceous Interior Seaway. The model predicts that a hyposaline plume of water entered the seaway from the Sevier Highlands to the west, enhancing organic carbon preservation near the plume source. To test this idea, Hattin (1985) examined the organic carbon content of 11 isochronous Bridge Creek Limestone beds in Kansas, Colorado, and New Mexico. Hattin discovered that, contrary to the Salinity Stratification Model, the organic carbon content of these beds increases toward the eastern margin of the seaway.

Finally, organic geochemical data fail to support the salinity stratification model. The model relies on greatly increased terrestrial runoff to produce the hyposaline surface layer. The volume of water needed to produce a brackish surface layer over the seaway would also deliver a significant amount of terrestrially derived organic matter. However, analyses of odd-carbon n-alkanes and long-chain paraffinic compounds that are typical of terrestrial plants, indicate that the fluctuating concentration of terrestrial organic matter is insignificant compared to marine derived organic matter (Pratt, 1984).

Carbonate Productivity Model

The failure of planktonic foraminifera data to support the Salinity Stratification Model lead Eicher and Diner (1985) to propose the Carbonate Productivity Model. Resembling the Salinity Stratification Model, this model invokes humid/arid climate cycles and seaway stratification to produce the Bridge Creek sedimentary cycles.

The Carbonate Productivity Model is based on the idea that ocean circulation during the Late Cretaceous was driven by the formation of warm saline bottom water (Brass et al., 1982). Eicher and Diner (1985) hypothesized that limestone was deposited when warm saline bottom water (WSBW) was produced during arid periods in the shallow, eastern margin of the seaway. Dense, hypersaline water flowing along the sea floor, drove vertical mixing, and oxygenated the sea floor. The vertical mixing would also transport nutrient-rich bottom water into the photic zone increasing planktonic carbonate production.

During humid periods, fresh water entering the seaway prevented the formation of WSBW and transported terrigenous material to the seaway. Without the WSBW to drive hypersaline circulation, the seaway became stratified and planktonic carbonate production diminished. The decreased carbonate production combined with the increased terrigenous input produced shale.

Like the Salinity Stratification Model, the data do not support the Carbonate Productivity Model. The paleontological data, and the stable isotope data contradict or fail to support the Carbonate Productivity Model, as discussed below.

In support of the Carbonate Productivity Model, Eicher and Diner (1989) suggested that a greater abundance of calcispheres in the limestone beds, relative to the shale beds reflects greater planktonic productivity during times of limestone deposition. Calcispheres are hollow calcareous spheres of unknown affinity, that range from 20-80 μm in diameter.

Paleozoic calcispheres have been attributed to charophytes while some Mesozoic spheres may have been produced by dinoflagellates.

Eicher and Diner's conclusions are not supported by interpretations of dinoflagellate data of this study and calcareous nannoplankton data of Watkins (1989). Phytoplankton evenness and richness values decrease with eutrophication because a few species dominate. Dinoflagellate and nannoplankton assemblages from the limestone beds exhibit greater evenness and richness values than assemblages from the shale beds. Contrary to the Carbonate Productivity Model, interpretations of nannoplankton assemblages and palynomorph assemblages are consistent with high surface water productivity during periods of shale deposition.

The $\delta^{13}C$ data are perhaps ambiguous as an indicator of planktonic productivity in this case. Because phytoplankton preferentially consume ^{12}C over ^{13}C, surface waters become ^{13}C enriched and the carbonate skeletons of planktonic organisms exhibit heavier $\delta^{13}C$. As phytoplankton die and settle to the sea floor, the ^{12}C is released and bottom waters become ^{12}C enriched.

Eicher and Diner's Carbonate Productivity Model states that the $\delta^{13}C_{carb}$ values measured in calcareous nannoplankton are influenced by upwelling and productivity. There are, however, two ways $\delta^{13}C_{carb}$ and productivity could be linked. First, as suggested by the Carbonate Productivity Model, the lighter $\delta^{13}C_{carb}$ measured in coccoliths from the limestone beds reflect ^{12}C enriched water being circulated upward when limestone was being deposited. Second, heavier $\delta^{13}C_{carb}$ values measured in the shale units may be a function of surface waters becoming depleted in ^{12}C due to increased uptake by phytoplankton. Thus, my interpretations suggest that the $\delta^{13}C_{carb}$ data are ambiguous with respect to the Carbonate Productivity Model.

Organic Productivity Model

Watkins (1989) proposed a third model that fits the paleontological, sedimentological, and geochemical data. He suggested that contrary to the Carbonate Productivity Model, in the Organic Productivity Model, planktonic productivity is greatest during times of shale deposition.

Paleontological Support of the Organic Productivity Model

Three paleontological studies of the Bridge Creek support the Organic Productivity Model. Calcareous nannofossil assemblages from the shale beds exhibit lower evenness and richness values than assemblages from the limestone beds (Watkins, 1989). Because algal assemblages have lower evenness and richness values in eutrophic conditions, the nannoplankton assemblages suggest surface water productivity was greater when shale was being deposited. Also, two nannoplankton taxa that are thought to reflect high surface water fertility, *Biscutum constans* and *Zeugrhabdotus spp.*, dominate nannoplankton assemblages from the shale beds (Watkins, 1989).

Courtinat (1993) studied palynomorphs from the lower half of the Bridge Creek and concluded that palynomorph diversity in the shale beds reflected mesotrophic conditions whereas diversity in the limestone beds reflected more oligotrophic conditions.

Data collected in this study indicate that dinoflagellate assemblages from the limestone beds exhibit greater evenness and richness values than assemblages from the shale beds suggesting planktonic productivity was greatest when shale was deposited.

Three studies involving two groups of microfossils are in general agreement with the possibility that surface water productivity was greatest during times of shale deposition, as stated in the Organic Productivity Model.

Sedimentological Support of the Organic Productivity Model

Organic geochemical studies indicate that the varying percent of organic carbon in the lime-shale cycles can only be explained by marine-derived organic carbon (Pratt, 1984). The lack of a terrestrial organic signal in the lime-shale cycles suggests that riverine runoff was not entirely responsible for the Bridge Creek stratigraphic cycles, although it did contribute terrigenous material during shale deposition.

Several studies have shown that organic rich strata result from either the preservation of organic carbon through anaerobic conditions, or high primary productivity and flux of organic material to the sea floor (Arthur et al., 1986; Arthur et al., 1988; Arthur et al., 1987; Calvert, 1987; Calvert and Pederson, 1992). The Salinity Stratification Model and the Carbonate Productivity Model invoke anoxia as the cause of organic-rich shale beds, whereas the Organic Productivity Model cites organic-rich sediments as the cause of anoxia. Paleontological evidence from the Bridge Creek indicates that deposition of the Bridge Creek Shale beds was associated with high surface water productivity and therefore, increase flux of organic material to the sea floor.

Stable Isotope Support of the Organic Productivity Model

The heavier $\delta^{13}C_{carb}$ values exhibited by calcareous nannoplankton from the Bridge Creek shale units are plausibly explained by the Organic Productivity Model. Because sequestering of ^{12}C by phytoplankton causes surface waters to become ^{13}C enriched, times of high primary productivity are reflected in ^{13}C enrichment in the carbonate skeletons of planktonic organisms. In the Organic Productivity Model, the heavier $\delta^{13}C_{carb}$ in nannoplankton from the Bridge Creek shale beds is explained by greater planktonic productivity during shale deposition.

There is concern regarding the diagenetic alteration of the $\delta^{18}O$ signal in the Bridge Creek. Several workers have suggested that, although diagenesis has probably decreased

$\delta^{18}O$ values, the relative difference between the limestone values and the shale values has remained unchanged (Arthur et al., 1985; Barron et al., 1985). If the $\delta^{18}O$ record is accepted as primary, the 2‰ to 3‰ negative shift from the limestones to the shales would translate to a 22‰ reduction in surface water salinity (Watkins, 1989). However, the palynomorph, nannoplankton, and planktonic foraminifera assemblages do not reflect a major change in surface water environments, suggesting that other factors, such as global ice volume or temperature, are responsible for a portion of the negative $\delta^{18}O$ shift from the limestone beds to the shale beds. A portion of the $\delta^{18}O$ signal may have been a result of fluctuating fresh water input that also supplied terrestrial detritus and nutrients during times of shale deposition.

Evidence exists that $\delta^{18}O$ may be linked to surface water fertility. In a study of Pliocene to Pleistocene planktonic foraminifera from the Mediterranean Sea, Lourens et al. (1992) correlated minimum $\delta^{18}O$ with warm, eutrophic conditions. Lourens' findings seem to apply to the Bridge Creek.

Nutrient Cycling and Circulation

Phytoplankton productivity depends on two main factors: solar intensity and nutrient availability. Phosphate (PO_4) is the limiting nutrient for marine phytoplankton and can only be replenished either by upwelling of nutrient rich water or by riverine input. Upwelling depends on surface winds and circulation patterns, and riverine input depends on rainfall.

Parrish and Curtis (1982) published qualitative circulation maps based on the effect of global geography on atmospheric circulation. They did not consider the seaway large enough to create the strong land-sea temperature contrast necessary for the development of independent circulation cells. Instead, according to their interpretation, the northern Pacific low pressure cell shifted east during the winter and the subtropical, high pressure cell

moved east during the summer (Figure 22). This configuration caused upwelling along the western margin of the seaway during winter and along the eastern margin during summer. Figure 22 shows the position of the subtropical high and northern Pacific low in winter and summer (Parrish and Curtis, 1982). If Milankovitch forcing favored the summer position for an extended period of time (e.g. half the obliquity cycle) the upwelling zone on the eastern margin of the seaway would be accentuated and phytoplankton productivity would be enhanced. During the other half of the cycle, east coast upwelling would be moderated by shifting the circulation cells westward and/or moderating the intensity of the cells.

Arthur et al. (1987) published predicted upwelling sites based on the National Center for Atmospheric Research (NCAR) Community Climate Model (Figure 23). Comparable to the Parrish model, their model also predicts upwelling during Bridge Creek deposition.

Riverine runoff is another way that nutrients can be transported to the photic zone. Fresh water input to the seaway would account for the lighter $\delta^{18}O$ values in the shale beds, and would provide clastic material necessary for shale deposition.

The paleontological, geochemical, and climatological data are consistent with a coupling between the Bridge Creek stratigraphic cycles and Milankovitch cycle-driven climate cycles. The coupling may occur through the following steps. Varying solar insolation driven by the Milankovitch obliquity or precessional cycle causes atmospheric circulation cells to advance and retreat over the seaway. The cyclic movement of the circulation cells triggers periodic upwelling of nutrient-rich bottom waters. The subsequent eutrophication of the photic zone stimulated phytoplankton productivity, producing

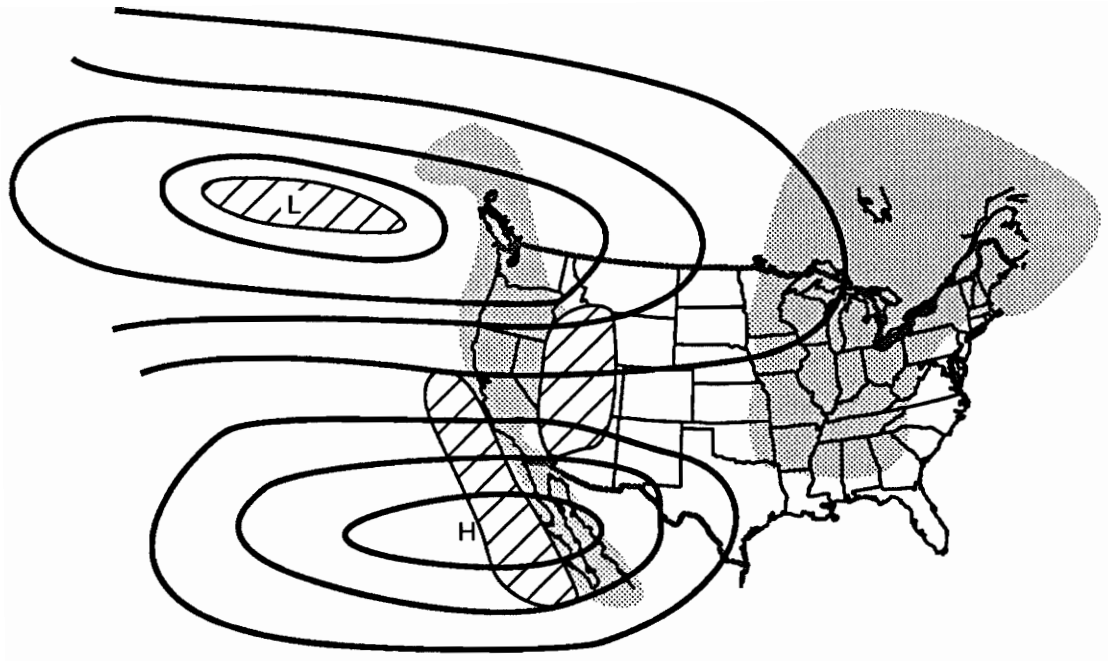

WINTER

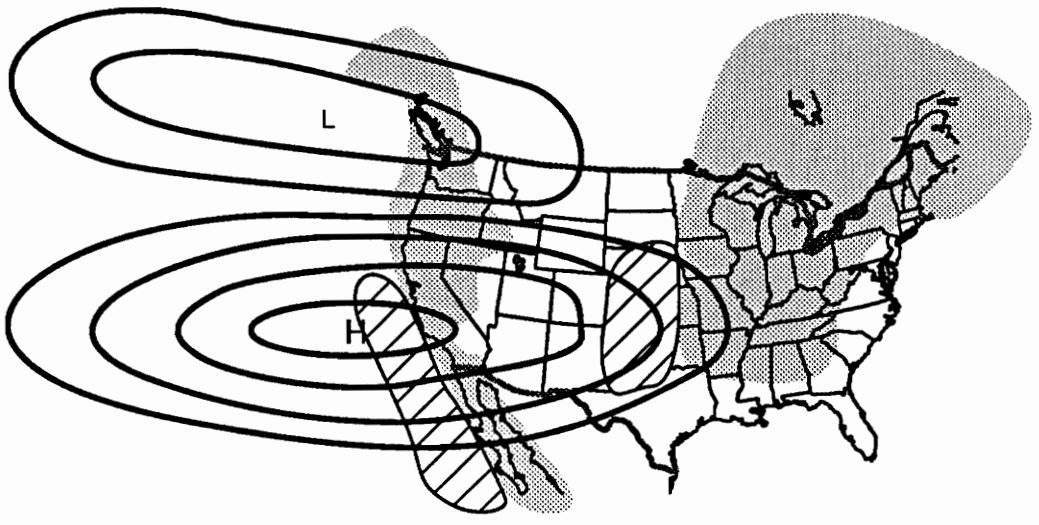

SUMMER

Figure 22. Circulation cells and expected upwelling zones (hatched areas). When the summer configuration was favored for an extended period, shale was deposited. When the winter configuration was favored, limestone was deposited. After Parrish and Curtis, 1982.

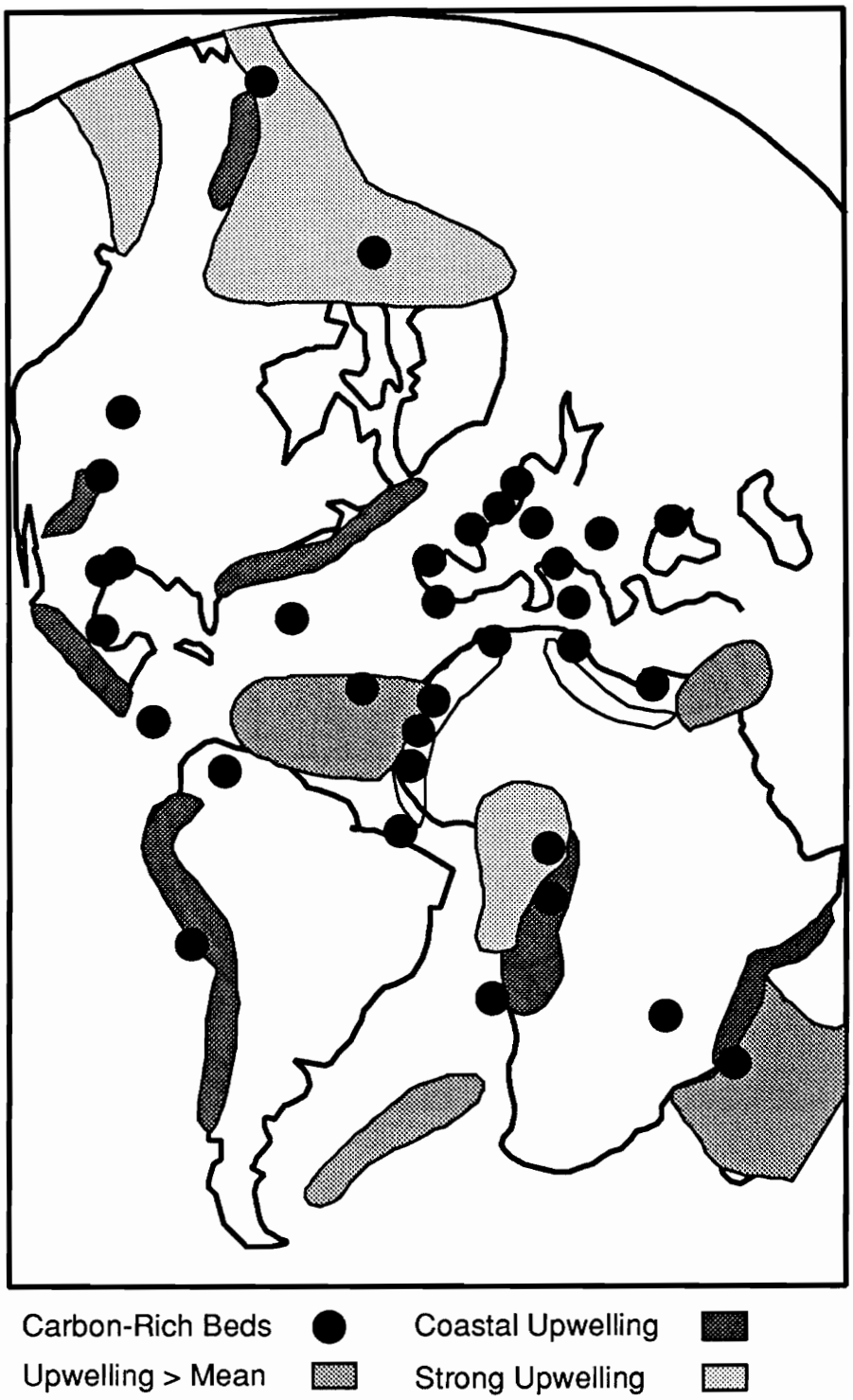

Figure 23. Predicted areas of upwelling during the Cretaceous (After Arthur et al., 1987).

organic-rich shale. Limestone was deposited during times of weakened and a decreased planktonic productivity. The effects of upwelling were probably augmented by humid/arid cycles and the flow of fresh water into the seaway. Riverine input of terrigenous material and isotopically-light fresh water provided the material necessary for shale deposition, and accounts for a part of the negative $\delta^{18}O$ shift from the limestone beds to the shale beds.

CONCLUSIONS

The following conclusions are based on statistical analyses of dinoflagellate, acritarch, and chlorophyte cysts studied during this investigation, and the integration of other paleontological data and stable isotope data.

1. Spectral analysis of the Bridge Creek lime-shale cycles indicates that the cycles are not random alternations, but are periodic cycles with a dominant period of 42 cm. Based on an average rock accumulation rate of 1 cm/ky (Elder and Kirkland, 1985), the Bridge Creek cycles correlate with the Milankovitch obliquity cycle.

2. Five informal palynomorph zones were established via cluster analysis. Two of the four palynomorph zone boundaries coincide with stratigraphic or biostratigraphic boundaries proposed by other workers.

3. Palynomorph assemblages from the limestone beds exhibit greater evenness and richness indices than assemblages from the shale beds. Since phytoplankton communities exhibit greater evenness and richness in oligotrophic conditions, these results are consistent with surface water eutrophication during times of shale deposition. This interpretation agrees with conclusions reached via coccolith studies (Watkins, 1989) and other palynomorph studies (Courtinat, 1993).

4. The lime-shale cycles in the Bridge Creek appear to be the result of fluctuating planktonic productivity and riverine runoff. Organic-rich shale beds were deposited when the oxidation of large amounts of organic detritus consumed the oxygen available at the sea floor, and high rainfall and terrestrial runoff provided the terrigenous material necessary for shale deposition. Micritic limestone beds were deposited when terrigenous and organic detritus decreased.

5. Circulation models suggest that the position and intensity of circulation cells produced periodic upwelling along the eastern margin of the Cretaceous Interior Seaway (Parrish and Curtis, 1982), which may have stimulated planktonic productivity. The movement of the circulation cells may also have produced humid/arid climate cycles that also contributed to cycle production. I propose that the position and intensity of the circulation cells may have been a function of Milankovitch cycle-driven fluctuations in insolation.

6. Testing of high resolution stratigraphic correlation using palynomorph assemblages was inconclusive. Statistical measures of sample similarity were used to attempt to correlate samples based on the palynomorph assemblages. Two similarity measurements, the Bray-Curtis Group Distance and the Chord Distance were used. In two test cases, one of the two distance measurements correctly correlated the samples. Additional testing is necessary to further evaluate the potential of high resolution correlation via phytoplankton assemblages.

REFERENCES

Arthur, M. A., D. J. Bottjer, W. E. Dean, A. G. Fischer, D. E. Hattin, E. G. Kauffman, L. M. Pratt and P. A. Scholle. 1986. Rhythmic Bedding in Upper Cretaceous Pelagic Carbonate Sequences: Varying Sedimentary Response to Climatic Forcing. Geology. v.14, p. 153-156.

Arthur, M. A., W. E. Dean, R. M. Pollastro and P. A. Scholle. 1985. "Comparative Geochemical and Mineralogical Studies of Two Cyclic Transgressive Pelagic Limestone Units, Cretaceous Western Interior Basin, U.S.". In: L. M. Pratt, E. G. Kauffman and F. B. Zelt (ed.) Fine-Grained Deposits and Biofacies of the Cretaceous Western Interior Seaway: Evidence of Cyclic Sedimentary Processes. SEPM Fieldrip Guidebook No.4, Golden, Colorado. p. 16-27.

Arthur, M. A., W. E. Dean and L. M. Pratt. 1988. Geochemical and climatic effects of increased marine organic carbon burial at the Cenomanian/Turonian boundary. Nature. v.335, p. 714-717.

Arthur, M. A., S. O. Schlanger and H. C. Jenkyns. 1987. "The Cenomanian-Turonian Oceanic Anoxic Event, II. Palaeoceanographic controls on organic-matter production and preservation". In: J. Brooks and A. J. Fleet (ed.) Marine Petroleum Source Rocks. Blackwell Scientific Publications, Oxford. p. 401-421.

Barron, E. J., M. A. Arthur and E. G. Kauffman. 1985. Cretaceous rhythmic bedding sequences: A plausible link between orbital variations and climate. Earth and Planetary Science Letters. v.72, p. 327-340.

Berger, A. 1980. The Milankovitch astonomical theory of paleoclimates: A modern review. Vistas in Astronomy. v.24, p. 103-122.

Brass, G. W., J. R. Southam and W. H. Peterson. 1982. Warm saline bottom water in the ancient ocean. Nature. v.296, p. 620-623.

Bray, J. H. and S. E. Maxwell. 1985. Multivariate Analysis of Variance. SAGE Publications, Beverly Hills. p. 79.

Brückner, W. D. 1953. Cyclic calcareous sedimentation as an index of climatic variations in the past. Journal of Sedimentary Petrology. v.4, p. 235-237.

Calvert, S. E. 1987. "Oceanographic controls on the accumulation of organic matter in marine sediments". In: J. Brooks and A. J. Fleet (ed.) Marine Petroleum Source Rocks. Blackwell Scientific Publications, Boston. p. 137-151.

Calvert, S. E. and T. F. Pederson. 1992. "Organic carbon accumulation and preservation in marine sediments: how important is anoxia". In: J. K. Whelan and J. W. Farrington (ed.) Organic Matter: Productivity, Accumulation, and Preservation in Recent and Ancient Sediments. Columbia University Press, New York. p. 231-264.

Calvert, S. E. and N. B. Price. 1971. Upwelling and nutrient regeneration in the Benguela Current, October 1968. Deep-Sea Research. v.18, p. 501-523.

Cobban, W. A. and G. R. Scott. 1972. Stratigraphy and Ammonite Fauna of the Graneros Shale and Greenhorn Limestone Near Pueblo, Colorado. U.S.G.S. Professional Paper 645. p. 108.

Courtinat, B. 1993. The significance of palynofacies fluctuations in the Greenhorn Formation (Cenomanian-Turonian) of the Western Interior Basin, USA. Marine Micropaleontology. v.21, p. 249-257.

Croll, J. 1875. Climate and Time in Their Geological Relations: A Theory of Secular Changes of Earth's Climate. Daldy, Isbister and Company, London. p. 175.

Eicher, D. L. 1969. Paleobathemetry of Cretaceous Greenhorn sea in eastern Colorado. American Association of Petroleum Geologists Bulletin. v.53, p. 1075-1090.

Eicher, D. L. and R. Diner. 1985. "Foraminifera as Indicators of Water Mass in the Cretaceous Greenhorn Sea, Western Interior". In: L. M. Pratt, E. G. Kauffman and F. B. Zelt (ed.) Fine-Grained Deposits and Biofacies of the Cretaceous Western Interior Seaway: Evidence of Cyclic Sedimentary Processes. SEPM Fieldtrip Guidebook No. 4, Golden, Colorado. p. 60-71.

Einsele, G. 1982. "Limestone-Marl Cycles (Periodites): Diagnosis, Significance, Causes - A Review". In: G. Einsel and A. Seilacher (ed.) Cyclic and Event Stratification. Springer-Verlag, Berlin. p. 8-53.

Einsele, G. and W. Ricken. 1991. "Limestone-marl alternation—an overview". In: G. Einsele, W. Ricken and A. Seilacher (ed.) Cycles and Events in Stratigraphy. Springer-Verlag, Berlin. p. 23-47.

Elder, W. P. 1985. "Biotic atterns across the Cenomanian-Turonian extinction boundary near Pueblo, Colorado". In: L. M. Pratt, E. G. Kauffman and F. B. Zelt (ed.) Fine-Grained Deposits and Biofacies of the Cretaceous Western Interior Seaway: Evidence of Cyclic Sedimentary Processes. SEPM Fieldtrip Guidebook No.4, Golden Colorado. p. 157-169.

Elder, W. P. and J. I. Kirkland. 1985. "Stratigraphy and Depositional Environments of the Bridge Creek Limestone Member of the Greenhorn Limestone at Rock Canyon Anticline Near Pueblo, Colorado". In: L. M. Pratt, E. G. Kauffman and F. B. Zelt (ed.) Fine-Grained Deposits and Biofacies of the Cretaceous Western Interior Seaway: Evidence of Cyclic Sedimentary Processes. SEPM Fieldtrip Guidebook No.4, Golden, Colorado. p. 122-134.

Ferris, T. 1989. Coming of Age in the Milky Way. Doubleday, New York. p. 495.

Fischer, A. G., T. Herbert and I. P. Silva. 1985. "Carbonate Bedding Cycles in Cretaceous Pelagic and Hemipelagic Sequences". In: L. M. Pratt, E. G. Kauffman and F. B. Zelt (ed.) Fine-Grained Deposits and Biofacies of the Cretaceous Western Interior Seaway: Evidence of Cyclic Sedimentary Processes. SEPM Fieldtrip Guidebook No.4, Golden, Colorado. p. 1-10.

Gilbert, G. K. 1895. Sedimentary Mesurement of Cretaceous Time. Journal of Geology. v.3, p. 121-127.

Goodwin, P. J. and E. J. Anderson. 1985. Punctuated Aggradational Cycles: A general hypothesis of episodic strtigraphic accumulation. Journal of Geology. v.93, p. 515-533.

Harris, G. P. 1986. Phytoplankton Ecology. Chapman and Hall, New York. p. 384.

Hattin, D. E. 1971. Widespread, Synchronously Deposited, Burrow-Mottled Limestone Beds in Greenhorn Limestone (Upper Cretaceous) of Kansas and Southeastern Colorado. American Association of Petroleum Geologists. v.55, p. 412-431.

Hattin, D. E. 1975. Stratigraphy and depositional environment of the Greenhorn Limestone (Upper Cretaceous) of Kansas. Kansas Geological Survey Bulletin 209. p. 128.

Hattin, D. E. 1985. "Distribution and significance of widespread, time-parallel pelagic limestone beds in the Greenhorn Limestone (Upper Cretaceous) of the central great plains and southern Rocky Mountains". In: L. M. Pratt, E. G. Kauffman and F. B. Zelt (ed.) Fine-Grained Deposits and Biofacies of the Cretaceous Western Interior Seaway: Evidence of Cyclic Sedimentary Processes. SEPM Fieldtrip Guidebook No.4, Golden, Colorado. p.

Hays, J. D., J. Imbrie and N. J. Shackleton. 1976. Variations in the Earth's Orbit: Pacemaker of the Ice Ages. Science. v.194, p. 1121-1131.

Jewell, P. W. 1993. Water-column stability, residence times, and anoxia in the Cretaceous North American seaway. Geology. v.21, p. 579-582.

Jørgensen, B. B. 1982. Ecology of the bacteria of the sulphur cycle with special reference to anoxic-oxic interface environments. Limnology and Oceanography. v.22, p. 814-832.

Kauffman, E. G. 1977. Upper Cretaceous Cyclothems, Biotas, and Environments, Rock Canyon Anticline, Pueblo, Colorado. The Mountain Geologist. v.14, p. 129-152.

Koerschner, W. F. and J. F. Read. 1989. Field and modelling studies of Cambrian carbonate cycles, Virginia Appalachians. Journal of Sedimentary Petrology. v.59, p. 654-687.

Leckie, R. M. 1985. "Foraminifera of The Cenomanian-Turonian Boundary Interval, Greenhorn formation, Rock Canyon Anticline, Pueblo, Colorado". In: L. M. Pratt, E. G. Kauffman and F. B. Zelt (ed.) Fine-Grained Deposits and Biofacies of the Cretaceous Western Interior Seaway: Evidence of Cyclic Sedimentary Processes. SEPM Fieldtrip Guidebook No.4, Golden, Colorado. p. 139-150.

Lourens, L. J., F. J. Hilgen, L. Gudjonsson and W. J. Zachariasse. 1992. Late Pliocene to early Pleistocene astronomically forced sea surface productivity and temperature variations in the Mediterranean. Marine Micropaleontology. v.19, p. 49-78.

Ludwig, J. A. and J. F. Reynolds. 1988. Statistical Ecology. John Wiley and Sons, New York. p. 337.

Martens, C. S. and J. V. Klump. 1984. Biogeochemical cycling in an organic rich coastal marine basin. An organic carbon budget for sediments dominated by sulfate reduction and methanogenesis. Geochemica et Cosmochima Acta. v.48, p. 1987-2004.

Mesolella, K. J., R. K. Matthews, W. S. Broecker and D. L. Thurber. 1969. The astronomical theory of climatic change: Barbados data. Journal of Geology. v.77, p. 250-274.

Müller, P. J. and E. Suess. 1979. Productivity, sedimentation rate and sedimentary organic matter in the oceans—I. Organic carbon preservation. Deep Sea Research. v.27A, p. 1347-1362.

Murray, J. W., V. Grundmanis and W. M. Smethie. 1978. Interstitial mater chemistry in the sediments of Saanich Inlet. Geochemica et Cosmochemica Acta. v.42, p. 1011-1026.

Parrish, J. T. and R. L. Curtis. 1982. Atmospheric cirulation, upwelling, and organic-rich rocks in the Mesozoic and Cenozoic Eras. Palaeogeography, Palaeoclimatology, Palaeoecology. v.40, p. 31-66.

Pratt, L. M. 1984. Influence of paleoenvironmental factors on preservation of organic matter in the Middle Cretaceous Greenhorn Formation, Pueblo, Colorado. American Association of Petroleum Geologists Bulliten. v.68, p. 1146-1159.

Sageman, B. B. and C. C. Johnson. 1985. "Stratigraphy and Paleobiology of the Lincoln Limestone Member, Greenhorn Limestone, Rock Canyon Anticline, Colorado". In: L. M. Pratt, E. G. Kauffman and F. B. Zelt (ed.) Fine-Grained Deposits and Biofacies of the Cretaceous Western Interior Seaway: Evidence of Cyclic Sedimentary Processes. SEPM Fieldtrip Guidebook No.4, Golden, Colorado. p. 100-109.

Shackleton, N. 1967. Oxygen isotope analysis and Pleistocene termperature re-assessed. Nature. v.215, p. 15-17.

Sheu, D. D. 1983. "The geochemistry of Orca Basin sediments". Ph.D. Dissertation, Texas A&M University.

Southam, J. R., W. H. Peterson and G. W. Brass. 1982. Dynamics of Anoxia. Palaeogeography, Palaeoclimatology, Palaeoecology. v.40, p. 183-198.

Thunell, R. D., D. Rio, R. Sproviere and I. Raffi. 1991. Limestone-marl couplets: Origin of the Early Pliocene Trubi Marls in Calabria, southern Italy. Journal of Sedimentary Petrology. v.61, p. 1109-1122.

Watkins, D. K. 1989. Nannoplankton productivity gluctuations and rhythmically-bedded pelagic carbonates of the Greenhorn Limestone (Upper Cretaceous). Palaeogeography, Palaeoclimatology, Palaeoecology. v.74, p. 75-86.

Whitney, B. L. 1976. "Campanian-Maastrichtian and Paleocene Dinoflagellat and Acritarch Assemblages from the Maryland-Delaware Coastal Plain". Dissertation, Virginia Polytechnic Institute and State University.

Witmer, R. 1975. "Taxonomy and Biostratigraphy of Lower Tertiary Dinoflagellate Assemblages from the Atlantic Coastal Plain Near Richmond, Virginia". Thesis, Virginia Polytechnic Institute and State University.

APPENDIX A

COMPUTER PROGRAMS

The following programs were used in data analysis. With the exception of the cluster program and the polar ordination program, which were run on an IBM 3090-300E mainframe computer, all other FORTRAN programs were run on a Macintosh Plus using MS-FORTRAN. The analysis of varience (ANOVA) and spectral analysis were run on the IBM 3090-300E using SAS®.

```
TITLE 'ANOVA OF CARBONATE DATA';
OPTIONS LS=80;
DATA ROCKS;
INPUT SAMPLE $ TYPE $ WTPCT WTCO3
CARDS;
PBC-1 LIMESTONE 94.14 236.62
.
.
.
.
.
.
.
.
.
PBC-40 MARLSTONE 87.76 73.56
PROC PLOT;
        PLOT WTCO3*TYPE;
        PLOT WTPCT*TYPE;

PROC ANOVA;
        CLASS TYPE;
        MODEL WTPCT=TYPE;
        MEANS TYPE/LSD;
        MEANS TYPE/SCHEFFE;

PROC ANOVA;
        CLASS TYPE
        MODEL WTCO3=TYPE;
        MEANS TYPE/LSD;
        MEANS TYPE/SCHEFFE;
```

Note: This program was also used for the ANOVA of species richness and evenness indices.

```
OPTIONS LS=80;
TITLE 'SPECTRAL ANALYSIS OF BRIDGE CREEK STRATA';
DATA TIME;
INPUT SAMPLE CODE;
CARDS;
1 1
.
.
.
.
.
.
.
.
154 2
PROC SPECTRA OUT=OUT1 P S WHITETEST;
    VAR CODE;
PROC PLOT DATA=OUT1;
    PLOT S_01*FREQ;
    PLOT P_01*FREQ;
PROC PRINT DATA=OUT1;
    VAR S_01 P_01 FREQ PERIOD;
```

```
C*************************************************************
C    PROGRAM PLANTS2 : PERFORMS CLUSTER ANALYSIS OF INPUT DATA.
C    WRITTEN BY PLANTS, REVISED BY ARNIE MILLER & TOM ROUNDS        C
MODIFIED BY BRET BENNINGTON
C
C    FILEDEFS : 04 = INPUT OF PLOTTING AND CONTROL PARAMETERS
C               05 = INPUT OF DATA SET
C               06 = OUTPUT OF TEXT OF RESULTS
C               07 = OUTPUT OF DATA SET (+/- INVERS. OR TRANSF.)
C               10 = OUTPUT OF PLOTTING INSTRUCTIONS
C
C*************************************************************
C THE INPUT DATA WILL USUALLY BE IN THE FOLLOWING FORM:
C
C              N ROWS    : FOR SAMPLES(I),I=1,N_SAMPLES
C         BY   M COLUMNS : FOR SPECIES(J),J=1,M_SPECIES
C
C*************************************************************
C CONTROL CARD PARAMETER: ITEST (USED TO SPECIFY Q OR R MODE)
C  ITEST = +1 : NO INVERSION OF DATA MATRIX (Q-MODE)
C  ITEST = -1 : INVERSION OF DATA MATRIX (R-MODE)
C  ITEST = 00 : ENDS RUN OF PROGRAM (THIS MUST BE ON THE VERY LAST
C               CARD FOR THE PROGRAM TO END SUCESSFULLY)
C              ALSO MAY BE USED TO CONVERT/INVERT DATA W/O CALCULATING
C              SIMILARITY COEFFICIENTS & W/O PLOTTING IF USED WITH
C              NCOEFF -1
C SIM. COEFF. CODE: MCOEFF
C  MCOEFF = 01 : NO TRANS. + JACCARD COEFF. (P/A)
C  MCOEFF = 02 : NO TRANS. + CZEK. (DICE) COEFF.
C  MCOEFF = 03 : PERCENT TRANS. + CZEK. COEFF.
C  MCOEFF = 04 : PERCENT MAX. TRANS. + CZEK. COEFF.
C  MCOEFF = 05 : LOG10 TRANS. + CZEK. COEFF.
C  MCOEFF = 06 : NO TRANS. + HOMOGEN. FUNCTION
C  MCOEFF = 07 : PERCENT TRANS. + HOMOGEN. FUNCTION
C  MCOEFF = 08 : PERCENT MAX. TRANS. + HOMOGEN. FUNCTION
C  MCOEFF = 09 : LOG10 TRANS. + HOMOGEN. FUNCTION
C  MCOEFF = 10 : D'BLE TRANS. IF INVERSION ELSE PERCENT TRANS., +DICE
C               D'BLE TRANS = PERCENT TRANS. FOLLOWED BY PERCENT
C                        TRANS. AFTER INVERSION.
C
C NEW SIM. COEFF CODE : NCOEFF
C  NCOEFF = -1 :TERMINATES RUN AFTER DATA TRANSFORMATION AND/OR
C               INVERSION WITHOUT CALCULATING SIMILARITY COEFFICIENTS
C               AND WITHOUT PRODUCING A DENDROGRAM IF USED WITH
C               ITEST 00
C  NCOEFF = 01 TO 09 : SAME AS MCOEFF
C*************************************************************
      INTEGER TITLE(20),FORMT(20),CSIM(7),LABEL(12),BLANK
     INTEGER M,N,ITEST,MCOEFF,NCOEFF,VAL1,VAL2,D,I,J,K,MT,NX,
    NPASS,IM1,LVROW,LVCOL,NBROW,NBCOL,NXM1,JADJ,NROWS,NUM,KOLT,KOLF,
     NROWT,IX,IXM1,NUMX,IC,NM1,NP1,IBOOK,INDEX1,INDEX2,NP,IPASS
     REAL
PERC,PMAX,PQ,PNO,V,W,VALMIN,VALMAX,SMAX,COMBO,HEIGHT,LENGTH,
    X,Y,YSCALE,CHARHT,XNUM,XSYM,YPOS,CONST
```

```
      INTEGER ROWCD(200,12),TEMCD(200,12),NUMBR(200)
      INTEGER    COLCD(125,12)
       REAL DATA(200,200),OUT(200,3),SIMCO(200,200),BOOK(200,200),
       SUM(200),T(200),PLOCX(200),PLOCY(200)
      EQUIVALENCE (SIMCO,BOOK)
      DATA BLANK,IPASS/0,0/
4839  CALL PLOTS(0,0,50)
C*************************************************************
C READ IN TITLE HEADING (UP TO 80 CHARACTERS)
4840  READ (5,100) TITLE
      WRITE (8,100) TITLE
      WRITE (6,100) TITLE
100   FORMAT(20A4)
C*************************************************************
C READ IN EXECUTION-TIME FORMAT FOR INPUT DATA
4841  READ (5,100) FORMT
      WRITE (8,100) FORMT
      WRITE (6,100) FORMT
C*************************************************************
C READ IN N (#ROWS/SAMPLES) & M (#COLS/SPECIES) AND FIND MAX. OF N OR M
4842  READ (5,101) N,M
      WRITE(6,101) N,M
      WRITE(8,101) N,M
101   FORMAT(I3,2X,I3)
      D=N
      IF(M.GT.N) D=M
C*************************************************************
C DIMENSIONALIZE ARRAYS
C FIND OUT HOW TO DIMENSIONALIZE ARRAYS AT EXECUTION TIME IF
POSSIBLE.
C*************************************************************
C INITIALIZE COLUMN AND ROW CODE ARRAYS
      DO 1234 J=1,M
      DO 5678 K=1,12
      COLCD(J,K)=BLANK
5678  CONTINUE
1234  CONTINUE
      DO 8765 I=1,N
      DO 4321 K=1,12
      ROWCD(I,K)=BLANK
4321  CONTINUE
8765  CONTINUE
C*************************************************************
C READ IN COLUMN CODES (12-A4 FIELDS EACH) FOR SPECIES, 1 TO A CARD.
23    DO 3 J=1,M
24    READ (5,100) (COLCD(J,K),K=1,12)
      WRITE (8,100) (COLCD(J,K),K=1,12)
3     CONTINUE
C*************************************************************
C READ IN ROW CODES (TWO 4-CHAR. FIELDS EACH) (USUALLY SAMPLES)
C  AND THE DATA MATRIX (N-ROWS BY M-COLUMNS)
25    DO 4 I=1,N
26    READ (5,100) (ROWCD(I,K),K=1,12)
      WRITE (8,100) (ROWCD(I,K),K=1,12)
27    READ (5,FORMT) (DATA(I,J),J=1,M)
```

```
C     READ (5,FORMT) (ROWCD(I),(DATA(I,J),J=1,M)
4     CONTINUE
12345 CONTINUE
C*************************************************************
C READ IN HEIGHT AND LENGTH OF DENDROGRAM PLOT IN INCHES, ALONG
WITH
C  THE VALUE OF "NEWPEN", THE PLOT LINE THICKNESS (1-NARROW TO 5-WIDE).
C  THEN CHECK FOR ILLEGAL VALUES AND SET TO MAXIMUM IF FOUND.
      READ (4,104) HEIGHT,LENGTH,NP
104   FORMAT(F4.1,1X,F4.1,1X,I1)
      IF(HEIGHT.GT.34.0) HEIGHT=34.0
C*************************************************************
C READ IN CONTROL CARD PARAMETER (ITEST), AND SIM. COEFF. CODE
(MCOEFF)
      READ (4,102) ITEST,MCOEFF,CONST
102   FORMAT(I2,1X,I2,1X,F7.3)
C*************************************************************
C TEST FOR ILLEGAL MCOEFF VALUE
      IF(MCOEFF.EQ.1.OR.MCOEFF.EQ.2.OR.MCOEFF.EQ.3.OR.MCOEFF.EQ.4
     *.OR.MCOEFF.EQ.5.OR.MCOEFF.EQ.6.OR.MCOEFF.EQ.7.OR.MCOEFF.EQ.8
     *.OR.MCOEFF.EQ.9.OR.MCOEFF.EQ.10)
     *GO TO 835
      WRITE(6,105) MCOEFF
105   FORMAT('SIM COEFF. VALUE OF ',I2,' IS ILLEGAL.')
      GO TO 999
C*************************************************************
C TEST FOR TRANSFORMATION TYPE (IF ANY)
835   IF(MCOEFF.EQ.1.OR.MCOEFF.EQ.2.OR.MCOEFF.EQ.6) GO TO 825
      IF(MCOEFF.EQ.4.OR.MCOEFF.EQ.8) GO TO 1226
      IF(MCOEFF.EQ.5.OR.MCOEFF.EQ.9) GO TO 1227
C*************************************************************
C CONVERTS RAW DATA TO PERCENTAGES : (MCOEFF=03,07,10)
1225  PERC=0.
      DO 89 I=1,N
      DO 87 J=1,M
     PERC=PERC+DATA(I,J)
87    CONTINUE
      DO 88 K=1,M
      DATA(I,K)=DATA(I,K)/PERC
88    CONTINUE
      PERC=0.
89    CONTINUE
      IF (IPASS.GT.0) GO TO 830
      GO TO 825
C*************************************************************
C COMPUTES A PERCENT MAXIMUM DATA TRANSFORMATION : (MCOEFF=04,08)
1226  PMAX=0.
      DO 96 I=1,M
      DO 97 J=1,N
      IF(DATA(J,I).GT.PMAX)PMAX=DATA(J,I)
97    CONTINUE
      DO 98 J=1,N
      DATA(J,I)=(DATA(J,I)/PMAX)*100.
98    CONTINUE
      PMAX=0.
```

```
96   CONTINUE
     GO TO 825
C*************************************************************
C COMPUTES A LOG10 TRANSFORMATION (MCOEFF=05,09)
C IF NO CONSTANT IS SPECIFIED A VALUE OF 1.0 WILL BE USED.
C (NOTE : DECILES WILL BE COMPUTED BASED ON A COUNT SIZE OF 300)
1227  IF(CONST.LT.0.0001) CONST=1.0
      DO 111 I=1,N
      DO 112 J=1,M
      DATA(I,J)=ALOG10((DATA(I,J)/30)+CONST)
112   CONTINUE
111   CONTINUE
C*************************************************************
C TEST FOR DATA INVERSION (ITEST NEGATIVE)
825   IF(ITEST.GT.0) GO TO 830
C*************************************************************
C INVERT 'DATA' MATRIX FOR R-MODE CLUSTERING.
800   DO 801 I=1,N
      DO 802 J=1,M
      SIMCO(J,I)=DATA(I,J)
802   CONTINUE
801   CONTINUE
      DO 805 I=1,N
      DO 806 J=1,M
      DATA(J,I)=SIMCO(J,I)
806   CONTINUE
805   CONTINUE
      DO 810 I=1,N
      DO 811 K=1,12
     TEMCD(I,K)=ROWCD(I,K)
811   CONTINUE
810   CONTINUE
      DO 815 J=1,M
      DO 816 K=1,12
    ROWCD(J,K)=COLCD(J,K)
816   CONTINUE
815   CONTINUE
      DO 821 I=1,N
      DO 822 K=1,12
     COLCD(I,K)=TEMCD(I,K)
822   CONTINUE
821   CONTINUE
      MT=M
      M=N
      N=MT
      IPASS = IPASS + 1
      IF(MCOEFF.EQ.10) GO TO 1225
C*************************************************************
C WRITE OUT DATA MATRIX (TRANSFORMED IF REQUESTED) TO FILEDEF UNIT
07
830   WRITE (7,100) TITLE
      IF(MCOEFF.EQ.1.OR.MCOEFF.EQ.2.OR.MCOEFF.EQ.6) WRITE(7,301)
      IF(MCOEFF.EQ.3.OR.MCOEFF.EQ.7) WRITE(7,302)
      IF(MCOEFF.EQ.4.OR.MCOEFF.EQ.8) WRITE(7,303)
      IF(MCOEFF.EQ.10.AND.ITEST.LT.0) WRITE(7,313)
```

```
      IF(MCOEFF.EQ.10.AND.ITEST.GT.0) WRITE(7,302)
      IF(MCOEFF.EQ.5.OR.MCOEFF.EQ.9) WRITE(7,310) CONST
301   FORMAT(' NO TRANSFORMATION')
302   FORMAT(' PERCENT TRANSFORMATION')
303   FORMAT(' PERCENT-MAXIMUM TRANSFORMATION')
313   FORMAT(' DOUBLE TRANSFORMED')
310   FORMAT(' LOG-10 TRANSFORMATION, CONSTANT = ',F7.3)
      WRITE(7,304)
304   FORMAT('DATA IS IN A (10(F7.3,1X)) FORMAT')
      WRITE (7,200)
200   FORMAT(' ')
      DO 5 J=1,M
      WRITE (7,100) (COLCD(J,K),K=1,12)
5     CONTINUE
      DO 6 I=1,N
      WRITE(7,100) (ROWCD(I,K),K=1,12)
      WRITE(7,201) (DATA(I,J),J=1,M)
201   FORMAT(10(F7.3,1X))
6     CONTINUE
      WRITE (7,200)
C*************************************************************
C TEST FOR END OF PROGRAM (USE TO CONVERT/INVERT DATA W/O
PERFORMING
C  CLUSTER ANALYSIS)
      READ(4,102) ITEST,NCOEFF,CONST
      IF(ITEST.EQ.0.AND.NCOEFF.LT.0) GO TO 9999
      IF(CONST.LT.0.0001) CONST=1.0
C*************************************************************
C INITIALIZE MATRICES.
      DO 8 I=1,N
      SUM(I)=0.
      T(I)=1.
      NUMBR(I)=1
      DO 9 J=1,N
      SIMCO(I,J)=0.
9     CONTINUE
8     CONTINUE
C*************************************************************
C TEST FOR SIM. COEFF. TYPE (JACCARD OR CZEKANOWSKI OR HQM)
      IF(MCOEFF.EQ.1) GO TO 125
      IF(MCOEFF.GE.6.AND.MCOEFF.LT.10) GO TO 126
C*************************************************************
C COMPUTE 'CZEKANOWSKI' COEFFICIENTS AND STORE IN LOWER TRIANGULAR
C  (LESS DIAGONAL) PART OF MATRIX 'SIMCO'. (MCOEFF=02,03,04,05)
      DO 10 I=1,N
      DO 20 J=1,M
20     SUM(I)=SUM(I)+DATA(I,J)
      DO 30 K=1,I
      IF (I.EQ.K)GOTO 30
      W=0.
      DO 40 J=1,M
      VALMIN=AMIN1(DATA(I,J),DATA(K,J))
40    W=W+VALMIN
      SIMCO(I,K)=(2.*W)/(SUM(I)+SUM(K))
30    CONTINUE
```

```
10    CONTINUE
      GO TO 15
C*************************************************************
C HQM : FREQUENCY MODULATED RELATIVE HOMOGENEITY FUNCTION (HALL
1967A)
C (MCOEFF=06,07,08,09)
126   DO 11 I=1,N
      DO 21 J=1,M
      SUM(I)=SUM(I)+DATA(I,J)
21    CONTINUE
      DO 31 K=1,I
      IF (I.EQ.K) GO TO 31
      W=0.0
      DO 41 J=1,M
      VALMIN=AMIN1(DATA(I,J),DATA(K,J))
      VALMAX=AMAX1(DATA(I,J),DATA(K,J))
     W=W+VALMIN
      V=V+VALMAX
41    CONTINUE
     SIMCO(I,K)=(W+(W*W/V))/(SUM(I)+SUM(K))
31    CONTINUE
11    CONTINUE
      GO TO 15
C*************************************************************
C COMPUTE JACCARD COEFF (MCOEFF=01)
125   DO 95 I=1,N
      DO 94 K=1,I
      IF(I.EQ.K)GO TO 94
      PQ=0.
      PNO=0.
      DO 93 J=1,M
      IF(DATA(K,J).GT.0..AND.DATA(I,J).GT.0.)PQ=PQ+1.
      IF(DATA(K,J).GT.0..AND.DATA(I,J).EQ.0.)PNO=PNO+1.
      IF(DATA(K,J).EQ.0..AND.DATA(I,J).GT.0.)PNO=PNO+1.
93    CONTINUE
     SIMCO(I,K)=PQ/(PNO+PQ)
94    CONTINUE
95    CONTINUE
C*************************************************************
C ARRAY'BOOK', WHICH OCCUPIES SAME LOCATIONS IN MEMORY AS ARRAY
'SIMCO'
C  IN ORDER TO CONSERVE SPACE, WILL BE USED FOR BOOKKEEPING PURPOSES.
C  ONLY THE UPPER TRIANGULAR (INCLUDING DIAGONAL) PART OF 'BOOK' WILL
BE
C  USED, SO VALUES CONTAINED IN 'SIMCO' WILL BE UNDISTURBED. EACH
COLUMN
C  IN ARRAY 'BOOK' CONTAINS THE NUMBERS OF THE SAMPLES CLUSTERED
C  TOGETHER IN THE OPPOSITE COLUMN IN 'SIMCO'.
15    DO 16 I=1,N
16    BOOK(1,I)=FLOAT(N-I)+1.
      NX=N
      NPASS=1
C*************************************************************
C 'SMAX' WILL CONTAIN THE LARGEST CORRELATION COEFFICIENT IN THE
CURRENT
```

```
C  'SIMCO' MATRIX. THE ROW AND COLUMN NUMBER OF THAT VALUE ARE
RECORDED
C  IN 'LVROW' AND 'LVCOL', RESPECTIVELY.  'SMAX' IS INITIALIZED AT THE
C  BEGINNING OF THE SEARCH TO A VALUE LOWER THAN THE FIRST
CORRELATION
C  COEFFICIENT ENCOUNTERED.  THE SAMPLES OR CLUSTERS WITH THESE
HIGHEST
C  VALUES WILL THEN BE CLUSTERED.
45    SMAX=SIMCO(2,1)-1.
      DO 50 I=2,NX
      IM1=I-1
      DO 51 J=1,IM1
      IF(SMAX.GE.SIMCO(I,J)) GO TO 51
      SMAX=SIMCO(I,J)
     LVROW=I
      LVCOL=J
51    CONTINUE
50    CONTINUE
C*****************************************************************
C SAMPLE (OR CLUSTER) NUMBERS ARE CLUSTERED AND THEIR SIMILARITY
C  COEFFICIENT IS RECORDED IN ARRAY 'OUT' FOR LATER PRINTOUT AND PLOT.
      COMBO=T(LVROW)+T(LVCOL)
      NBCOL=N-LVCOL+1
     NBROW=N-LVROW+1
      OUT(NPASS,1)=BOOK(1,NBCOL)
     OUT(NPASS,2)=BOOK(1,NBROW)
      OUT(NPASS,3)=SMAX
C*****************************************************************
C SIMILARITY COEFFICIENTS ARE CALCULATED FOR THE NEW CLUSTER &
COMPUTED
C  AND STORED IN 'SIMCO'. 'SIMCO' IS THEN COMPACTED BY REMOVING THE
ROW
C  AND COLUMN OF THE SAMPLE WITH THE LARGER NUMBER WHICH WAS
CLUSTERED.
C  ARRAY 'BOOK' IS ALSO UPDATED TO REFLECT THE CHANGE DUE TO THE NEW
C  CLUSTERING.
      DO 60 I=1,NX
      IF(I.EQ.LVCOL) GO TO 60
      IF(I.LT.LVCOL) SIMCO(LVCOL,I)=
     *(T(LVCOL)*SIMCO(LVCOL,I)+T(LVROW)*SIMCO(LVROW,I))/COMBO
      IF(I.GT.LVCOL.AND.I.LT.LVROW) SIMCO(I,LVCOL)=
     *(T(LVCOL)*SIMCO(I,LVCOL)+T(LVROW)*SIMCO(LVROW,I))/COMBO
      IF(I.GT.LVROW) SIMCO(I,LVCOL)=
     *(T(LVCOL)*SIMCO(I,LVCOL)+T(LVROW)*SIMCO(I,LVROW))/COMBO
60    CONTINUE
      T(LVCOL)=COMBO
      NXM1=NX-1
      DO 70 I=LVROW,NXM1
      JADJ=0
      DO 75 J=1,I
     IF (J.EQ.LVROW) JADJ=1
     SIMCO(I,J)=SIMCO(I+1,J+JADJ)
75    CONTINUE
70    CONTINUE
C*****************************************************************
```

```
C ARRAY 'NUMBR' CONTAINS THE NUMBER OF SAMPLES COMPRISING EACH
CLUSTER.
      NROWS=NUMBR(LVCOL)
      NUM=NUMBR(LVROW)
      KOLT=NBCOL
      KOLF=NBROW
      DO 501 I=1,NUM
      NROWT=NROWS+I
      BOOK(NROWT,KOLT)=BOOK(I,KOLF)
501   BOOK(I,KOLF)=0.
      IF(LVROW.EQ.NX)GO TO 535
      DO 505 I=LVROW,NXM1
      IX=N-I+1
      IXM1=IX-1
      NUMX=MAX0(NUMBR(I),NUMBR(I+1))
      DO 515 IC=1,NUMX
      BOOK(IC,IX)=BOOK(IC,IXM1)
515   CONTINUE
505   CONTINUE
535   NUMBR(LVCOL)=NUMBR(LVCOL)+NUMBR(LVROW)
      IF(LVROW.EQ.NX) GO TO 545
      DO 510 I=LVROW,NXM1
510   NUMBR(I)=NUMBR(I+1)
545   NUMBR(NX)=0
      DO 550 I=1,NX
550   SIMCO(NX,I)=0.
      NPASS=NPASS+1
      NX=NX-1
      IF (NX.EQ.1) GO TO 80
      GO TO 45
80    CONTINUE
      NM1=N-1
C**********************************************************
C WRITE OUT RESULTS AS TEXT FILE TO FILEDEF UNIT 06
      WRITE(6,100) TITLE
2001  FORMAT(I5)
      IF(ITEST.EQ.1) WRITE(6,305)
305   FORMAT(' Q-MODE')
      IF(ITEST.EQ.-1) WRITE(6,306)
306   FORMAT(' R-MODE')
      IF(MCOEFF.EQ.1) WRITE(6,307)
307   FORMAT(' JACCARD COEFFICIENT')
      IF(MCOEFF.GE.2.AND.MCOEFF.LE.5) WRITE(6,308)
308   FORMAT(' CZEKANOWSKI COEFFICIENT')
      IF(MCOEFF.GE.6.AND.MCOEFF.LE.9) WRITE(6,309)
309   FORMAT(' HOMOGENEITY FUNCTION')
      IF(MCOEFF.EQ.1.OR.MCOEFF.EQ.2.OR.MCOEFF.EQ.6) WRITE(6,301)
      IF(MCOEFF.EQ.3.OR.MCOEFF.EQ.7) WRITE(6,302)
      IF(MCOEFF.EQ.4.OR.MCOEFF.EQ.8) WRITE(6,303)
      IF(MCOEFF.EQ.5.OR.MCOEFF.EQ.9) WRITE(6,310) CONST
      WRITE(6,200)
      WRITE(6,202)
202   FORMAT('SIM. COEFF. VALUES FOR DENDRO. BRANCHES:')
      DO 90 I=1,NM1
      VAL1=IFIX(OUT(I,1))
```

```
      VAL2=IFIX(OUT(I,2))
     WRITE(6,203) OUT(I,1),(ROWCD(VAL1,K),K=1,12),OUT(I,2),
     *(ROWCD(VAL2,K),K=1,12),OUT(I,3)
203   FORMAT(F4.0,'=',12A4,5X,F4.0,'=',12A4,5X,F5.3)
90    CONTINUE
     WRITE(6,200)
     WRITE(6,204)
204   FORMAT('DENDRO. BRANCH CODES IN DENDROGRAM ORDER')
     DO 91 I=1,N
     IBOOK=IFIX(BOOK(I,N))
     WRITE(6,205) BOOK(I,N),(ROWCD(IBOOK,K),K=1,12)
205   FORMAT(F4.0,' = ',12A4)
91    CONTINUE
     WRITE(6,200)
C*************************************************************
C PLOT THE DENDROGRAM. (SENDS PLOTTING INSTRUCTIONS TO FILEDEF UNIT
10)
C 34 INCHES IS THE MAXIMUM WORKING HEIGHT FOR THIS ROUTINE ON THE
C VERSATEC PLOTTER, WHILE THE LENGTH MAY BE CHOSEN AS DESIRED.
C THE VALUE OF "NEWPEN" DETERMINES THE PLOT LINE THICKNESS.
     CALL NEWPEN(NP)
C-------------------------------------------------------------------
C THIS DRAWS THE AXIS.
     DATA CSIM /4HCOEF,4HFICI,4HENT ,4HOF S,4HIMIL,4HARIT,4HY   /
      CALL SAXIS(0.0,(HEIGHT+0.1),CSIM,25,LENGTH,0.0,0.1,0.1,
     *(LENGTH/10),(LENGTH/10))
C-------------------------------------------------------------------
C THIS SCALES THE DENDROGRAM.
     NP1=N+1
     YSCALE=HEIGHT/FLOAT(N)
      XNUM=LENGTH+0.2
     XSYM=LENGTH+0.9
     CHARHT=0.2
      IF(YSCALE.LT.0.25) CHARHT=0.075
      IF(YSCALE.LT.0.25) XSYM=LENGTH+0.7
     DO 601 I=1,N
     IBOOK=IFIX(BOOK(I,N))
     Y=FLOAT(NP1-I)
     PLOCX(IBOOK)=LENGTH
     PLOCY(IBOOK)=Y*YSCALE
C     IF(YSCALE.LT.0.15) GO TO 601
C-------------------------------------------------------------------
C THIS NUMBERS AND LABELS THE BRANCHES OF THE DENDROGRAM.
     YPOS=PLOCY(IBOOK)-(CHARHT/2)
     CALL NUMBER(XNUM,YPOS,CHARHT,BOOK(I,N),0.0,0)
      DO 71 K=1,12
     LABEL(K)=ROWCD(IBOOK,K)
71    CONTINUE
     CALL SYMBOL(XSYM,YPOS,CHARHT,LABEL,0.0,48)
601   CONTINUE
C-------------------------------------------------------------------
C THIS DRAWS THE DENDROGRAM'S BRANCHES.
     NM1=N-1
     DO 610 I=1,NM1
      X=LENGTH*OUT(I,3)
```

```
      INDEX1=IFIX(OUT(I,1))
      INDEX2=IFIX(OUT(I,2))
      CALL PLOT(PLOCX(INDEX1),PLOCY(INDEX1),3)
      CALL PLOT(X,PLOCY(INDEX1),2)
      CALL PLOT(X,PLOCY(INDEX2),2)
      CALL PLOT(PLOCX(INDEX2),PLOCY(INDEX2),2)
      PLOCX(INDEX1)=X
      PLOCY(INDEX1)=(PLOCY(INDEX1)+PLOCY(INDEX2))/2.
610   CONTINUE
      CALL PLOT(PLOCX(INDEX1),PLOCY(INDEX1),3)
      CALL PLOT(0.0,PLOCY(INDEX1),2)
C*************************************************************
C TEST CONTROL CARD VALUE FOR END OF PROGRAM OR FOR RE-EXECUTION
OF
C  PROGRAM (IF REQUESTED)
      IF(ITEST.EQ.0)GO TO 999
      CALL PLOT(LENGTH+3.,0.,-3)
      GO TO 825
C END PROGRAM
*************************************************************
999   CONTINUE
      CALL PLOT(LENGTH+3.,0.,999)
      RETURN
9999  END
```

```
      PROGRAM DISTANCE
C*************************************************************
C     This program compiles a distance matrix between an unknown
C     sample and each sample in a series of known samples.
C     The distance measurement used is the chord distance as
C     described by Pielou (1984).
C     Witten by Scott Rutherford
C*************************************************************
C     FILE DEFS
C     12--INPUT OF UNKNOWN SAMPLE
C     10--INPUT DATA SET
C     11--OUTPUT OF DISTANCE MATRIX
C
C     Input file format is as follows:
C           Title(40)
C           Number of samples and number of species (3 digits each
C           with 2 spaces between the numbers; ie. 036  052)
C           Species list (30 characters per species)
C           The data set (this also applies to the unknown sample):
C                 Sample No. (12)
C                 Species abundance counts for sample in free format
C
C*************************************************************
      INTEGER NSAMP,NSPEC,I,J,K,L,M,N,O,DATA(200,200),UDATA(200)
      REAL CHORD(200)
      CHARACTER TITLE*40,SAMPLE(200)*12,SPECIE(200)*30,UNKNOWN*12
C*************************************************************
C     -NSPEC AND NSAMP ARE THE NUMBER OF SPECIES AND SAMPLES
C     -I THRU O ARE COUNTERS
C     -DATA IS THE ACTUAL COUNT OF SPECIES IN A SAMPLE
C     -SAMPLE AND SPECIE ARE THE SAMPLE NUMBER AND SPECIES NAME
C     -UDATA AND UNKNOWN ARE THE DATA AND SAMPLE NUMBER OF THE
C      UNKNOWN SAMPLE
C*************************************************************
      OPEN(10,FILE='INPUT',STATUS='OLD')
      OPEN(12,FILE='COMPARE',STATUS='OLD')
      OPEN(11,FILE='OUTPUT',STATUS='NEW')
C
      CALL INDATA(NSAMP,NSPEC,DATA,TITLE,SAMPLE,SPECIE,UNKNOWN,
     &UDATA)
      CALL COMPUTE(NSAMP,NSPEC,DATA,SPECIE,SAMPLE,UDATA,CHORD)
      CALL WRITIT(NSAMP,NSPEC,DATA,TITLE,SAMPLE,SPECIE,UNKNOWN,
     &UDATA,CHORD)
      STOP
      END
C-------------------------------------------------------
C-------------------------------------------------------
C     SUBROUTINE TO READ IN DATA
C
      SUBROUTINE INDATA(NSAMP,NSPEC,DATA,TITLE,SAMPLE,SPECIE,
     &UNKNOWN,UDATA)
      INTEGER NSAMP,NSPEC,DATA(200,200),UDATA(200)
      CHARACTER TITLE*40,SAMPLE(200)*12,SPECIE(200)*30,UNKNOWN*12
```

```
      INTEGER I,J,K,L
      READ(10,300)TITLE
300   FORMAT(A40)
      READ(10,100)NSAMP,NSPEC
100   FORMAT(I3,2X,I3)
      DO 10 K=1,NSPEC
            READ(10,*)SPECIE(K)
10    CONTINUE
      DO 20 I=1,NSAMP
            READ(10,*)SAMPLE(I)
                  READ(10,*)(DATA(I,J),J=1,NSPEC)
20    CONTINUE
C     READ IN UNKNOWN SAMPLE
      READ (12,*)UNKNOWN
      READ (12,*)(UDATA(L),L=1,NSPEC)
      RETURN
      END
C-------------------------------------------------------------
C-------------------------------------------------------------
C     SUBROUTINE TO WRITE OUTPUT FILE
      SUBROUTINE WRITIT(NSAMP,NSPEC,DATA,TITLE,SAMPLE,SPECIE,
     &UNKNOWN,UDATA,CHORD)
      CHARACTER TITLE*40,SAMPLE(200)*12,SPECIE(200)*30,UNKNOWN*12
      INTEGER NSAMP,NSPEC,I,J,K,L,M,N,O,DATA(200,200),UDATA(200)
      REAL CHORD(200)
      WRITE(11,*)TITLE
      WRITE(11,100)NSAMP,NSPEC
100   FORMAT(I3,2X,I3)
      DO 5 K=1,NSPEC
            WRITE(11,*)SPECIE(K)
5     CONTINUE
      DO 10 I=1,NSAMP
            WRITE (11,400)SAMPLE(I)
            WRITE(11,300)(DATA (I,J),J=1,NSPEC)
20          CONTINUE
10    CONTINUE
300   FORMAT (10(I3,2X))
400   FORMAT (A12)
      WRITE(11,*)'UNKNOWN SAMPLE DESIGNATION IS ',UNKNOWN
      WRITE(11,*)(UDATA(L),L=1,NSPEC)
      WRITE(11,*)'---------------------------------'
      WRITE(11,*)'SAMPLE      CHORD DISTANCE'
      DO 50 M=1,NSAMP
            WRITE(11,500)SAMPLE(M),CHORD(M)
50    CONTINUE
500   FORMAT(A15,F4.3)
      RETURN
      END
C-------------------------------------------------------------
C-------------------------------------------------------------
C     SUBROUTINE TO CALCULATE A DISTANCE MEASUREMENT
C     BETWEEN A SERIES OF KNOWN SAMPLES AND 1 UNKNOWN SAMPLES
      SUBROUTINE
COMPUTE(NSAMP,NSPEC,DATA,SPECIE,SAMPLE,UDATA,CHORD)
      INTEGER NSAMP,NSPEC,I,J,K,L,M,N,O,DATA(200,200),UDATA(200),
```

```
      &NUMER(200)
          REAL CCOS(200),CHORD(200),DENOM(200)
          CHARACTER TITLE*40,SAMPLE(200)*12,SPECIE(200)*30,UNKNOWN*12
C-------------------------------------------------------------
C         NUMER, DENOM, AND CCOS ARE USED IN THE CALCULATION OF THE
C         CHORD DISTANCE.  CHORD IS THE DISTANCE BETWEEN 2 SAMPLES.
C-------------------------------------------------------------
C         LOOP TO CALCULATE THE NUMERATOR FOR EACH COMPARISON
          DO 15 J=1,NSAMP
                DO 20 K=1,NSPEC
                NUMER(J)=NUMER(J)+(DATA(J,K)*UDATA(K))
20              CONTINUE
15        CONTINUE
C
C         LOOP TO CALCULATE THE DENOMINATOR
          DO 30 I=1,NSAMP
                X=0
                Y=0
                DO 40 L=1,NSPEC
                      X=X+DATA(I,L)**2
                      Y=Y+UDATA(L)**2
40              CONTINUE
          DENOM(I)=SQRT(X*Y)
30        CONTINUE
          DO 50 M=1,NSAMP
                CCOS(M)=NUMER(M)/DENOM(M)
                CHORD(M)=SQRT(2*(1-CCOS(M)))
50        CONTINUE
          RETURN
          END
```

```
      PROGRAM EVENNESS
C*************************************************************
C     This program computes an evenness index for up to 200 samples
C     With 200 species per sample.  The equation for calculation is
C     from Hill (1973) as. cited in Ludwig and Reynolds (1988).
C     Program written by Scott Rutherford
C*************************************************************
C     FILE DEFS
C     10--INPUT DATA SET
C     11--OUTPUT OF EVENNESS INDEX FOR EACH SAMPLE
C*************************************************************
      INTEGER NSAMP,NSPEC,I,J,K,L,M,N,O,DATA(200,200)
      REAL EVEN(200)
      CHARACTER TITLE*40,SAMPLE(200)*12,SPECIE(200)*30,UNKNOWN*12
C*************************************************************
C     -NSPEC AND NSAMP ARE THE NUMBER OF SPECIES AND SAMPLES
C     -I THRU O ARE COUNTERS
C     -DATA IS THE ACTUAL COUNT
C     -SAMPLE AND SPECIE ARE THE SAMPLE NUMBER AND SPECIES NAME
C     -UDATA AND UNKNOWN ARE THE DATA AND SAMPLE NUMBER OF THE
C      UNKNOWN SAMPLE
C*************************************************************
      OPEN(10,FILE='INPUT',STATUS='OLD')
      OPEN(11,FILE='OUTPUT',STATUS='NEW')
C
      CALL INDATA(NSAMP,NSPEC,DATA,TITLE,SAMPLE,SPECIE)
      CALL CALCULATE(NSAMP,NSPEC,EVEN,DATA,SAMPLE)
      CALL WRITIT(NSAMP,NSPEC,DATA,TITLE,SAMPLE,SPECIE,EVEN)
      STOP
      END
C-------------------------------------------------------
C-------------------------------------------------------

C     SUBROUTINE TO READ IN DATA
C
      SUBROUTINE INDATA(NSAMP,NSPEC,DATA,TITLE,SAMPLE,SPECIE)
      INTEGER NSAMP,NSPEC,DATA(200,200)
      CHARACTER TITLE*40,SAMPLE(200)*12,SPECIE(200)*30
      INTEGER I,J,K,L
      READ(10,300)TITLE
300   FORMAT(A40)
      READ(10,100)NSAMP,NSPEC
100   FORMAT(I3,2X,I3)
      DO 10 K=1,NSPEC
            READ(10,*)SPECIE(K)
10    CONTINUE
      DO 20 I=1,NSAMP
            READ(10,*)SAMPLE(I)
                  READ(10,*)(DATA(I,J),J=1,NSPEC)
20    CONTINUE
      RETURN
      END
C-------------------------------------------------------
C-------------------------------------------------------
```

```
C       SUBROUTINE TO WRITE OUTPUT FILE
        SUBROUTINE WRITIT(NSAMP,NSPEC,DATA,TITLE,SAMPLE,SPECIE,EVEN)
        CHARACTER  TITLE*40,SAMPLE(200)*12,SPECIE(200)*30
        INTEGER NSAMP,NSPEC,I,J,K,L,M,N,O,DATA(200,200)
        REAL EVEN(200)
        WRITE(11,*)TITLE
        WRITE(11,*)'--------------------------------'
        WRITE(11,*)'OUTPUT OF EVENNESS VALUE FOR SAMPLES'
        WRITE(11,*)' '
        WRITE(11,*)'SAMPLE                EVENNESS VALUE'
        WRITE(11,*)'------                --------------'
        DO 40, I=1,NSAMP
                WRITE(11,500)SAMPLE(I),EVEN(I)
40      CONTINUE
500     FORMAT(A12,20X,F6.4)
        RETURN
        END
C-------------------------------------------------------------
C-------------------------------------------------------------
C       SUBROUTINE TO CALCULATE EVENNESS INDEX OF HILL(1973)
C
        SUBROUTINE CALCULATE(NSAMP,NSPEC,EVEN,DATA,SAMPLE)
        INTEGER NSPEC,NSAMP,DATA(200,200)
        REAL EVEN(200),HHAT,MINUSHP,LAMBDA,X,SAMPSUM,NUMER,DENOM
        CHARACTER SPECIE*30,SAMPLE*12
C
        DO 10 I=1,NSAMP
        HHAT=0
        LAMBDA=0
        SAMPSUM=0
                DO 20 J=1,NSPEC
                        SAMPSUM=SAMPSUM+FLOAT(DATA(I,J))
20              CONTINUE
                DO 30 K=1,NSPEC
                        LAMBDA=LAMBDA+((FLOAT(DATA(I,K))*
   &            (FLOAT(DATA(I,K))-1))/(SAMPSUM*(SAMPSUM-1)))
                        X=FLOAT(DATA(I,K))/SAMPSUM
                        IF (X.EQ.0) GOTO 30
                        HHAT=HHAT+FLOAT((DATA(I,K))/SAMPSUM*LOG(X))
30              CONTINUE
                MINUSHP=-HHAT
                NUMER=1/LAMBDA
                DENOM=EXP(MINUSHP)
                EVEN(I)=(NUMER-1)/(DENOM-1)
10      CONTINUE
        RETURN
        END
```

```
      PROGRAM BC-DISTANCE
C*****************************************************************
C     This program compiles a distance matrix between an unknown
C     sample and each sample in a series of known samples.
C     The distance measurement used is the BC-Group distance as
C     introduced by Bray and Curtis (1957) as sited in Ludwig and
C     Reynolds (1988).
C     Program written by Scott Rutherford
C*****************************************************************
C     FILE DEFS
C     12--INPUT OF UNKNOWN SAMPLE
C     10--INPUT DATA SET
C     11--OUTPUT OF DISTANCE MATRIX
C
C     Input file format is as follows:
C           Title(40)
C           Number of samples and number of species (3 digits each
C           with 2 spaces between the numbers; ie. 036  052)
C           Species list (30 characters per species)
C           The data set (this also applies to the unknown sample):
C                 Sample No. (12)
C                 Species abundance counts for sample in free format.
C
C*****************************************************************
      INTEGER NSAMP,NSPEC,I,J,K,L,M,N,O,DATA(200,200),UDATA(200)
      REAL DIST(200)
      CHARACTER TITLE*40,SAMPLE(200)*12,SPECIE(200)*30,UNKNOWN*12
C*****************************************************************
C     -NSPEC and NSAMP are the number of speceis and the number of
C      samples/
C     -I through O are counters
C     -DATA is the count of species I in the sample
C     -SAMPLE and SPECIE are the sample and specie designations
C     -UDATA and UNKNOWN are the data and sample designation for
C      the unknown sample.
C*****************************************************************
      OPEN(10,FILE='INPUT',STATUS='OLD')
      OPEN(12,FILE='UNKNOWN',STATUS='OLD')
      OPEN(11,FILE='OUTPUT',STATUS='NEW')
C
      CALL INDATA(NSAMP,NSPEC,DATA,TITLE,SAMPLE,SPECIE,
     &UNKNOWN,UDATA)
      CALL COMPUTE(NSAMP,NSPEC,DATA,SPECIE,SAMPLE,UDATA,DIST)
      CALLWRITIT(NSAMP,NSPEC,DATA,TITLE,SAMPLE,SPECIE,
     &UNKNOWN,UDATA,DIST)
      STOP
      END
C-------------------------------------------------------
C-------------------------------------------------------
C     SUBROUTINE TO READ IN DATA
C
```

```
      SUBROUTINE INDATA(NSAMP,NSPEC,DATA,TITLE,SAMPLE,SPECIE,
     &UNKNOWN,UDATA)
      INTEGER NSAMP,NSPEC,DATA(200,200),UDATA(200)
      CHARACTER TITLE*40,SAMPLE(200)*12,SPECIE(200)*30,UNKNOWN*12
      INTEGER I,J,K,L
      READ(10,300)TITLE
300   FORMAT(A40)
      READ(10,100)NSAMP,NSPEC
100   FORMAT(I3,2X,I3)
      DO 10 K=1,NSPEC
            READ(10,*)SPECIE(K)
10    CONTINUE
      DO 20 I=1,NSAMP
            READ(10,*)SAMPLE(I)
                  READ(10,*)(DATA(I,J),J=1,NSPEC)
20    CONTINUE
C     READ IN UNKNOWN SAMPLE
      READ (12,*)UNKNOWN
      READ (12,*)(UDATA(L),L=1,NSPEC)
      RETURN
      END
C-------------------------------------------------------------
C-------------------------------------------------------------
C     SUBROUTINE TO WRITE OUTPUT FILE
      SUBROUTINE WRITIT(NSAMP,NSPEC,DATA,TITLE,SAMPLE,SPECIE,
     &UNKNOWN,UDATA,DIST)
      CHARACTER TITLE*40,SAMPLE(200)*12,SPECIE(200)*30,UNKNOWN*12
      INTEGER NSAMP,NSPEC,I,J,K,L,M,N,O,DATA(200,200),UDATA(200)
      REAL DIST(200)
      WRITE(11,*)TITLE
      WRITE(11,100)NSAMP,NSPEC
100   FORMAT(I3,2X,I3)
      DO 5 K=1,NSPEC
            WRITE(11,*)SPECIE(K)
5     CONTINUE
      DO 10 I=1,NSAMP
            WRITE (11,400)SAMPLE(I)
            WRITE(11,300)(DATA (I,J),J=1,NSPEC)
20          CONTINUE
10    CONTINUE
300   FORMAT (10(I3,2X))
400   FORMAT (A12)
      WRITE(11,*)'UNKNOWN SAMPLE DESIGNATION IS ',UNKNOWN
      WRITE(11,*)(UDATA(L),L=1,NSPEC)
      WRITE(11,*)'---------------------------------'
      WRITE(11,*)'SAMPLE      PERCENT SIMILARITY'
      DO 50 M=1,NSAMP
            WRITE(11,*)SAMPLE(M),DIST(M)
50    CONTINUE
500   FORMAT(A15,F10.7)
      RETURN
```

```
      END
C-------------------------------------------------------------
C-------------------------------------------------------------
C     SUBROUTINE TO CALCULATE A DISTANCE MEASUREMENT
C     BETWEEN A SERIES OF KNOWN SAMPLES AND 1 UNKNOWN SAMPLE
      SUBROUTINE
COMPUTE(NSAMP,NSPEC,DATA,SPECIE,SAMPLE,UDATA,DIST)
      INTEGER NSAMP,NSPEC,I,J,K,L,M,N,O,DATA(200,200),UDATA(200),
     &NUMER,SPECTOT
      REAL DIST(200)
      CHARACTER TITLE*40,SAMPLE(200)*12,SPECIE(200)*30,UNKNOWN*12
C-------------------------------------------------------------
      DO 15 J=1,NSAMP
      NUMER=0
      SPECTOT=0
            DO 20 K=1,NSPEC
            SPECTOT=SPECTOT+DATA(J,K)+UDATA(K)
                  IF (DATA(J,K).LT.UDATA(K)) THEN
                  NUMER=NUMER+DATA(J,K)
                  ELSE
                  NUMER=NUMER+UDATA(K)
                  END IF
20          CONTINUE
      DIST(J)=(2*FLOAT(NUMER)/FLOAT(SPECTOT))*100
15    CONTINUE
      RETURN
      END
```

```
      PROGRAM RICHNESS
C*****************************************************************
C     This program calculates a species richness measure for a series of samples.
C     The measurement used is the Margalev index as cited in Ludwig and
C     Reynolds (1988).
C     Program written by Scott Rutherford
C*****************************************************************
C     FILE DEFS
C     10--INPUT DATA SET
C     11--OUTPUT OF DISTANCE MATRIX
C
C     Input file format is as follows:
C           Title(40)
C           Number of samples and number of species (3 digits each
C           with 2 spaces between the numbers; ie. 036  052)
C           Species list (30 characters per species)
C           The data set (this also applies to the unknown sample):
C                 Sample No. (12)
C                 Species abundance counts for sample in free format
C
C*****************************************************************
      INTEGER NSAMP,NSPEC,I,J,K,L,M,N,O,DATA(200,200)
      REAL RICH(200)
      CHARACTER TITLE*40,SAMPLE(200)*12,SPECIE(200)*30
C*****************************************************************
C     -NSPEC AND NSAMP ARE THE NUMBER OF SPECIES AND SAMPLES
C     -I THRU O ARE COUNTERS
C     -DATA IS THE ACTUAL COUNT OF SPECIES IN A SAMPLE
C     -SAMPLE AND SPECIE ARE THE SAMPLE NUMBER AND SPECIES NAME
C     -UDATA AND UNKNOWN ARE THE DATA AND SAMPLE NUMBER OF
C     THE UNKNOWN SAMPLE
C*****************************************************************
      OPEN(10,FILE='INPUT',STATUS='OLD')
      OPEN(11,FILE='OUTPUT',STATUS='NEW')
C
      CALL INDATA(NSAMP,NSPEC,DATA,TITLE,SAMPLE,SPECIE)
      CALL COMPUTE(NSAMP,NSPEC,DATA,SPECIE,SAMPLE,RICH)
      CALL WRITIT(NSAMP,NSPEC,DATA,TITLE,SAMPLE,SPECIE,RICH)
      STOP
      END
C-------------------------------------------------------
C     SUBROUTINE TO READ IN DATA
C
      SUBROUTINE INDATA(NSAMP,NSPEC,DATA,TITLE,SAMPLE,SPECIE)
      INTEGER NSAMP,NSPEC,DATA(200,200)
      CHARACTER TITLE*40,SAMPLE(200)*12,SPECIE(200)*30
      INTEGER I,J,K,L
      READ(10,300)TITLE
300   FORMAT(A40)
      READ(10,100)NSAMP,NSPEC
100   FORMAT(I3,2X,I3)
```

```
      DO 10 K=1,NSPEC
            READ(10,*)SPECIE(K)
10    CONTINUE
      DO 20 I=1,NSAMP
            READ(10,*)SAMPLE(I)
                  READ(10,*)(DATA(I,J),J=1,NSPEC)
20    CONTINUE
      RETURN
      END
C-------------------------------------------------------
C     SUBROUTINE TO WRITE OUTPUT FILE
C-------------------------------------------------------
      SUBROUTINE WRITIT(NSAMP,NSPEC,DATA,TITLE,SAMPLE,SPECIE,
     &RICH)
      CHARACTER TITLE*40,SAMPLE(200)*12,SPECIE(200)*30
      INTEGER NSAMP,NSPEC,I,J,K,L,M,N,O,DATA(200,200)
      REAL RICH(200)
C-------------------------------------------------------
      WRITE(11,*)TITLE
      WRITE(11,100)NSAMP,NSPEC
100   FORMAT(I3,2X,I3)
      DO 5 K=1,NSPEC
            WRITE(11,*)SPECIE(K)
5     CONTINUE
      DO 10 I=1,NSAMP
            WRITE (11,400)SAMPLE(I)
            WRITE(11,300)(DATA (I,J),J=1,NSPEC)
20          CONTINUE
10    CONTINUE
300   FORMAT (10(I3,2X))
400   FORMAT (A12)
      WRITE(11,*)'----------------------------------'
      WRITE(11,*)'SAMPLE      SPECIES RICHNESS'
      DO 50 M=1,NSAMP
            WRITE(11,*)SAMPLE(M),RICH(M)
50    CONTINUE
      RETURN
      END
C-------------------------------------------------------
C     Subroutine to calculate species richness coeficient.
      SUBROUTINE COMPUTE(NSAMP,NSPEC,DATA,SPECIE,SAMPLE,RICH)
      INTEGER NSAMP,NSPEC,I,J,K,L,M,N,O,DATA(200,200)
      REAL RICH(200)
C*************************************************************
      DO 10, I=1,NSAMP
      SPECTOT=0
      SAMPTOT=0
            DO 20, J=1,NSPEC
                  IF (DATA(I,J).NE.0) THEN
                  SPECTOT=SPECTOT+1
                  END IF
```

```
                    SAMPTOT=SAMPTOT+DATA(I,J)
20              CONTINUE
        RICH(I)=(SPECTOT-1)/LOG(SAMPTOT)
10      CONTINUE
        RETURN
        END

C*************************************************************************
*
```

APPENDIX B

DATA TABLES

Data Table 1. Palynomorph counts by sample and species.

Sample number	Lithology	P. infusorioides	S. Ramosus	Cyclonephelium sp. A	O	Macrolatesporites spp.	Apteodinium?	Leiosphaerida sp.	Odontochitina Sp.	AA	V	U	F	AC	Pterospermopsis sp.	Tanyosphaeridium sp.	Lepodinium sp. A	Cyclonephelium compactum?	Hystrichodinium pulchrum	Lepodinium sp B	Spinidinium?	W	A	Acritarch form A	I	J	T	L	S	C. oceanica	Microdinium sp.	Non-cavate no hair	Polygonal no Hair	Dinogymnium spp.	Pterodinium sp.	Hystrichosphaera spp.	AI	Deflandrea sp.	E	O	C	D	N	Z	K	P	AH	Veryhachium?	AE	AL	AN	X	AB	AD	Litosphaeridium spp.	M	AF	AG	AJ	AK	AM	B	Cymatosphaera	G	H	R	Y	Total
PBC-1	Limestone	110	47	39					3			2	1				7		1	0	6	10	4	5				14			9	8		4				1	2		5	2	0		1					3	1	3	1		1				1			1	1					295
PBC-2A	Shale	139	23	12			8		2	5		25	4	9	12		2	1		2	3			3		1					1	11	7	4			4	2				1											1						1		1	1			232
PBC-3	Limestone	13	36						33				2	1			13			20	1	1		2	4	1					1													2		1	2			1		1			2			1	1											139
PBC-6	Limestone	2	7	1					35						7		8							8			1			5		1			2		1				0		3																											81
PBC-9	Marlstone	93										50		12	3		2									10			9			10					11					1				4																									205
PBC-9A	Shale	18	109	2			12	10	5	8		4	12		2	12	2	6			1		2	1	1	3				3	1				3					3		1			3																1				1		228
PBC 13	Marlstone	5	44	14			5	12	5	2		2	3			1	3						3					1		6			2	1		1			1	2																													113
PBC-14	Shale		72	179				29	20				1											4		1		3	2													2			0																1								314
PBC-15	Limestone	3	9	6		4	1	12	5		1	1			3		1				1	2		8	1	3		2			4		3	1										1										1																75
PBC-16	Limestone	89	40	66		27		3	14		3		9			5		25				4	1		4					2							7																2						2												305
PBC-19	Shale	16	14	62		186	1	2	5	4			2			2	2	9	2			3														3	3	1																																317
PBC-20	Shale	19	71	10	7	25	65	14	2	38		4	5			3		3			11									2				1			1		3		1		1																										316
PBC-21	Limestone	50	24	17		37	52	8	6		3		10		1	2	6	1			1	1	7			1				3				1									2																										233
PBC-23	Limestone	7	1			2	13	9	1	21	36		2	19	1		1						1			1				1			1		1																																	118
PBC-23A	Shale				1		23	3		6			11	2						1								1																																									48
PBC-26	Limestone		3	6			4	18	2		4		3			7	2	1		3		2	1			1																																										1	58
PBC-27	Marlstone	10	27	9	7	30	3	24	18	20	16		13	8	1	8	1		5				3							1							2		1				3				2																					212
PBC-28	Marlstone	3	5		1			5	2	5	4		1	1		2															1							1																																30
PBC-31	Marlstone	1	7	1		9		3			6		3	1	1	8			2	5					1																																											48
PBC-32A	Shale	2			255	2	3			3				9	13											10		1																																								298
PBC-34	Marlstone	2	9	70	1		2	28	1		3			2	1	3	2		17				2							1					1				1													1																		147
PBC-36	Limestone		9	31	3	1	1	7		11	17		6			4	2		8	1																	1					1																										103
PBC-39A	Shale	3	1	1	139			1		6	3			1	15												12		6							2			3										2																				197
PBC-40	Marlstone	2	17	9		2		14					1	1	1				5			2			4											1				1			5																										65
Totals		585	575	540	414	325	221	202	159	129	96	88	72	75	63	57	54	46	40	31	27	25	24	23	23	22	22	21	21	20	20	19	18	13	15	14	13	12	10	8	7	7	6	6	5	5	4	4	3	3	3	3	2	2	2	2	1	1	1	1	1	1	1	1	1	1	1	4225

Limestone

Shale

Marlstone

Data Table 2. General data grouped by palynomorph zone.

Sample Number	Lithology	Weight % Carbonate	Bed Thickness	Weight of Carbonate	Species Richness	Hill's Modifie Evenness
PBC-1	Limestone	94.14	45.72	108.00	5.081	0.5023
PBC-2A	Shale	40.67	12.70	11.88	4.603	0.4006
PBC-3	Limestone	83.92	15.24	32.40	4.053	0.6827
PBC-6	Limestone	84.49	15.24	32.60	2.731	0.6024
PBC-9	Marlstone	71.62	15.24	26.85	1.879	0.6118
Average		**74.968**	**20.828**	**42.346**	**3.6694**	**0.55996**
PBC-9A	Shale	41.03	19.05	17.89	4.77	0.3947
PBC-13	Marlstone	71.66	12.7	22.39	4.004	0.5437
PBC-14A	Shale	73.30	7.62	12.85	1.911	0.6121
PBC-15	Limestone	88.93	21.59	28.60	4.914	0.8999
PBC-18	Limestone	84.64	7.62	16.30	2.95	0.6881
PBC-19	Shale	75.04	7.62	13.15	2.84	0.4729
Average		**72.43**	**12.70**	**18.53**	**3.56**	**0.60**
PBC-20	Shale	68.40	3.81	5.99	3.458	0.6452
PBC-21	Limestone	94.82	15.24	36.56	3.527	0.7199
PBC-23	Limestone	79.13	15.24	30.50	3.527	0.722
PBC-23A	Shale	84.85	19.05	37.18	2.015	0.7056
Average		**81.80**	**13.34**	**27.56**	**3.13**	**0.70**
PBC-26	Limestone	89.53	15.24	34.50	3.679	0.7452
PBC-27	Marlstone	73.62	6.35	11.50	4.1	0.8499
PBC-28	Marlstone	88.26	11.43	24.82	3.234	0.166
PBC-31	Limestone	94.57	11.43	27.40	3.306	0.9944
Average		**86.50**	**11.11**	**24.56**	**3.58**	**0.69**
PBC-32A	Shale	67.27	35.56	55.02	1.579	0.3779
PBC-34	Marlstone	90.52	22.96	50.90	3.597	0.5296
PBC-35	Limestone	90.32	11.43	26.00	3.223	0.7398
PBC-39A	Shale	69.46	19.05	30.43	2.645	0.3933
PBC-40	Marlstone	87.76	15.24	32.90	3.114	0.7948
Average		**81.066**	**20.848**	**39.05**	**2.8316**	**0.56708**

Data Table 3. Carbonate data for each sample.

Sample Number	Lithology	Wt. % Carbonate	Bed Thickness (cm.)
PBC-1	Limestone	94.14	45.7
PBC-2	Marlstone	54.00	10.2
PBC-2A	Shale	40.67	12.7
PBC-3	Limestone	83.92	15.2
PBC-6	Limestone	84.49	15.2
PBC-6A	Shale	48.22	11.4
PBC-6C	Shale	29.54	7.6
PBC-7	Limestone	89.15	12.7
PBC-8	Marlstone	69.77	25.4
PBC-9	Marlstone	71.62	15.2
PBC-9A	Shale	41.03	19.1
PBC-10	Limestone	72.04	22.9
PBC-11A	Shale	66.39	10.2
PBC-12	Marlstone	76.68	11.4
PBC-12A	Shale	51.05	10.2
PBC-13	Marlstone	71.66	12.7
PBC-13A	Shale	64.52	10.2
PBC-14	Limestone	83.32	22.9
PBC-14A	Shale	73.30	7.6
PBC-15	Limestone	88.93	21.6
PBC-15A	Shale	53.43	20.3
PBC-16	Marlstone	80.03	12.7
PBC-18	Limestone	84.64	7.6
PBC-19	Shale	75.04	7.6
PBC-19A	Marlstone	78.94	19.1
PBC-19B	Shale	43.79	15.2
PBC-20	Shale	68.40	3.8
PBC-21	Limestone	94.82	15.2
PBC-21A	Shale	62.30	15.2
PBC-22	Marlstone	82.43	7.6
PBC-22A	Shale	62.07	15.2
PBC-23	Limestone	79.13	15.2
PBC-23A	Shale	84.85	19.1
PBC-24	Marlstone	88.40	11.4
PBC-24A	Shale	72.54	11.4
PBC-25	Marlstone	86.74	10.2
PBC-25A	Shale	72.45	27.9
PBC-26	Limestone	89.53	15.2
PBC-26A	Shale	77.26	5.1
PBC-27	Marlstone	73.62	6.4
PBC-27A	Shale	73.84	5.1
PBC-28	Marlstone	88.26	11.4
PBC-28A	Shale	72.89	20.3
PBC-29	Limestone	82.92	7.6
PBC-30	Shale	63.19	26.7
PBC-31	Limestone	94.57	11.4
PBC-32A	Shale	67.27	35.6
PBC-33	Marlstone	92.13	19.1
PBC-33A	Shale	86.75	17.8
PBC-34	Marlstone	90.52	23.0
PBC-34A	Shale	86.58	22.9
PBC-35	Limestone	90.32	11.4
PBC-35A	Shale	81.27	41.9
PBC-36	Marlstone	73.15	5.1
PBC-36A	Shale	62.19	15.2
PBC-37	Marlstone	83.80	11.4
PBC-38	Shale	68.94	22.9
PBC-39	Marlstone	76.54	7.6
PBC-39A	Shale	69.46	19.1
PBC-40	Marlstone	87.76	15.2

VITA

Name:	Scott David Rutherford
Date of Birth:	June 28, 1967
Place of Birth:	Philadelphia, Pennsylvania
Present Address:	9104 Dentana Court, Richmond, Virginia 23228
Telephone:	(804) 672-6543
Marital Status:	Married LeAnn Swartz on August 24, 1991
Education:	B.S. Geology, 1992; Temple University, Philadelphia, Pennsylvania
Teaching Experience:	Graduate Teaching Assistant, Department of Geological Sciences, Virginia Polytechnic Institute and State University; September, 1991 to August, 1993
Awards:	C.G. Tillman Award for Teaching Excellence, 1993
Research Interests:	Climate and oceanic productivity